Evaluation of hydrogen sensors and location inside a metering cabinet

Barrie van der Goes

MSc Thesis

Delft University of Technology

kiwa

TU Delft

(Cover photo source:

https://www.kiwa.com/nl/en/themes/renewable-energy-transition/hydrogen-house/hydrogen-training)

Evaluation of hydrogen sensors and location inside a metering cabinet

By

Barrie Reinier van der Goes

In partial fulfillment of the requirements for the degree of

Master of Science

In Sustainable Energy Technology

at the Delft University of Technology

to be defended publicly on Thursday February 24, 2022

Student number:	4134036	
Thesis committee:	Prof. dr. A. J. M. van Wijk	TU Delft, supervisor
	Prof. dr. ir. Z. Lukszo	TU Delft
	Dr. Ir. S. A. Saadabadi	TU Delft, supervisor
	R. J. M. Hermkens	Kiwa, supervisor

Preface

My thesis, with the title ‘Evaluation of hydrogen sensors and location inside a metering cabinet’, was part of the Hydrogen heating project. With this final work, I will conclude my time as a student at Delft University of Technology and complete my master Sustainable Energy Technology. I enjoyed the fulfillment of my thesis very much, where I gained a lot of knowledge in the field of hydrogen and developed my research skills. I also learned a lot about working in a company and how to approach an experimental study.

I would like to go on by thanking all the people for their assistance during the past months. This pleasant process was due to the nice cooperation with my supervisors, for which I would like to thank: Ad van Wijk, Ali Saadabadi, René Hermkens, Zofia Lukszo and all people of the Kiwa technology department PSM. They all provided key support during the research, since they pushed me to not only think in systems, like a typical engineer, but to also to try to find out what was hidden behind the findings of measurements. Especially Ali, for the daily supervision and helpful comments about technical academic writing during this journey.

Ultimately, I would like to thank my loved ones for their support and companionship during the hours that were invested in this master’s thesis: My parents, Brigit, Jasper and all of my friends. Without them this master’s thesis would not have been possible.

Barrie van der Goes
Kwintsheul, February 2022

Abstract

Limiting the emissions of CO_2 from conventional residential heating methods in the built environment is key to reducing all-round greenhouse gas emissions. The Hydrogen Heating Studies project in the Green Village at the TU Delft provides research on the safe application of hydrogen as a more sustainable alternative to conventional heating methods. This thesis contributes to this research by evaluating different hydrogen sensor technologies, as well as determining the sensor location with the fastest response to potential leakages of hydrogen gas inside a standard (Dutch) metering cabinet.

A range of commercially available sensor technologies were assessed to determine which type is most suitable for residential applications. A multi-criteria analysis was applied to evaluate each sensor technology with respect to various criteria such as accuracy, selectivity, maintenance, and calibration. From this analysis the thermal conductivity sensors outperformed the other sensor technologies, albeit only by a small margin versus the catalytic hydrogen sensors.

Investigation of the optimal location of the sensor within the cabinet was made possible with the support of Kiwa Technology. The aim was to find the sensor location enabling the quickest response to high hydrogen concentration levels. An experimental research approach was applied using seven different conditions (e.g., with open ventilation) and seven different sensor locations inside the metering cabinet to determine in which location the sensor response time is faster. A standard leakage flow rate of five liters per hour was applied, which is the highest rate of gas leakage currently allowed in existing buildings. The experiment results indicate the top-center backside of the metering cabinet as the location for the sensor with the fastest response.

The results of this research also confirmed that the condition of closed ventilation leads to a constant increase of hydrogen concentration in the metering cabinet. This has implications for managing the risks associated with high hydrogen concentration levels because of hydrogen leakage. It was found that sensors located at the top-center of the metering cabinet showed the highest concentrations. With closed ventilation, the alarm level at 10 %LEL hydrogen concentration is sufficient to provide early detection.

Ventilation causes changes in the distribution mechanism, resulting in better mixing of the hydrogen which reduces its concentrations. With open ventilation, the hydrogen concentration levels to trigger the alarm inside the metering cabinet should be lowered. Based on the results gathered, it is advised to set the alarm to trigger in the event of hydrogen concentration levels reaching 5 %LEL hydrogen concentration.

Moreover, the release of hydrogen gas leads to a more buoyant gas mixture that rises quicker and mixes more easily with the surrounding air compared to a methane leakage. The time required for the methane gas to reach the sensors at the top-center of the cabinet was three times longer than in the event of a hydrogen leakage. In open ventilation conditions, similar response times for both methane and hydrogen gases close to the leakage were found. Finally, further research on worst-case scenarios is relevant to make specific recommendations for safe and economically feasible residential heating appliances.

Contents

List of Figures

List of Tables

Acronyms

AC	Acoustic
ANSI	American National Standards Institute
Atm	Standard atmospheric pressure defined as 101325 Pa
bar	Unit of pressure defined as 100000 Pa
bara	Unit of absolute pressure
CFD	Computational fluid dynamics model(ling)
CH_4	Methane
CO	Carbon monoxide
CO_2	Carbon dioxide
DIN	Deutsches Institut für Normung (German institute for standardization)
EC	Electrochemical
H_2	Hydrogen
H_2O	Water
IEC	International Electrotechnical Commission
ISO	International Organization for Standardization
LDL	Lower detection limit
LEL	Lower Explosion Limit
LFL	Lower Flammability Limit
mbar	millibar unit of pressure
MCA	Multi-Criteria Analysis
MCDM	Multi criteria decision-making method
MEMS	Micro Electro-Mechanical System
MFC	Mass flow controller
min	Minutes
MOS	Metal-oxide semiconductor
MOX	Metal-oxide
NEN	Nederlandse Norm (Dutch standard)
NFPA	National Fire Protection Association
OPT	Optical
PE	Polyethylene, material of pipe (plastic)
ppb	Parts per billion
ppm	Parts per million
PVC	Polyvinyl chloride, material of pipe (plastic)
QCM	Quartz crystal microbalance
Re	Reynolds number
TC	Thermal conductivity
vol	Volume
WPM	Weighted product model
WSM	Weighted sum model

1

Introduction

1 Introduction

In the universe there is plenty of hydrogen around us. Almost 74% of the weight of the universe exists in the form of hydrogen. On earth, however, hydrogen is normally not found in gaseous form in nature but is bound to other elements and form water, for example.

Hydrogen is the lightest element with a low density, making it lighter than air. It is a very buoyant gas, meaning that when it is released into the air, it rises quickly and rapidly mixes with the ambient air. Hydrogen gas is considered an ideal gas over a wide temperature range and even when stored at high pressures. The molecules of ideal gasses do not attract or repel each other. In standard conditions (ambient temperature and pressure) it is a non-toxic, colorless and odorless gas [1].

Hydrogen gas is also highly versatile in use. In the future it could be widely used for energy storage and for the transportation of energy. In fuel cells the hydrogen could be used for electricity generation, for example in the residential sector to provide electricity or in the transportation sector to power hydrogen vehicles. Hydrogen could also be burned and used as a heat source in heating systems for buildings. Besides, it is an important fuel and feedstock in the industrial sector. Hydrogen gas could play a major role in the energy transition as it is an important energy carrier thanks to its high energy density per weight.

When hydrogen is produced using renewable energy sources such as wind and solar energy, it is called green hydrogen. Green hydrogen is mainly produced through electrolysis (Figure 1-1), whereby water is split into hydrogen and oxygen, after which the hydrogen could be used as a fuel to convert back to electricity or heat. No CO_2 will be emitted the only by-product is water(vapor).

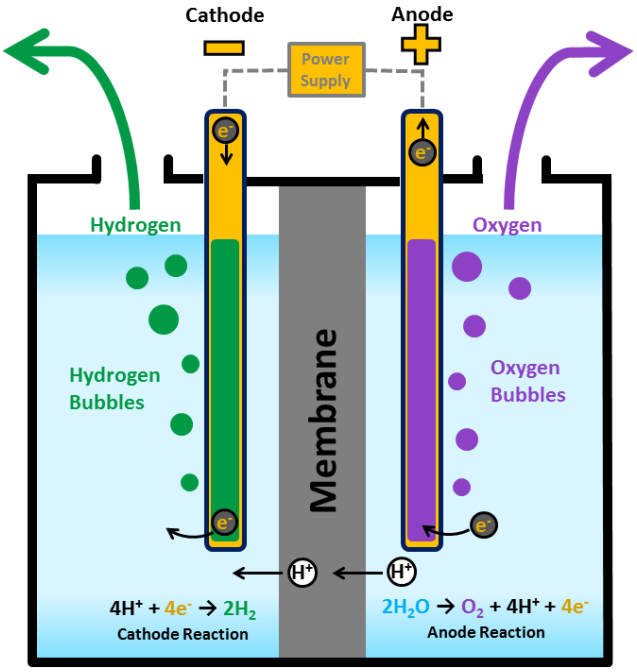

Figure 1-1 Schematic of an electrolyser process to produce green hydrogen (and oxygen) from electricity [2].

Nowadays a major share of hydrogen is produced as grey hydrogen in the industrial sector. This type of hydrogen is produced through methane reforming of hydrocarbon fuels, thereby emitting CO_2.

Blue hydrogen, meanwhile, is produced in a way which is better for the environment than grey hydrogen. The emitted gas, including CO_2, is captured and re-used or stored underground (or underseas). For instance, captured CO_2 can be stored in empty gas fields or under the North Sea [3].

In the future, green hydrogen production is preferred being the most sustainable. Hydrogen production from renewable resources got more attention. The production of green limits the emission of CO_2 when the electricity is generated fully out of renewable energy sources.

To use hydrogen in all of its diverse applications it has to be stored and transported. Hydrogen can be either stored in gaseous form under pressure or as a liquid at extremely low temperature (-253 °C). Hydrogen storage facilitates energy demand to compensate fluctuation of electricity intermittency of renewable energy. The storage of energy is important to structurally have enough energy, even when there are periods with less wind or sun to produce enough renewable energy. At peak moments the stored hydrogen can be turned into electricity without the need for burning fossil fuels. An option for the short term could be energy storage in batteries. Where hydrogen especially is important is for long-term (seasonal) storage. An example could be that a high amount of energy is needed in winter, but there is not enough generation by the solar panels. In the summer, however, a lot of extra generation was available which has been converted to hydrogen and then later used in winter.

These applications of hydrogen storage range from a small system that is meant for households or to replace a battery, up to larger (megawatt) systems that are designed to supply power in electricity grids for a whole village.

1.1 Background - Hydrogen heating

At the residential level, if we want to reach to net zero emissions by 2050 then we must also reduce or remove the carbon emissions from the heating of water and homes (particularly during the winter season). Hydrogen gas is used for heating residential buildings using a hydrogen boiler (Figure 1-2) whereby hydrogen gas is burned in the boiler to heat the residential building.

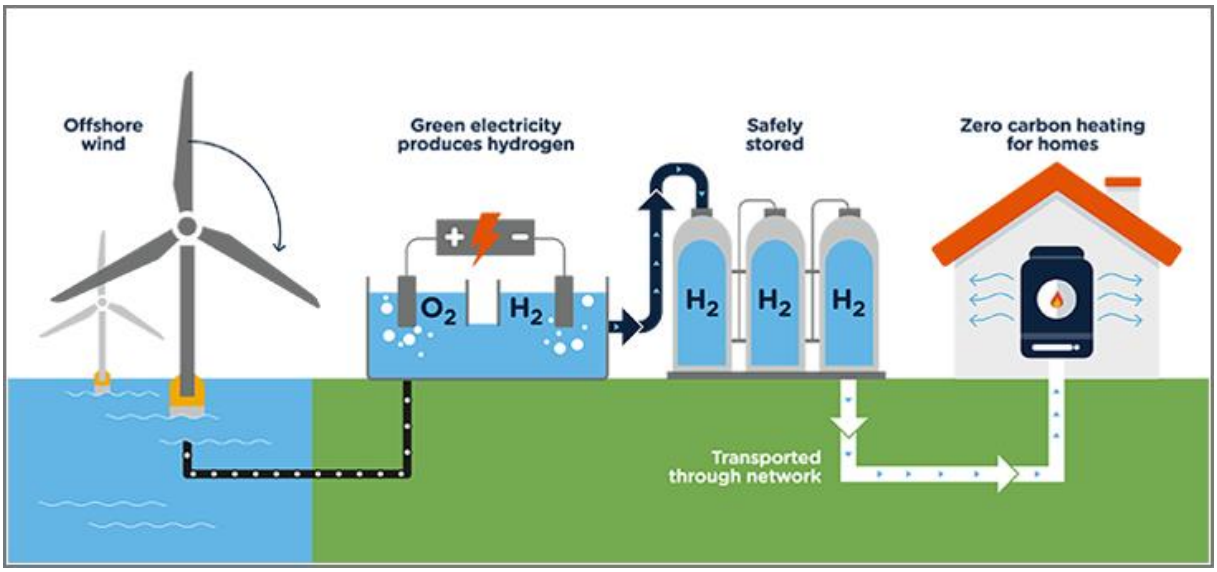

Figure 1-2 Schematic of the generation and supply of green hydrogen (SGN H100 Fife project) [4].

Regarding boilers, part of central heating units in new-built houses, future generations are considered as 'hydrogen ready', meaning the newest boilers can operate both on natural gas as well as hydrogen. In the early 2020s, these hydrogen ready boilers are not yet on the market in the Netherlands.

An electric heat pump is an alternative solution to heat the house in the future. It uses a vapor compression system which is used to extract heat from the surrounding air. Electricity is used to distribute this heat around the house. This is the same principle as used in a refrigerator that moves heat. The electric heat pump moves heat during the heating season from the cool outdoors into the house to get it warm and during the cooling season, the heat goes from the cool house to the warm outdoors [5].

There are water-source heat pumps that also circulate water through underground pipes. This way they are very energy efficient during extreme weather conditions [6]. But for it to work best the rest of the house needs to be very well insulated. Large fluctuations in the temperature should be prevented. The heat pump does not adapt very quickly to the outside climate. If it is freezing during the morning and later in the afternoon there are clear skies with a lot of sunshine, the change would likely be too large for a heat pump. A gas boiler however would just burn more or less amounts of gas when it needs to and withstand every situation.

Green hydrogen gas could be a good option for older buildings and historical city centers. At these locations a connection to a low temperature heat network is not possible. Or an electric heat pump is not a possibility. These buildings are not able to have good insulation. The old buildings could also be monumental buildings that do not allow big changes made to the building. Therefore, they still rely on heating with gas [7].

This applies to old houses that have been built before 1980. The insulation of these older houses just is not good enough. Therefore, they are hard to warm with electric heat pumps [8]. Hydrogen boilers would be a good solution for these older houses to replace the CO_2-emitting natural gas boilers with a sustainable hydrogen boiler.

Next to these two options, a third type is available. This is an electric heat pump including a hydrogen boiler called a hybrid heat pump boiler. Hydrogen will be used as back up and supports the heat pump when there is a peak in the demand. This way it could also help to prevent the electricity grid from overloading and failing.

1.2 Background - The gas network

In the past we have used hydrogen in our Dutch homes before. Until the 1960s the use of “town gas”, a mixture out of which 50 % hydrogen that was made by the thermolytic heating of coal. Later Natural gas became the most important gas used after the discovery of big natural gas reserves in Groningen and forced the “town gas” out of the market [9].

At present, the Netherlands has an advanced natural gas network throughout the country. Gas network providers Liander and Stedin stated that 90 % of residential buildings have a connection to the natural gas grid [8].

Plans are there to make the current natural gas grid suitable for the distribution of hydrogen. There are several projects going on to test the hydrogen in the built environment. The suitability of the gas network is researched on the changes that have to be made to the grid, the safety and the cost. The government wants to make distribution of gas affordable; they want to monitor the safety and have a balanced market. They also want to provide space to network providers to make investments.

The network providers all work together in their research and share the knowledge they have. Without doing this the hydrogen network would not get off the ground and it would be difficult to make a bigger grid [10].

Currently, it is still not possible because of legal aspects to have hydrogen flowing through the existing gas grid. But, from a technical perspective it is advancing rapidly. Likely, this happens in steps in the future. First a hydrogen so called 'backbone' is going to be constructed. It will connect the important industrial locations of the Netherlands. And the import and export connections to the neighboring countries will be made to make the exchange of hydrogen possible from 2030 [11].

Kiwa [12] concludes that the materials from the current gas network are suitable for hydrogen. Existing gas network infrastructure can be used for the transportation of hydrogen. The main materials used for pipeline are PE (polyethylene) and PVC (polyvinyl chloride).

The costs are still a subject of discussion. The advantage of a gas network is the transport of big volumes of energy at fairly low cost. The yearly extra costs for containing the gas grid happens to be in the range of 5-10 euro per home equivalent per year.

There is still a lot of research going on around transporting hydrogen through the same natural gas grid. The government has to make well thought choices [13].

1.3 Background – Hydrogen safety

Safety is an important aspect to keep in mind if someone is working with hydrogen. But this is true for all types of energy and gases. When does hydrogen gas become flammable and what properties do affect safety? To get more insight, the characteristics of hydrogen are compared to natural gas.

1.3.1 Hydrogen compared to natural gas

The density of gaseous hydrogen is only 0.0813 kg/m^3, while methane has a density of 0.657 kg/m^3 [14]. The largest substance as a fraction that is present in natural gas is methane gas (82 %) [15]. The energy density per weight (per kg) of hydrogen is higher than methane, but it has a low energy density per volume (per m^3) compared to methane (see Table 1-1). This also implies that even if there is a higher leakage rate of hydrogen it does not mean that the amount of energy that leaks is also high. The determination of the energy densities is dependent on two other properties in Table 1-1 (between brackets). Depending on the heat produced by a complete combustion of the gas that is measured, they are expressed as the HHV (higher heating value) and the LHV (lower heating value). Both are a unit of energy per unit mass or volume of the substance.

Hydrogen is highly flammable. The lower flammability limit (LFL) or lower explosion limit (LEL) of hydrogen is 4.0 volume% or mol% and the upper explosive limit is 75 volume% (in air). This is the concentration at which the gas and air will result in a flammable mixture at given. Regarding the terms LFL and LEL, both are used in the literature and have a similar meaning. Hydrogen has a wider flammability range in air (4 vol% - 75 vol%) in comparison to methane (5 vol% - 15 vol%), which increases the explosion risk.

In case of a leak, the hydrogen has higher leakage flow rates than natural gas. It is due to the small size of the H_2 molecule and a low viscosity (8.8 * 10^{-6} Pa·s). The H_2 leakage through small gaps in fittings or seals is higher than natural gas leakage (with methane viscosity of 11.0 * 10^{-6} Pa·s [16]).

Because the density of hydrogen is the lowest at standard conditions in comparison to other gases, it therefore has a high buoyancy. Hydrogen gas is about 14 times lighter than air in normal conditions compared to 2 times for methane (Table 1-1). This high value for the buoyancy of hydrogen helps with respect to hydrogen safety concerns. Because in open environments hydrogen could easily escape.

This makes it safer in these conditions than natural gas. In the case of a hydrogen leakage inside a confined space, after accumulation on the top, it rapidly mixes with air [1].

Table 1-1: Properties of hydrogen and methane (adjusted) [14].

Property	Unit	Hydrogen	Methane
Density (gaseous)	kg/m^3 (25 °C, 1 bar)	0.0813	0.657
Density (liquid)	kg/m^3	71.14 (−253 °C, 1 bar)	422.6 (−162 °C, 1 bar)
Boiling point	°C at 1 bar	−252.76	−161.6
Mass energy density	MJ/kg (HHV) MJ/kg (LHV)	141.8 120.0	55.5 50.0
Volume energy density (25 C, 1 bar)	MJ/m^3 (HHV) MJ/m^3 (LHV)	11.54 9.76	36.46 32.85
Auto-ignition Temp.	°C	500	580
Flammability limits	% in air by volume	4%–75%	5%–15%
Ignition energy	MJ	0.02	0.28
Buoyancy	Relative to Air	14 × lighter	2 × lighter (natural gas)
Rising speed in air	m/s	20	3.3 (natural gas)

1.3.2 Safety guidelines and standards

To distribute guiding on safety, safety standards were created. A standard is a set of guidelines and definitions and instructions for system designers, manufacturers and users. It is developed by a number of experts in the field and by national and international standard organizations, such as ISO, NEN, IEC, NFPA, ANSI and DIN.

The following part is a summary of some important takes on the Safety Standard **NPR-ISO/TR 15916 (2015)** [17] containing the basic considerations for the safety of hydrogen systems. Hydrogen systems should always be installed and located according to the specific requirements found in relevant safety standards. Because of the lightness and size of hydrogen molecules, they pass through smaller leaks and rise faster than other gasses because of its greater buoyancy [1]. When the gas is present in a confined space the gas accumulates in high spots and could reach concentrations above the limit that it can ignite (4.0 vol%). Therefore, hydrogen leaks should always be prevented in piping systems with proper sealing.

The hazards caused by the flammability of hydrogen are: Thermal effects, pressure effects and easy ignitability of mixtures with air. The main hazard in the application of hydrogen systems is the uncontrolled combustion of accidentally released hydrogen. This only happens when a leakage forms combustible mixtures under favourable circumstances (air is present and a source of ignition). Upon release of compressed hydrogen, strong pressure effects can be generated. When hydrogen flow into the air cannot be avoided, the formation of ignitable mixtures should be prevented no ignition sources should be present.

1.3.3 Environmental effects of hydrogen

There are less effects to the environment when using hydrogen systems compared to natural gas systems. Hydrogen boilers do not emit any CO_2 unlike natural gas boilers (Table 1-2). Then, there is a safety concern when incomplete combustion of natural gas takes place, CO is emitted. Above a concentration of 150 to 200 ppm the inhalation of CO gas is lethal [18]. In hydrogen boilers, no CO is emitted. The emission of NOx happens for both hydrogen and natural gas. However, in case of hydrogen the amount is less. The emission specifications as well as the efficiency and the heat output for both hydrogen and natural gas boilers are found in Table 1-2.

Table 1-2: Remeha Hydra boiler specifications for hydrogen and natural gas [19].

	Unit	**Hydrogen**	**Natural gas**
CO_2	g/kWh kg/year*	0 0	190 2500
CO	ppm	0	48
NOx	Mg/kWh Hs	20	30
Efficiency**	% LHV % HHV	115 97	108 97
Output Heating	kW	24	24

* At average gas consumption ** Temperature retour = 30 °C, 30 % load

1.4 Relevancy of this study - Hydrogen sensors

The presence and use of pure hydrogen inside residential buildings will require safety measures. If there are any leaks present, then they are difficult to detect. Hydrogen is colourless, odourless and tasteless and burns with an invisible flame. A good way to detect hydrogen is by using hydrogen sensors. To ensure safety inside the house, hydrogen sensors will find their application and there will be a growing demand for hydrogen detectors. The dedicated sensors should be mounted at the right location for the sensor to detect the leak as soon as possible.

The high hydrogen concentrations can be caused by leaks from hydrogen equipment like boilers and fuel cells or from piping in the distribution network. Hydrogen, being the smallest molecule and the lightest element, can leak through very small cracks and holes at high leakage rates. This higher leaking risk makes the need of a safety system more crucial. The monitoring enables a better understanding of the leakage behavior of hydrogen and helps the prevention of ignitable gas mixtures.

In the near future, the market for residential hydrogen sensors could likely be quite large. The future deployment of hydrogen sensors can be comparable to home CO detectors nowadays. These CO detectors are priced well below €80 ($100) [20].

The hydrogen sensors should satisfy a number of characteristics to ensure the safety and reliable response to any leaks of hydrogen gas. Based on the system a sensor should take action as alarming or shutting down the system at a high concentration of hydrogen.

What are the most important characteristics of given hydrogen sensors and how would the most appropriate ones for residential use be selected?

Requirements for a reliable hydrogen gas sensor are the following [21]–[23]:

- Detection of gases with precision and accuracy in ppm range.
- Sensitively detect small hydrogen leakages (0.01 vol%) to moderate level of gas concentrations [23]. It should have good sensitivity well before the Lower Explosive Limit (LEL) of 4.0 vol%.
- A fast response time under 2 seconds is desired to trigger the sensor for an early warning.
- The lifetime of hydrogen sensors is defined as the maintenance and replacement period according to the application.
- Calibration of the sensor is needed annually. But hydrogen sensors should be operational without cleaning, frequent calibration, or replacements in the local environmental conditions.
- Good stability of the sensor is necessary for the long term and it should have consistent reproducibility.
- Low power consumption could also influence the choice of the sensor type (preferably less than 100 mW).
- Other unfavorable operating conditions, such as high pressure (800 mbar) or temperature (-30 to 80 °C), should also not cause problems to the sensors.
- The sensors should have minimum interference with other gases. The selectivity of the sensor must be adequate so that it indicates the presence of hydrogen specifically. It should respond to the target gas without the influence of other present contaminants. This way it will not lead to false alarms of the sensor.
- The cost of the used technology should be justified. This includes the purchase, installation, calibration and maintenance.

In this thesis, the abovementioned requirements will be used to evaluate the sensors. The next section continues with the objective of this study.

1.5 Research objective and research questions

More research is needed on how to safely use hydrogen in houses and the built environment. The objective of this thesis is to contribute to the assessment and design of a hydrogen leakage detection system in residential buildings. With a better understanding of the behaviour of a hydrogen leakage inside a closed space, this research will provide insight in the way hydrogen sensors should be applied in a residential setting.

The research objective is formulated as follows:

Evaluation of hydrogen sensor technologies for residential safety and determination of the sensor location with the fastest response to high hydrogen concentrations inside a metering cabinet.

This main objective can be fulfilled by dividing the thesis structure into two parts. The first part is an evaluation of the different hydrogen sensor technologies. The second part is an assessment of an experiment of the behaviour of a hydrogen gas leakage inside a metering cabinet.

The main objective is answered with three sub research questions. It is divided into the following questions:

1. **What type of hydrogen sensor technology is most suitable based on the relevant criteria for residential use?**
2. **What location of the hydrogen sensor shows the fastest response to high hydrogen concentrations inside the metering cabinet?**
3. **Which conditions lead to the highest risk of hydrogen leakage inside the metering cabinet?**

The method used to answer these questions is the following. Sub-research question 1 is addressed by doing literature research on the different hydrogen sensor technologies. Furthermore, a multi-criteria analysis was performed to find out which sensor technology is the best suited for the residential application.

To gain more knowledge of applying these sensors, experimental research was carried out with support of the company Kiwa Technology in Apeldoorn. To answer sub-research questions 2 and 3, measurements in various conditions were performed on the set up of a Dutch metering cabinet. Attempted is to find the difference in concentration levels of hydrogen by putting several hydrogen sensors in strategic places inside the metering cabinet. The answers to these questions will be discussed during this thesis research report.

1.6 Outline of this thesis

This thesis has started off with an introduction leading to the research objective and sub research questions. It will continue in two parts. The first part focuses on an evaluation of different types of hydrogen sensor technologies. The second part consists of the theory of hydrogen in a closed space and an experimental study of a hydrogen leakage inside a metering cabinet.

The first part, chapter 2, starts off with an evaluation of different available sensor technologies used to measure hydrogen. Afterwards, these technologies are assessed in an analysis based on selected performance criteria found in previous research on commercially available hydrogen sensors.

The second part of this thesis, starting off with chapter 3, begins with the theory of hydrogen gas dispersing into a closed space. The fourth chapter discusses the experimental methods of the study on the behaviour of hydrogen gas in a metering cabinet. Subsequently, the fifth chapter contains the data and figures of the experiment results, followed by the discussion of these results. This thesis report ends with the conclusions and recommendations for future research in respectively the sixth and seventh chapter.

2

Evaluation of different hydrogen technologies

2 Evaluation of different hydrogen sensor technologies

Hydrogen gas sensors are devices that detect the presence of hydrogen in the air, producing an electrical signal that is proportional to the measured hydrogen concentration. There are many different types of hydrogen sensor technologies commercially available or in development. Most hydrogen sensing principles have already been known for decades [23].

Hydrogen sensors are continuously redesigned and improved over the past years [24]. Nowadays, even detection on ppb (parts per billion) level of hydrogen gas concentration is possible [22]. There are different kinds of hydrogen sensors, each with its own way of measurement. Some measure by a change in physical properties, others work chemically or mechanically.

2.1 Hydrogen sensor technologies

2.1.1 Thermal conductivity

The first type of sensor reviewed is the thermal conductivity sensor. Thermal conductivity is a property of each type of gas: the amount of heat loss depends upon the thermal conductivity of the surrounding gas. The thermal conductivity of hydrogen is 0.174 W/mK at 20 °C compared to 0.026 W/mK of air [23]. The difference between these numbers, which is reasonably large, allows the measurement of the concentration of hydrogen in air. If the hydrogen concentration in air increases, so will the heat dissipation due to the increase in thermal conductivity of the medium.

The measuring principle of a thermal conductivity sensor involves the measurement of the heat loss from a hot body to the surrounding gas [22]. It works with an electrically heated sensing element (as seen in Figure 2-1 and Figure 2-2).

An existing type of this sensor is a pellistor-like sensor that has two parts of resistors, an electrical component that creates resistance in the electrical circuit. One part of these resistors is dependent on temperature, called a thermoresistor. One part is exposed to the measured gas and the other contains a reference gas which is usually air. With these parts, it measures the thermal conductivity of a sample gas and compares it to the thermal conductivity of the reference gas. If both cells of the sensor only contain air, the resistors lose heat equally and give the same reading. Depending on the type of gas running through the cell, the heat loss of the resistor will differ from the air resistor. When the target gas, hydrogen, enters the measuring cell, the heat loss will increase [22], [23].

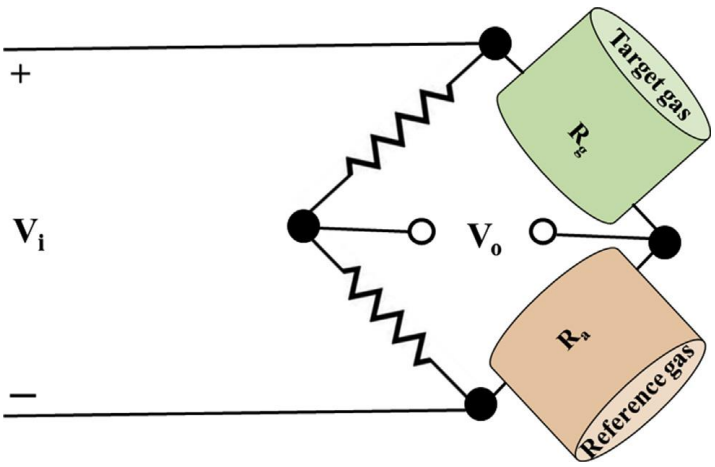

Figure 2-1 Global schematic for a thermal conductivity sensor [22].

The sensor detects the change in thermal conductivity by the sensing elements, also called thermistors. These lose heat to the surrounding gas at a rate that is proportional to the thermal conductivity. The equilibrium temperature of the sensing element after the heat loss determines the electrical resistance of the element. The change in electrical resistance is the final signal from the sensor and is proportional to the hydrogen gas concentration [25], [26].

The sensors are connected in a Wheatstone bridge circuit (Figure 2-2). A Wheatstone bridge is an electrical circuit that is used to measure the unknown electrical resistance with two other resistances contained in two legs of a bridge circuit [27]. The output signal will be the change in resistance that is caused by the resulting heat loss difference.

Another variant of a thermal conductivity sensor has a design without using a reference cell. The detection is based on the heat lost compared to a test gas. It works by using a reference point that is set at the moment when the target gas is absent [21].

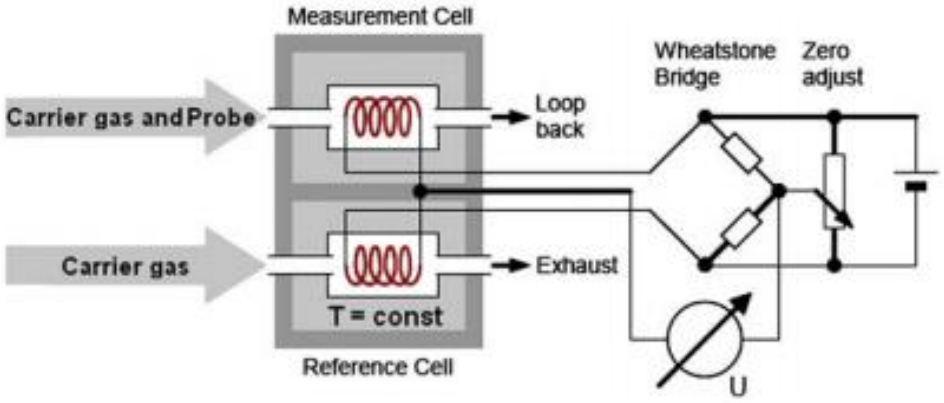

Figure 2-2 Thermal conductivity hydrogen gas sensor in a Wheatstone bridge circuit [28].

2.1.2 Catalytic

Catalytic sensors are based on gas oxidation on the surface of an electrically heated element, called a sensor bead which is coated with a hydrogen sensitive catalyst material. Catalytic sensors are built according to the principle of heat release from the oxidation reaction with oxygen of a combustible gas at the surface of the catalyst [22], [29].

The oxidation uses oxygen from the air and the reaction causes an increase in temperature of the sensing element. Because hydrogen is a combustible gas it will release heat (the combustion energy of hydrogen gas is 141.9 kJ/g) [22], [30]. The heat is proportional to the concentration of the hydrogen that is present. This heat will increase the temperature of the wire coil which increases its resistance.

The most common type of this sensor, same as for thermal conductivity sensors is of the pellistor type which is a combination of the words pellet and resistor [23]. Here, there are two resistor beads present where one of the beads is coated with a hydrogen-sensitive catalyst material and the other is used as a reference element for the ambient conditions (Figure 2-3).

An electrical current is passed through the coil in the ceramic beads which heat it up to approximately 550 °C [24]. At these high temperatures the hydrogen gas molecules get adsorbed on the surface of the catalyst. The adsorbed gas molecules get oxidized by the adsorbed oxygen and form water molecules [22]. This is an exothermal process as the gas oxidation of hydrogen produces a temperature increase of the catalyst bead. After that, the increase in the temperature of the active bead causes a change in the electrical resistance of the platinum wire inside. Consequently, the increase in resistance is measured as an electrical signal.

A Wheatstone bridge circuit is created to which both the beads are attached (see Figure 2-3). This way, the resistance change can be measured. If the resistance of the measuring resistor bead is not the same as the reference bead, then a resistance imbalance is measured. This resistance imbalance in the Wheatstone bridge can be considered a signal of the presence of hydrogen.

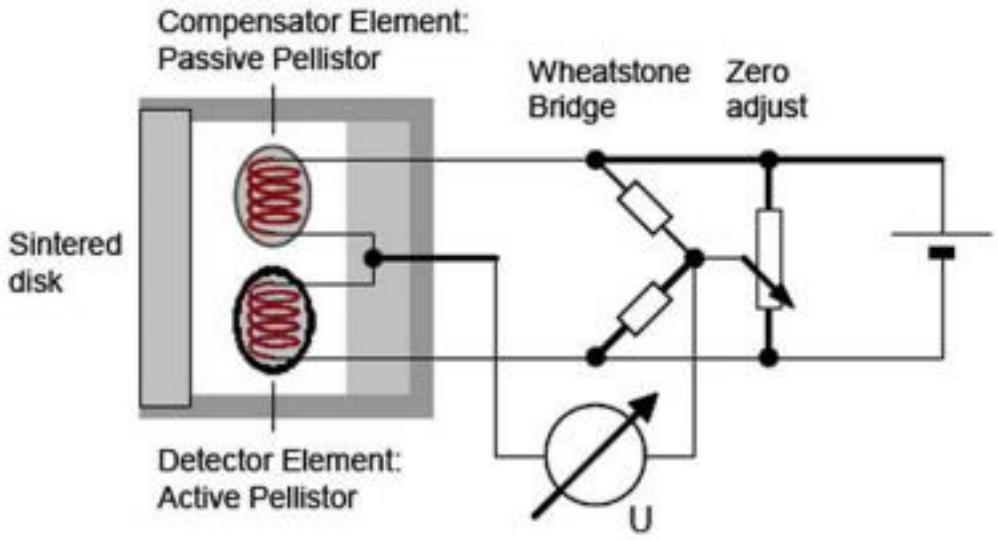

Figure 2-3 Schematic of a catalytic hydrogen gas sensor in a Wheatstone bridge circuit [28].

A second type of this sensor is the thermoelectric type catalytic sensor [23]. The same principle is involved, however, this sensor uses the thermoelectric effect to directly convert the temperature difference to electrical voltage. The temperature differs in two points of the conductor. The part that corresponds to these to points also has a different voltage. The oxidation reaction due to the presence of hydrogen increases the temperature at the active part of the sensor. This way the sensor also generates the desired electrical signal proportional to the hydrogen concentration.

2.1.3 Electrochemical

Electrochemical sensors operate on the principle of electrical current that is caused by electrochemical reactions at its electrode surfaces. Electrochemical sensors detect changes in charge transport of electrons, or the electrical properties caused by these electrochemical reactions.

The sensing electrodes (cathode and anode) are placed in an electrolyte medium. The electrolyte with an electrolytic solution allows ion transport between the electrodes. It has a similar working principle to batteries. The reactions take place at the surface of the electrodes coated with a catalyst.

The hydrogen gas gets oxidised at the sensing electrode according to the following equation:

$2H_2 \rightarrow 4H+ + 4e-$

It releases electrons and therefore its potential changes. At the other electrode, reduction of oxygen takes place with the following reaction:

$O_2 + 4H+ + 2e- \rightarrow 2H_2O$

The electrons flow from the anode to the cathode (see Figure 2-4). The amount of electric current that is flowing depends on the hydrogen gas concentration that is measured [23]. More hydrogen means more electrons are generated.

Electrochemical sensors can be of amperometric type or potentiometric type depending on the signal that results from these sensors [22]. Amperometric sensors work at a constant applied voltage and measure the current. Hydrogen gas diffuses through the porous membrane and is oxidized at the sensing electrode. [24] The flow of electrons from the anode to the cathode causes an electric current, which is proportional to the hydrogen gas concentration [23].

Potentiometric sensors are different from amperometric sensors in the way that they operate at zero current. They measure the potential or voltage difference between the electrodes [23]. This value of the electrode potential is related to the hydrogen gas concentration.

The structure of potentiometric sensors is similar to the amperometric type. It consists of an electrolyte and two electrodes made from noble metals, such as palladium, platinum, gold or silver [23].

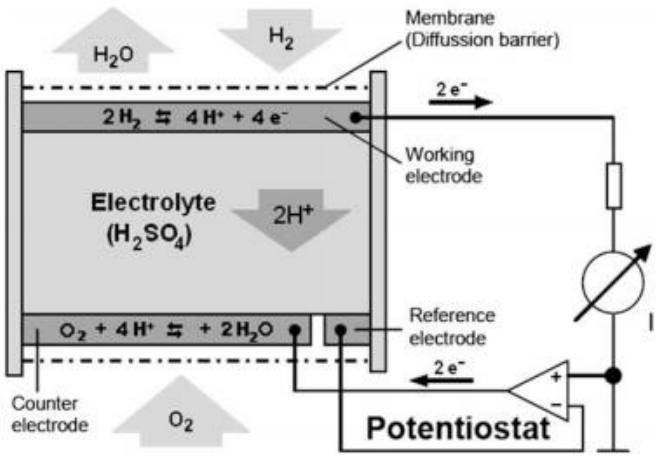

Figure 2-4 Schematic of an electrochemical hydrogen gas sensor [28].

2.1.4 Metal - oxide

Another type of hydrogen sensor are the metal-oxide sensor (MOX sensor) and metal oxide semiconductor sensor (MOS). They have a surface interaction between the hydrogen gas and a gas-sensitive semiconductor. A metal-oxide film that has sensitivity towards hydrogen gas, is applied on a substrate material between two electrodes (Figure 2-5). The interaction that proceeds, changes the conductivity of the semiconductor and this measures the concentration of hydrogen gas [25].

Metal oxide based semiconducting materials mostly respond through a change in resistance in the presence of hydrogen gas. Semiconductor hydrogen sensors typically measure resistance changes under a fixed applied voltage. Some metal oxides have been found to work at a relatively high temperature with the need for a heating element (Figure 2-6) [22].

The reactions taking place inside the metal-oxide sensor that provide the sensing mechanism are as follows. First, oxygen is adsorbed on the surface of the metal oxides and captures free electrons:

$O_2 + 2e^- \rightarrow 2O^-$

Second, because of these captured free electrons, the conductivity of the material reduces or the resistance increases. If there is hydrogen gas present, the adsorbed oxygen reacts with adsorbed hydrogen molecules. The product of the reaction is a water molecule and at the same time a free electron gets released:

$H_2 + O^- \rightarrow H_2O + e^-$

Again, the electrical signal that is produced by the sensor is again connected via a Wheatstone bridge (Figure 2-6).

2.1.4.1 N-type and P-type

Most of the metal oxide based semiconducting sensors are defined as n-type meaning the charge carriers are electrons (n refers to negative charge carriers). They will show a decrease in resistance in presence of hydrogen gas. However, there are also some p-type semiconducting materials for sensors. The p-type semiconducting materials have holes (p refers to the positive charge carriers) as the important electron distributor, so they are called the majority charge carriers. If hydrogen gas is present, the release of captured electrons results in the recombination of a hole and an electron. In this case the resistance of the p-type material increases [22]. The previously mentioned reactions decrease the resistance in n-type material and increase the resistance in p-type material.

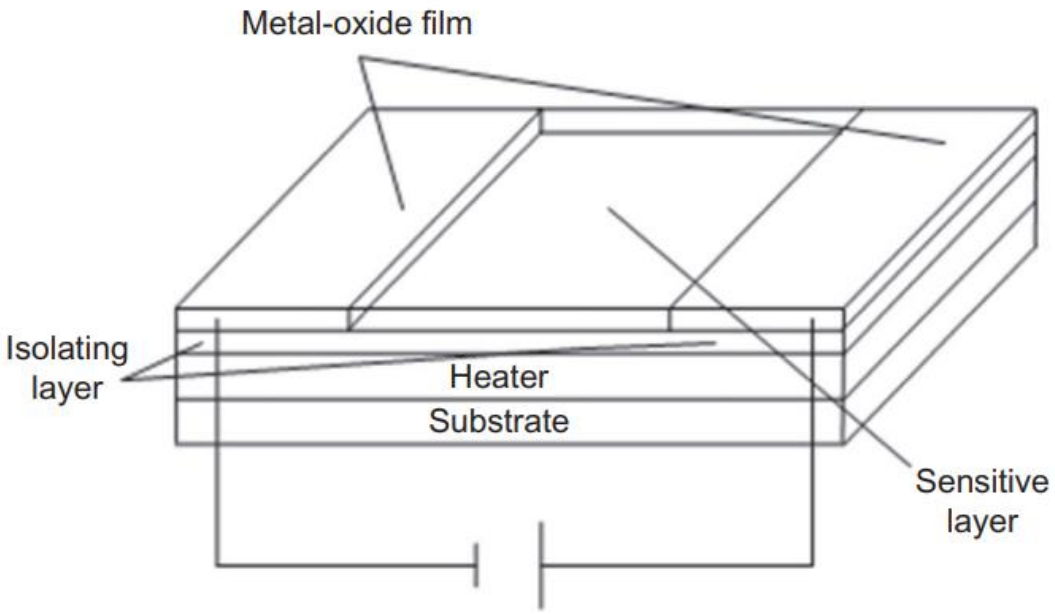

Figure 2-5 Global schematic of a metal-oxide hydrogen gas sensor [25].

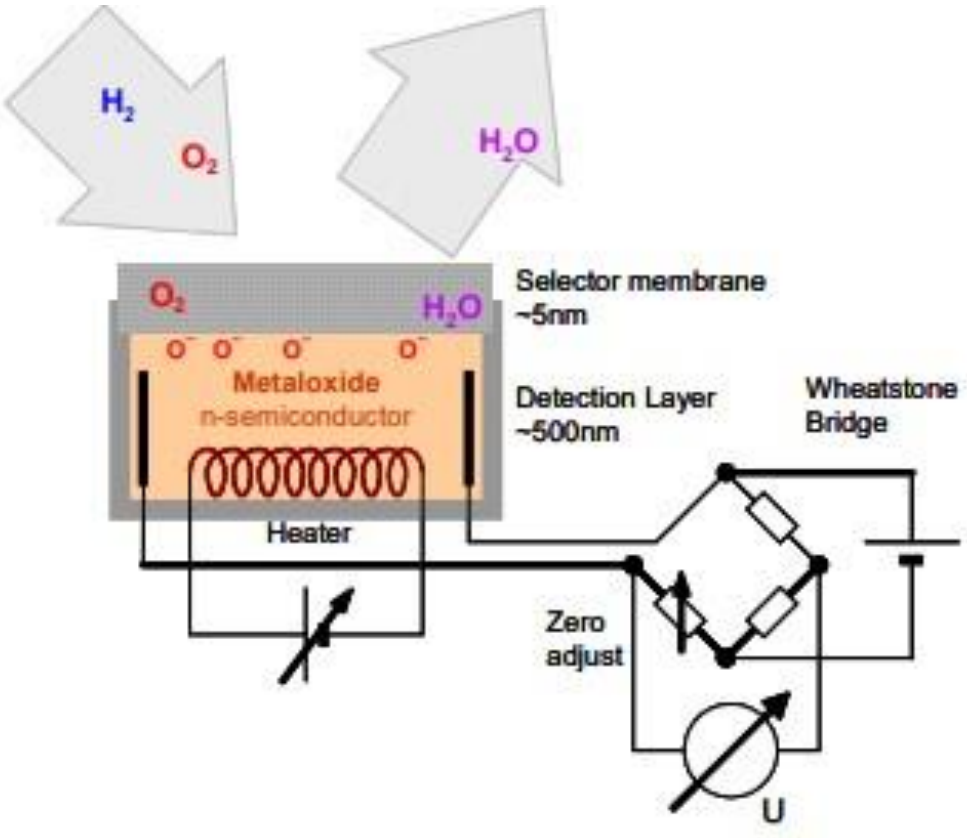

Figure 2-6 Detailed schematic of a metal-oxide hydrogen gas sensor in a Wheatstone bridge circuit (adjusted) [31].

2.1.4.2 Work function based

There are also types of Metal-oxide sensors with a different working principle. They have the same three layers: metal, oxide and semiconductor (MOS) structure. But this type of sensor is based on the change of the work function caused by hydrogen molecules. The work function is the minimum energy required (which is typically measured in electron volts) to remove an electron completely from the surface of a metal [22], [23]. Hydrogen gas atoms diffuse through the metallic layer and get adsorbed at the interlayer of metal and the oxide. The hydrogen atoms get polarized at this stage which changes the work function of the metal. This change in work function is measured as voltage change and indicates the presence of hydrogen gas [22].

2.1.5 Mechanical

A mechanical sensor is based on the fact that the measurement method of the sensor involves a material that changes its physical property. An example of such a material is palladium, which is sensitive to hydrogen gas. A thin film of palladium is coated over one side of the sensor, forming a microcantilever. This film absorbs hydrogen gas into interstitial sites of the metal surface causing it to expand. The expansion of the volume on the absorption of hydrogen takes place only at the surface but does not take place at the substrate on which the film is coated. The induced stresses cause mechanical bending or curvature of the cantilever (see Figure 2-7). The result is a deflection or bending of the microcantilever [22], [23].

This sensing technology has a lot of disadvantages such as complex fabrication and delamination of the coating. Also, the application of mechanical sensors is only suited in the case when gas selectivity is not an issue. The sensor gives a signal for more than one gas [22].

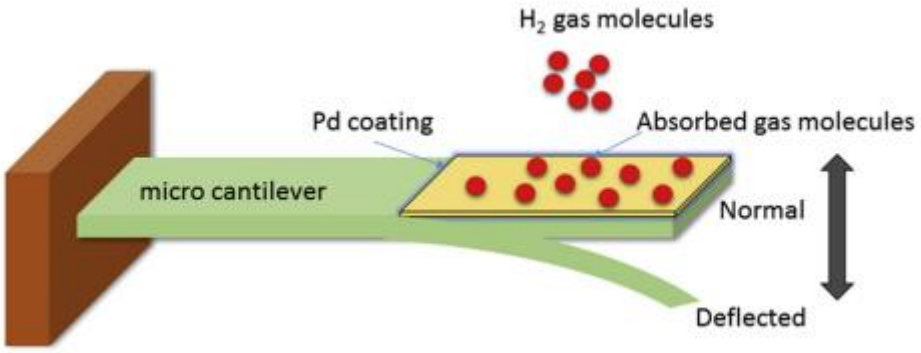

Figure 2-7 Schematic of a microcantilever mechanical hydrogen sensor [22]

2.1.6 Optical

Optical type sensors use an optical signal originating from an optically active material. Optical sensors use materials that change properties when they absorb hydrogen gas molecules. This phenomenon can be used as a means of hydrogen detection. Many types of optical sensors exist. But the main type is where the device is based on optical properties of palladium films (see Figure 2-8). An optical fiber cable is coated along a small part of its length with palladium. When this metallic palladium coating is exposed to hydrogen gas, it stretches the fiber as it gets expanded axially and radially. The reflectivity of the palladium surface changes at the place where hydrogen molecules get absorbed. When a light beam is passed through the optical cable and received back, there is a change in its optical path and therefore its reflectivity. This value of reflectivity can be linked to the concentration of hydrogen gas [22], [23].

The optical signal can be measured with various techniques such as interferometric and reflectivity measurements [25]. An interferometer operates by splitting a light beam into two parts, a reference and the sensing beam. This sensing beam is changed by the variable to measure. The creation of an interference pattern gives information about the desired measurement variable.

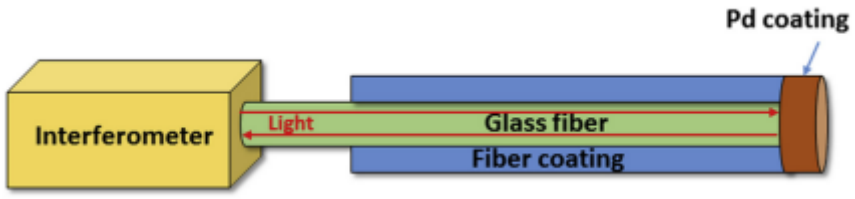

Figure 2-8 Schematic of an optical hydrogen gas sensor, interferometer and Pd reflector [22]

2.1.7 Acoustic

Acoustic gas sensors detect changes in the properties of acoustic waves. The surface-generated acoustic waves can be measured and be linked to the hydrogen concentration in the sensor's area. The working principle of acoustic gas sensors are based on the detection of changes in the properties of acoustic waves by using an adsorbate on a piezoelectric material. A change in the mechanical properties of the piezoelectric material happens due to the adsorption of hydrogen gas molecules.

A quartz crystal microbalance (QCM) is one of the devices to measure acoustic waves. A QCM has a small and thin quartz disc with electrodes on each side (see Figure 2-9). These are used to cause deformation in the structure and result in resonance in the disk. Gas molecules get adsorbed on the surface of the disk. The material of this disk is sensitive to hydrogen gas. When the gas molecules get adsorbed on the coated surface of the disk, the mass of the surface film changes. Due to the change in mass the resonance frequency changes. By measuring the resonance frequency the presence of hydrogen gas in its environment can be measured with this type of sensor [22], [23]. A disadvantage of the QCM sensor, however, is that other gases and the temperature highly interfere with the measurements [22].

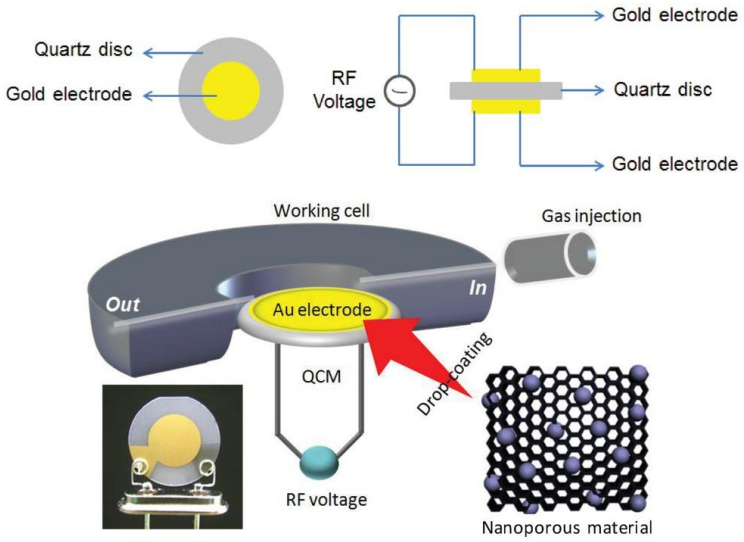

Figure 2-9 Schematic of a quartz crystal microbalance gas sensing device [32]

2.1.8 MEMS

The micro-electro-mechanical sensor technology type, shortly MEMS, consists of miniature gas sensors that are several orders of magnitude smaller than conventional gas sensors. At the same time, their power consumption, response time and production costs are reduced [33], [34].

Thermal conductivity sensor devices could be applied in MEMS technology, which reduces the power requirements. And making this technology in miniature version resulted in faster response times [24]. There has been good progress in silicon-based MEMS technology. Silicon-based MEMS technology has made it possible to fabricate low-cost micro gas sensors. And the silicon technology also provided high-performance gas sensors that combine good electrical and thermal functionalities and this could all be produced within a single piece of silicon [34].

MEMS and nano-technology sensors are still in ongoing research for the measurement of hydrogen to improve the sensor characteristics: a faster response time, even lower power consumption, higher selectivity and better handling of critical operating conditions [22].

2.1.9 Combination of sensor types

It is possible to think of a combination of different detection technologies incorporated in one sensor. For example, a combination between a catalytic and a thermal conductivity sensor. The advantage of such a sensor would be that it measures the hydrogen concentrations over a wide range. Also, combining the older sensor techniques with new nano-material technology improves the performance of the sensors [21].

Another example of a combination of technologies incorporated in one sensor is a semiconductor gas sensor element combined with a thermal conductivity element. Semiconductor-based hydrogen sensors have a limited measuring range. The lower limit of detection is typically as low as 10 ppm but have a limited upper measuring range for hydrogen. Also, the presence of oxygen or humidity can influence the sensor's response. Thermal conductivity sensors however can detect hydrogen concentrations up to 100 vol% [35]. And the advantage of thermal conductivity sensors is that it does not need oxygen to operate. This is why these sensors could complement each other. Thus, if one sensor's properties do not comply with the requirements. One can choose to use a combination of sensors.

This discussion of hydrogen detection was mainly about using the previous mentioned sensor technologies. Nevertheless, different methods of detection could be explored. One approach comprises a type of indicator such as a material that changes colour in the presence of hydrogen gas that can be found in Appendix D.

2.2 Advantages and disadvantages of the sensor technologies

2.2.1 Thermal conductivity

Starting with the advantages of thermal conductivity sensors. They have a fast response, are low cost and are stable devices. It has a wide measuring range with simple construction and the sensors are robust [22].

There is no chemical interaction, and this is why they are less susceptible to contamination. The wide detection range and long operation lifetime are advantages. The reliability is very good and they have high accuracy [25]. The TC sensor also does not require oxygen for its operation. And it requires less power than is required for catalytic combustion sensors [21].

A disadvantage of this type of sensor is that they are sensitive to interfering gases. The heating elements could react with the gas [22]. They might struggle with detecting a very low concentration of hydrogen. The lower detection limit is still quite high. Therefore, they are usually used in combination with other types of sensors. Furthermore, this type of sensor has a low gas selectivity which is not a problem when only a single gas combustible is present that needs to be detected [25].

2.2.2 Electrochemical

Advantages of Electrochemical sensors are that the sensors have a high sensitivity to hydrogen and they are well-established commercially [25]. Other advantages are the low cost and good selectivity. It is also still possible that the sensors work at high temperatures. A heating element is not required, so they have a low power consumption during operation [22].

The disadvantages of this type of sensor are the lower lifetime. Typical lifetimes for stable electrochemical sensors can be up to 2 years. The restricted temperature range of the liquid electrolyte is a limitation for the lifetime. Furthermore, this type of sensor has moderate selectivity and is affected by environmental pressure [21]. Also, the requirement for a specific electrolyte and regular calibration can both be a disadvantage [22].

2.2.3 Catalytic

Advantages of catalytic sensors are the wider operating temperature and stability of the sensors [22]. The catalytic sensor is a well-developed technology and this small type of sensor can be used to detect any combustible gas [25].

Disadvantages are the high power requirement, and a higher response time [22]. Catalytic sensors are not specific to hydrogen, they cannot differentiate between combustible gases. They are therefore not very selective. Regular calibration and replacement are needed. And oxygen presence is required for the operation of the sensor.

2.2.4 (Semi conductive) Metal-oxide sensors (resistive)

The MOX resistive sensors have a fast response and acceptable lifetime. The high sensitivity of the resistive sensor is an advantage. The wide range of the operating temperature is an advantage as well. Furthermore, they are low cost and have a low power consumption [22], [25].

A disadvantage is that it has cross-sensitivity with interfering gases and humidity. They are sensitive to water vapor and many other gases [25]. It requires oxygen to work and parts can be affected by higher gas pressure [22].

2.2.5 Metal-oxide semiconductor (work function)

The advantages of work function sensors are that they are small in size, have a fast response and have a low power requirement. They have high sensitivity and selectivity, are low cost and ambient conditions have a smaller influence.

The disadvantages are the existence of hysteresis losses and the possibility of drift [22], [23]. Due to hysteresis, the state of the signal depends on a state that happened earlier. Drift occurs when there is electron movement caused by an electric field.

2.2.6 Mechanical

The advantages of a mechanical type of sensor are the small size and the ability to work in an explosive atmosphere. Micromachining is possible and it does not require oxygen to operate. The disadvantages are that they are hard to fabricate and have cross-sensitivity with interfering gases. The mechanical sensors have a slow response and an aging effect [22].

2.2.7 Optical

Optical sensors eliminate a few risks that other types of sensors have. For example, the risk of providing a source of ignition in the hydrogen leaking area. In this sensor, the signal is an optical signal rather than an electrical one. This will eliminate the risk of ignition. In the same way, it is also less sensitive to electromagnetic noise [25]. Oxygen is not needed for the operation of the sensor. They also have the advantage of a fast response [22]. The disadvantages are their cross-sensitivity with interfering gases [22] and that they are sensitive to interference from ambient light and temperature changes [25].

2.2.8 Acoustic

The advantages of acoustic sensors are the high sensitivity, the low power consumption and the wide range of detection. It can operate without oxygen and has a fast response. A disadvantage is the sensor's sensitivity to interfering sound waves and vibrations. It is unable to operate at high temperature and humid environments and has the possibility of interference of other gasses [22], [23]. An overview of the advantages and disadvantages of the technologies used for hydrogen sensing is found in Table A7 at the end of Appendix A.

2.3 Multi-criteria analysis

Currently, the most common hydrogen sensors commercially available are electrical sensors including catalytic (CAT) sensors, thermal conductivity (TC) sensors, electrochemical (EC) sensors, and metal-oxide semiconductor (MOX or MOS) sensors. These hydrogen sensors have existed for relatively long periods of time and their technologies are quite well developed. These mentioned types were found in a book from 1992: "A Survey and Analysis of Commercially Available Hydrogen Sensors" by Gary W. Hunter, reflecting how long they have been commercially available.

Many resources have been dedicated to the research and development of new types of sensors. For example, optical fiber sensors, based on palladium films. There has also been recent research on metal hydride-based optical hydrogen sensors with promising properties. However, they still suffer from a short lifetime, decreased accuracy, low stability and weak humidity resistance. At the moment this still challenges their widespread application [36].

Next to the optical sensors, acoustic sensors and MEMS are also not widely available yet. According to the level of maturity from **Buttner (2011)** [24] (Table A6 in Appendix A) the choice has been made to only include the sensor technologies that have the largest level of maturity. Therefore, these last-mentioned sensor types will be excluded from the following analysis of sensors.

For the analysis, a selection of the most widely used sensors was made. Three research works studied different commercially available types of sensors [28], [37], [38]. These studies are used to analyse the sensor types to evaluate their performance at different criteria and operating conditions. The paper of **Jallais et al. (Hyindoor) (2015)** included three different kinds of catalytic hydrogen sensors, which the first one (Cat1) was chosen based on its accurate performance and low pricing according to the paper. The other two (Cat2 and Cat3) are more conventional and robust sensors with protection against explosive environments. They were selected to verify the first (Cat1) sensor on the influence of the packaging and the overall performance of catalytic sensors [38]. The paper unfortunately does not mention the difference in material of these three catalytic sensors and therefore no further explanation of the differences between these could be given.

Next to the catalytic sensors, the outcomes of a tested thermal conductivity (TC) sensor, an electrochemical (EC) sensor and a metal-oxide (MOX) semiconductor sensor are chosen for analysis [28]. They are all assessed based on the most important performance criteria in the residential use of the sensors.

The relevant data needed for the multi-criteria analysis is extracted from 3 literature studies about commercially available hydrogen sensors. This is done in order to find the performance of the technologies subjected to the analysis on these criteria. The hydrogen sensors will be assessed on a selection of relevant criteria. The criteria were selected from reviewing the following reports and papers:

Jallais et al. (Hyindoor) (2015) [38] described the safety design guidelines for indoors in the Hyindoor project. They have examined the hazardous consequences of hydrogen release in confined environments. Also, a market survey was performed regarding commercially available hydrogen sensors. The performances of three types of hydrogen sensors from five brands were tested: Three different catalytic sensors, one thermal conductivity sensor, and one electrochemical sensor.

From the commercially available sensors mentioned in the Hyindoor final report [38], the data for three catalytic sensors was used. The first catalytic sensor was examined on good performances combined to a low pricing. Furthermore, two conventional catalytic sensors are to verify the first (Cat1) sensor and the overall performance of catalytic sensors. The results are found in Table A1 (Appendix A).

The paper of **Boon-Brett et al. (2009)** [28], described an extensive test on the performance of multiple commercially available hydrogen safety sensors. Seven performance tests were done on 39 hydrogen sensors of four sensor types from which some were unsuccessful. The performance four CAT sensors, four MOX sensors, eight EC sensors and two TC sensors were successfully tested. The results that stand out for each type are found in Table A2 and Table A3 (Appendix A). Table A2 shows the detection limit and cross-sensitivity against CO of each type of sensor. Table A3 gives the important results that strike from the remainder of the tests. These results have been verified by comparing the outcomes to the results of the research of **Hübert et al. (2011)** [23] found in Table A5 (Appendix A).

Many types of commercially available hydrogen sensors for industrial applications provide reliable detection under a given range of ambient conditions. But if the sensor is deployed in new applications it will lead to more performance requirements. The selectivity of the sensors and their robustness against poisoning gas species, other substances that will influence the measurements, are very important factors to prevent false alarms.

Palmisano et al. (2015) [37] tested three sensor types (catalytic, electrochemical and metal-oxide semiconductor) based on their measuring range and cross-sensitivity to H_2S, NO_2 and SO_2. The cross-sensitivity to these other gasses is important to rate the selectivity of these sensor types. During these measurements, the sensors were exposed to gas flows containing 1 vol% hydrogen and the contaminants (H_2S, NO_2 and SO_2). The results are found in Table A4 (Appendix A).

Finally, the pros and cons for all performance criteria were double checked per sensor type. This was done with the advantages and disadvantages of the different sensor technologies determined earlier through the researches of **Chauhan an Bhattacharya (2019)** [22]**, Hübert (2011)** [23] and **Manjavacas and Nieto (2016)** [25].

The criteria obtained for the sensor types were analysed in an analysis on multiple criteria. Specifically, a multi criteria decision-making method (MCDM) was used. A matrix is created and arranged to be

used for analyzing different type of sensors. For the type of MDCM analysis, a Weighted Sum Model (WSM) analysis is chosen. To select the most suitable sensor from the list of available sensors, they are assessed on multiple criteria. Both quantitative and qualitative parameters can be used as input and are translated to numbers representing the score [39].

For the scoring of the sensors, a so called 'Likert' scale of 1 – 4 is used. This scale will provide the ranking of the different criteria. The higher a numerical score, the better the expected performance is for a sensor. In the analysis, the score 1 – 4 is given based on the performance in each of the criteria. These numbers represent 1: 'low', 2: 'medium', 3: 'good' to scoring 4: 'excellent'. A 4 number Likert scale is chosen to provide specific responses. This scale lacks a neutral number. A neutral result is not of value in reviewing the sensors with the goal of finding the ones that score a pass grade.

There are two types of criteria, the beneficial criteria and non-beneficial criteria. For beneficial criteria, the score will be higher on the scale when the criteria score is higher for each sensor. A higher value is desired. Examples of this are the accuracy and stability of the sensor.

Non-beneficial criteria are the ones where a lower value is desired. Examples of this type are response time and the price of the sensor. In this case, the non-beneficial criteria in this analysis get a higher score if the value for the criteria is lower. In the analysis, the non-beneficial criteria are therefore not treated differently than beneficial criteria. And a maximum score is preferred for every criterion. The scores for all performance criteria are found in Table 2-1.

In the last column, values for weights are assigned to the different performance parameters. An important one will get a higher factor and will therefore have a higher impact on the final score. An example to illustrate this, is that selectivity of the sensor is much more important than pressure for the residential application of sensors. Therefore, the weight assigned to selectivity has a higher value than the weight value for the pressure.

The importance of the values for the weights were determined by the study of **Buttner et al. (2011)** [20] A table in this study was considered that states the importance of the different performance criteria for residential applications. This table specified for residential applications (Table B1) is found in Appendix B together with the determination and calculation of the weights.

In this table, practical criteria primarily were regarded as more important for the residential application. For this reason, some of the criteria such as cost, lifetime, calibration and maintenance got more importance. Therefore, these criteria have a significant influence in the decision of the sensor technology type. The determination of total of the weights is found in Appendix B (section B.2). The total of the values for the weights added up must be equal to the total number of criteria (15).

Table 2-1: Scoring per sensor type on the different performance criteria [22], [23], [25], [28], [37], [38].

	Scoring per sensor type						
Criteria description	**Cat1**	**Cat2**	**Cat3**	**TC**	**EC**	**MOX**	**Weights**
Accuracy	4	2	2	3	2	3	1.5
Lower Detection Limit (LDL)	3	3	2	3	4	3	1.5
Response time/Recovery time	3	2	2	4	1	3	1
Measuring range	3	2	2	3	2	2	1.3
Selectivity	1	3	2	2	2	3	2
Lifetime	3	3	3	3	1	2	1.3
Relative Humidity	3	2	3	2	2	1	0.5
Pressure	3	2	2	4	2	2	0.5
Temperature	2	3	2	4	1	3	1
Stability	2	3	3	3	2	2	1.3
Calibration/Maintenance	2	1	2	3	1	2	1
Flow rate	2	3	2	4	1	2	0.3
Robustness	2	3	3	2	3	3	0.3
Price	4	2	2	3	3	3	1
Power consumption	2	2	2	3	3	3	0.5
						Total	15

To continue, a normalization of the scores is conducted to allow forming a similar scale for comparing all performance parameters using the below equation [39].

Normalization for a maximization problem:

$$N = \frac{Xi\ j}{Xi\ j\ max}$$

Hence, the criteria score is divided by the maximum score received for those criteria. After the normalized matrix is calculated, the values of the weights are transformed to a percentage. In this case, the total value of the weights will be equal to 1.

For each sensor alternative, the criteria weight and the normalized value are multiplied, and the summation of all criteria for the sensor in the product with the weights results in the sensor's final score. The results are found in Table 2-2.

Table 2-2: Normalized scores per sensor type and final scores on the performance criteria [22], [23], [25], [28], [37], [38].

	Normalized scores per sensor type						Normalized Weights (%)
Criteria description	**Cat1**	**Cat2**	**Cat3**	**TC**	**EC**	**MOX**	
Accuracy	1.000	0.500	0.500	0.750	0.500	0.750	0.100
Lower Detection Limit (LDL)	0.750	0.750	0.500	0.750	1.000	0.750	0.100
Response time/Recovery time	0.750	0.500	0.500	1.000	0.250	0.750	0.067
Measuring range	1.000	0.667	0.667	1.000	0.667	0.667	0.087
Selectivity	0.333	1.000	0.667	0.667	0.667	1.000	0.133
Lifetime	1.000	1.000	1.000	1.000	0.333	0.667	0.087
Relative Humidity	1.000	0.667	1.000	0.667	0.667	0.333	0.033
Pressure	0.750	0.500	0.500	1.000	0.500	0.500	0.033
temperature	0.500	0.750	0.500	1.000	0.250	0.750	0.067
Stability	0.667	1.000	1.000	1.000	0.667	0.667	0.087
Calibration/Maintenance	0.667	0.333	0.667	1.000	0.333	0.667	0.067
Flow rate	0.500	0.750	0.500	1.000	0.250	0.500	0.020
Robust	0.667	1.000	1.000	0.667	1.000	1.000	0.020
Price	1.000	0.500	0.500	0.750	0.750	0.750	0.067
Power consumption	0.667	0.667	0.667	1.000	1.000	1.000	0.033
						Total	1.000

WSM	**Cat1**	**Cat2**	**Cat3**	**TC**	**EC**	**MOX**
Final score	0.749	0.724	0.667	0.871	0.586	0.742
Rank	2	4	5	1	6	3

2.4 Ranking of the different sensor types

The multi-criteria analysis resulted in the following ranking of the different sensor technologies:

1. Thermal conductivity sensor
2. Catalytic #1 sensor
3. Metal Oxide (Semiconductor) sensor
4. Catalytic #2 sensor
5. Catalytic #3 sensor
6. Electrochemical sensor

Thermal conductivity sensors showed the highest performance overall. The type out-performed the rest on stability, response time and selectivity. However, it is costly and with future improvements on the detection limit, it could be considered suitable for residential applications.

Catalytic sensors had a good performance overall, during the evaluation. They are accurate in measuring hydrogen and methane concentrations. However, they are not selective and detect different combustible gases simultaneously. Their response is influenced by operating conditions, such as the gas leakage rate.

Metal oxide sensors had an acceptable performance and they are unexpensive and the power consumption is reasonably low. However, the detection accuracy needs to be improved.

Electrochemical sensors showed a variation in performance. They are highly accurate on the lower detection limits (in ppm range) but showed uncertainty of detection. The impact of environmental conditions, such as temperature and gas leakage rate, on the hydrogen detection are considerable. They also suffer from a lower lifetime.

As a sensitivity analysis, a check of the Weighted Sum Model was done by redoing the calculation in Matlab with a designated function for the WSM method. The outcomes of the scores of the WSM in Matlab were the same as the final scores from the WSM in Excel.

Also, another variation of the multi criteria decision-making analysis methods was used to check if the results would differ and if the other method, with a slight difference in the calculation, will lead to a different winner. This other method is the Weighted Product Model (WPM) and is conducted to check if this would make a difference in rankings of the sensors compared to the WSM. When using the WPM method, only the ranking of the best catalytic sensor and the metal oxide sensor changed the position of second place with a slightly different final score as seen in table C1 in Appendix C. The Matlab script with the Weighted Sum Model and the Weighted Product Model is found in Appendix C.

3

Behaviour of hydrogen in an enclosed space

3 Behaviour of hydrogen in an enclosed space

3.1 Hydrogen-air mixture

Hydrogen is the smallest molecule, the diffusion coefficient is high in comparison to other molecules [31]. Hydrogen easily diffuses through air after release. The time to reach a homogeneous hydrogen-air mixture significantly depends on the diffusion of the hydrogen gas.

High buoyancy provides the ability to hydrogen to rapidly rise and mix with ambient air [40]**.** In case of hydrogen leakage inside a closed compartment, hydrogen rises and accumulates on the top part of the closed space [41].

3.1.1 De-mixing of hydrogen and air

Hydrogen accumulates at the top of a closed space [42] because the density of hydrogen is very low. However, in case of a hydrogen leakage that diffuses into air, hydrogen mixes with air.

Hydrogen mixes well in air in normal conditions. When hydrogen separates from the air because of the lower density it is called de-mixing of hydrogen and air. This effect of de-mixing is only small at low heights (below 3 meter). The hydrogen concentration in air is dependent on the pressure. Thus, the mixing depends on the pressure and changes with respect to the height (elevation). At a height of several kilometers, the pressure is lower compared to the pressure at sea-level.

In a mixture of 0.4 vol% hydrogen in air (10% of LEL) the de-mixing is less than 2 ppm (only 0.05%) at a 3-meter height [42]. De-mixing is predominantly observed above heights of the general living space. The effect of the density differences of air and hydrogen on the de-mixing is small at normal heights in the bottom 3 meter. Spontaneous de-mixing therefore does not occur at these heights.

3.2 Hydrogen leakage into different enclosures

Inside an enclosed space, hydrogen rises quickly toward the ceiling and slowly back towards the lower section [43]. The hydrogen gas is not able to exit the closed compartment and there is a build-up of gas concentration.

In open spaces, the risk is caused by the leakage rate of the hydrogen. The volume of the hydrogen gas is not important anymore. When there is no enclosure, hydrogen rises and there is no longer the risk of accumulation. Once the hydrogen flow is stopped, the combustible concentration of hydrogen is gone immediately.

In partially enclosed spaces, including spaces with ventilation, the volume and the leakage rate of the escaping gas both affect the safety risk of explosion. This risk depends on the geometry of the partially enclosed space and the location of the hydrogen leak. The location of the leakage determines the direction of the hydrogen leakage. When the enclosed space is designed with proper ventilation at the right location, the risk caused by hydrogen leakage is reduced.

The location of the vents strongly affects the risk of a hydrogen leakage. Due to the low density of hydrogen, the hydrogen rises toward the ceiling. Therefore, the ventilation openings need to be near the top of the enclosure allowing the hydrogen to exit effectively. It is necessary to have an opening (ventilation grill) near the bottom of the enclosure as well. These allow fresh air to enter and replace the exhausted hydrogen-air mixture from the top ventilation grill. This helps to improve air recirculation and more effective ventilation.

3.3 Hydrogen leakage

3.3.1 Leakage types

There are two types of hydrogen leakage, convection and permeation [44]. Convection causes hydrogen to leak through connections or joints of the piping equipment. Convection results from a pressure difference at openings in the walls or defects at joints or bends. Hydrogen molecules could easily leak through these openings.

The second type, permeation, is caused by large concentration differences of hydrogen molecules. Due to the small molecular size, hydrogen permeates through the material of the pipe[45]. The material of the walls of the piping equipment permits hydrogen molecules to pass through the walls of the pipes.

Piping, seals and Joints should be suitable for hydrogen. The material of the pipelines are PE (polyethylene) and PVC (polyvinyl chloride). Caution is required with these materials, more than in case of steel pipelines.

The rate of permeation mainly depends on the kind of material, concentration and temperature. Also, increasing pressure and aging of the material affect the amount of permeation**.** Permeation is identified as slow long term hydrogen release. Permeation occurs continuously over the whole surface of a pipe and not just locally at one spot. The driving force is the absolute pressure difference of inside and outside the component.

The permeation coefficient of PE (at room temperature) is assumed to be 156 [(cm^3 * mm) / (m^2 * day * atm)] for hydrogen and for methane 21-56 [(cm^3 * mm) / (m^2 * day * atm)] [12]. So, under equal conditions, the permeation of hydrogen is 3 - 5 times higher than for methane.

For PVC, the permeation coefficient for hydrogen at 20 ° C is assumed to be 112 [(cm^3 * mm) / (m^2 * day * atm)]. Whereas, the methane permeation coefficient is 1.9 [(cm^3 * mm) / (m^2 * day * atm)] [12]. The following formula applies [46]:

$$PC = \frac{Q_{p\times e}}{A \times \Delta p}$$

Where PC is the permeation coefficient [(cm^3 * mm) / (m^2 * day * bara)], Q_P is the permeated volume [cm^3 day-1], e is the wall thickness [mm], Δp is the difference in partial pressure (absolute pressure) [bara] and A is the area of the pipe [m2]. This area is calculated with the average of the inner and outer diameter and with the length of the pipe. Considering the permeation, the leakage rate of the hydrogen on a particular location is very low. It is negligible in such a way that the hydrogen-air mixture is not ignitable [45].

3.3.2 Flow regime

The gas behaviour of the leakage flow of hydrogen gas depends on the flow characteristics. The flow is similar to laminar flow or turbulent flow. Laminar flow is characterized by smooth streamlines and highly ordered motion [47]. Whereas turbulent flow is characterized by a flow with fluctuations and highly disordered motion (Figure 3-1). In case of turbulent flow, the flow zigzags at random. Due to these fluctuations, when two fluids meet, the fluid particles from different layers rapidly start mixing. Apart from laminar or turbulent, the flow can also be in between laminar and turbulent: transitional flow.

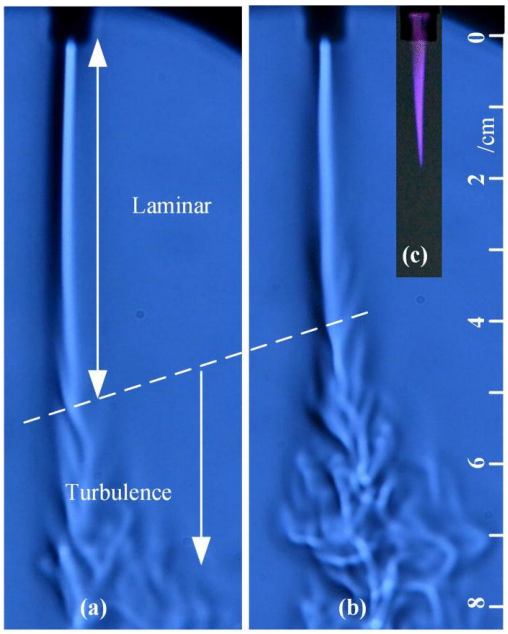

Figure 3-1: A laminar and turbulent section of the flow of helium gas[48].

The Reynolds number (Re), the ratio of inertial forces (inertia) to viscous forces (viscosity) occurring in a fluid, is used to determine if a flow is laminar flow or turbulent flow. The Reynolds number is different for different geometries and flow conditions [47].

The Re number is calculated with the following formula:

$$Re_D = \frac{\rho v D}{\mu}$$

Where ρ is the density (kg/m^3), v is average flow velocity (m/s), D is characteristic length of the geometry (m), and μ is dynamic viscosity of the fluid (m^2/s) or (Pa · s).

Based on the Reynolds number:

At small Reynolds number: Re < 2300, the flow is laminar.

If it is large: Re > 4000, the flow is turbulent.

In between these two limits, there is a transitional flow.

The geometrics of the leak opening, the gas pressure in combination with the gas characteristics inside determine the flow type [49]. The hydrogen leakage flow velocity in the case of a leakage in the gas network is in the order of 0.5 m/s and the Reynolds number is below 100. In case of a small leakage size, for it to reach turbulent flow the leakage mass flow rate needs to be very high. The pressure of the service line in the Netherlands is 100 mbar. After passing the gas meter the pressure is reduced to 25 mbar. At these low pressures, the hydrogen leakage would not normally have enough kinetic energy to enable the gas to reach a turbulent outflow.

3.3.3 Effect of buoyancy and diffusion

Valuable experimental research in a thorough experimental study has been done by **M. De Stefano (2019)** [50]. In this research, a small amount of hydrogen is leaked into a small enclosure: a scale

version conclusion drawn from this study is that the hydrogen is dispersed homogeneously in the room with a higher leakage rate. The kinetic energy dominates at a high leakage rate in the order of 100 liters per hour. But by decreasing the leakage rate, the buoyancy force becomes more dominant. So due to the density difference between hydrogen and air, the hydrogen rises quickly towards the ceiling.

A turbulent flow moves in all directions and causes a uniform distribution of hydrogen gas layers. The hydrogen concentration is more evenly mixed with air. The concentration is then approximately even throughout the gas, also said to be homogeneous (Figure 3-2).

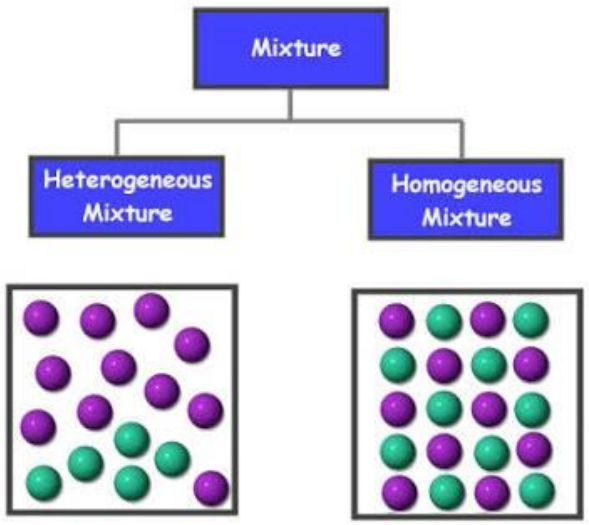

Figure 3-2: Schematic of a heterogeneous (not uniformly distributed) mixture with layers of gas and a homogeneous (uniformly distributed) mixture[51].

In the case of a laminar flow, the gas causes another type of distribution at the top of a compartment where there are multiple layers of hydrogen gas with different concentrations. This phenomenon of formed layers of different concentrations is called stratification [50]. This means you get the highest concentrations on top of the space and comparably low concentrations at the bottom. The hydrogen rises to the highest level of the space because of the buoyancy. It therefore creates a layering effect within the top half of the confined space [41].

After the phase of the initial dispersion of hydrogen into the compartment with a leakage rate of 100 liters per hour, homogenization is eventually reached in the mixture in 130 seconds [50]. The homogenization occurs mainly horizontally because of the molecular diffusion. Consequently, the concentration is different in the vertical aspect. Therefore, hydrogen layers are formed at different heights.

In the same phase (homogenization phase) of the experiment of the laminar flow hydrogen leakage, the buoyancy forces of the hydrogen gas began dominating the inertia forces. If the hydrogen flow is laminar the hydrogen does not mix with the air at the top of the compartment. Different hydrogen layers with different hydrogen concentrations are observed close to the ceiling. The concentration of hydrogen in these layers gradually differs.

At a low leakage flow rate, the hydrogen build-up in the top of the enclosed space might create a peak concentration. The level of concentration is higher compared to uniformly distributed layers that exist if hydrogen gas leaks at a higher leakage rate.

3.4 Ventilation effect

When there are ventilation openings present in a confined space filled with air, the results of a leakage of hydrogen depends on several things. As discussed in a study of **Prasad (2010)** [52], these are: release rate, volume of hydrogen released, location of the vent(s), cross-sectional area of the vent(s), thermal effects and air movement around the building caused by outdoor wind. The type of ventilation that occurs in the situation of the metering cabinet is natural ventilation. The natural flow of air through the ventilation grilles creates the ventilation flow. When more air enters through the ventilation grill or when ventilation grill is larger, this causes a lower hydrogen volume fraction in the air of an enclosure [52]. In the situation where hydrogen is fully mixed with the air in a ventilated space with a ventilation grill positioned at the top and at the same time, the incoming hydrogen flow might still be at the bottom of the compartment. The more hydrogen that flows into the fully mixed compartment, the greater the decrease in density of the air, which affects the ventilation behaviour.

The study of **Lowesmith (2009)** [53] concludes that hydrogen gas flowing into an enclosure causing a rising hydrogen concentration increases the volume of the region where it accumulates. A higher hydrogen concentration in air leads to enhancing the buoyancy. This could cause an even greater increase in ventilation airflow.

3.5 Schlieren technique

3.5.1 Schlieren technique method

To get more insight in the outflow of hydrogen, an experiment of the so called Schlieren technique or Schlieren photography is conducted [54], [55]. Schlieren photography is used to make the flow of fluids with varying densities visible to the camera. The technique could be used to visualise the dispersion of the gas flow. Hydrogen and air have different densities and thus an image of the outflow of the hydrogen can be created. The equipment for this type of measurement was available at Kiwa and was ready to be used (Figure E1 and Figure E2 in Appendix E).

Set-up necessities:

- Spherical Mirror
- Light source
- Knife (razorblade)
- High-resolution photo – video camera

To reach to the best result a suitable digital camera which provides different ISO settings and a high resolution. It is useful to have sharp images at higher zoom levels. An extra feature that enhances the result is a high-speed function (with a high number of frames per second).

The light source should be approaching a point source light. It should focus its light on a spherical mirror that allows to see small changes in the index of refraction in air. When there is a change in the refractive index of the gas in the air, the image from the point light source will be deflected slightly. The razor blade is placed in the light pathway from the mirror to the camera (Figure 3-3). It should block half the light and is positioned at the focal point. Some of the light rays bend above the knife edge and some to bend below the knife edge. The Schlieren effect makes it possible to see differences of brightness and darkness that are in the image that is caused by the particle differences.

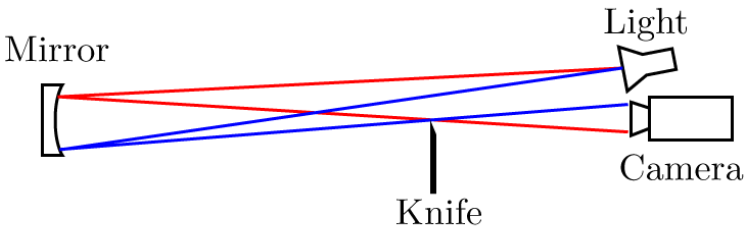

Figure 3-3: Schematic of the Schlieren experiment set-up with the spherical mirror, light camera and the knife (razorblade)[54].

3.5.2 Results of the hydrogen outflow visualised with the Schlieren technique

The flow of hydrogen from a standard metal pipe (D=4 mm) is seen in Figure 3-4.The hydrogen gas slowly exits and rises immediately. When a nozzle is added to the outlet pipe the flow is similar. Also, in Figure E3 (b) clear disturbances of the hydrogen plume were seen caused by (ventilation) airflow.

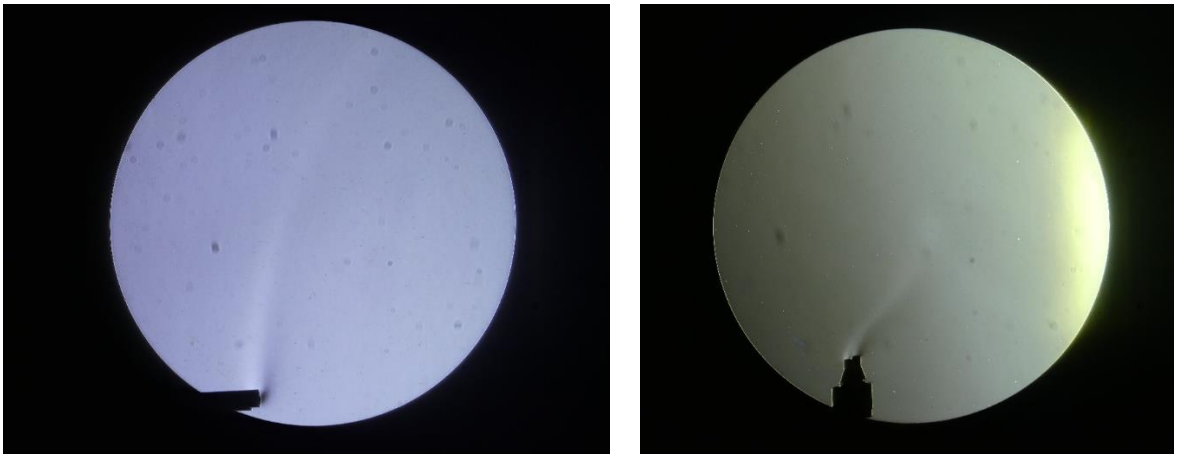

(a) (b)

Figure 3-4: Images that result from the camera: (a) without a nozzle the flow will be directed upward. (b) Disturbances because of (ventilation) airflow.

From the pictures created of the hydrogen flow of the nozzle outflow configuration in Figure 3-5 it became clear that there is a small plume exiting the nozzle to the upside. This flow with the leakage rate of 5 liters per hour hydrogen has a low exit speed of the gas even with the small opening of the nozzle (D=2 mm). The discovered fluent flow and calm behaviour of the plume resulted in the idea that the hydrogen outflow is laminar.

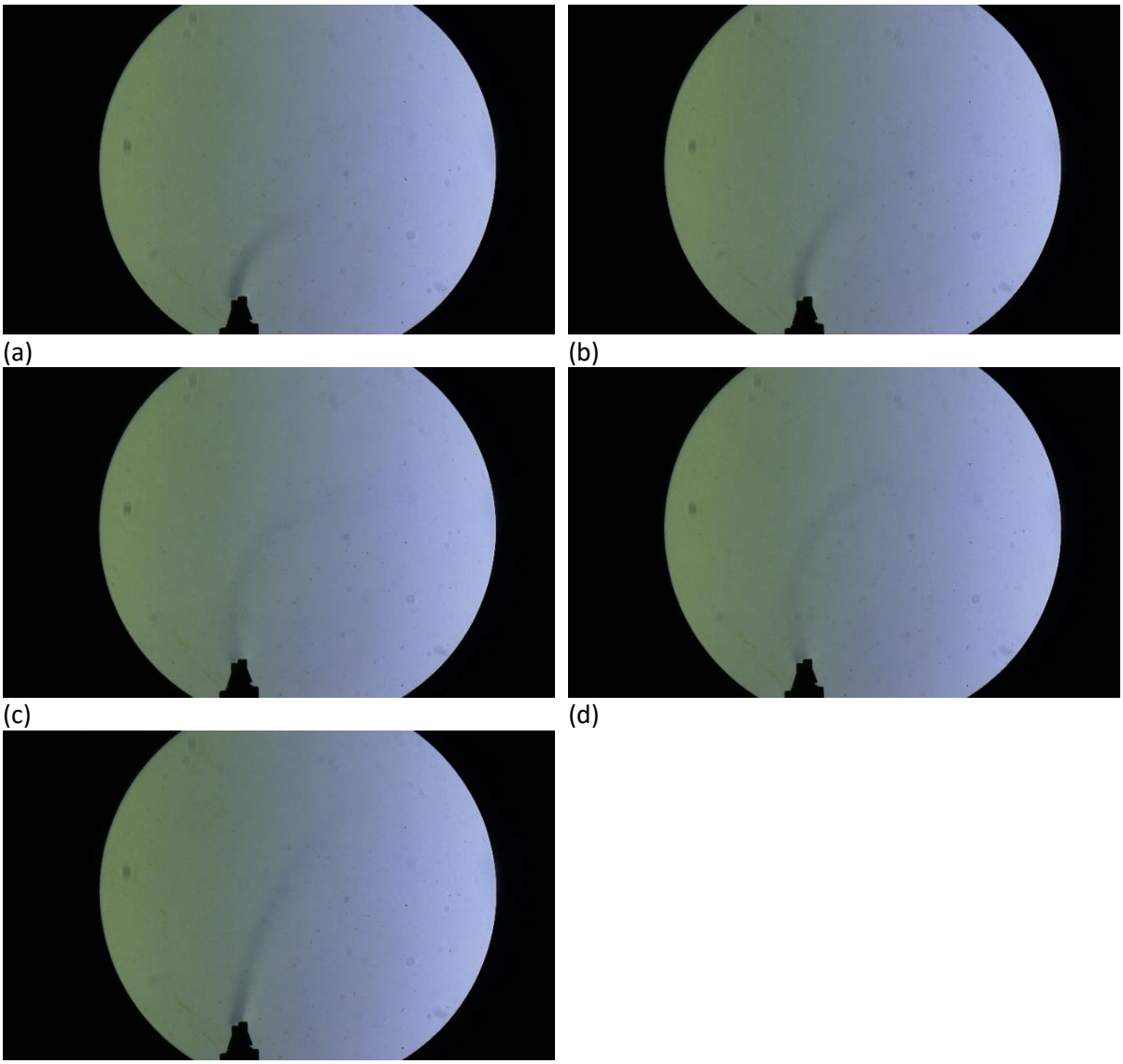

Figure 3-5: Stills of the camera from the Schlieren experiment in order: (a) - (e).

4

Experimental method

4 Experimental method

4.1 Introduction

After the assessment of the different hydrogen sensors the objective of the research is to evaluate a hydrogen leakage in a standard Dutch metering cabinet or otherwise called meter cupboard. The main question of the experiments inside the metering cabinet was: Which location of the hydrogen sensor could deliver the fastest detection of hydrogen concentrations?

The measurements were carried out by putting eight hydrogen sensors in specific places inside the metering cabinet. The objective is to find the difference in concentration levels of hydrogen at these places. The process of doing the measurements was carried out under seven different conditions in order to understand the hydrogen leakage in different situations.

The conditions of the 7 cases have been chosen to find out how hydrogen gas is distributed inside the metering cabinet in case of hydrogen leakage. In order to find out if the preferred detection location would be close to the leakage or on a spot at the ceiling where the gas could accumulate.

4.1.1 Test Location

The test location was in within a small building (indoors) that is specifically used to provide trainings to get hands-on experience with hydrogen. This small wooden house, called the Hydrogen Experience Centre, is located near the Kiwa company building in Apeldoorn. The heat demand of this building is supplied by a hydrogen boiler connected to a hydrogen pipeline.

4.1.2 The metering cabinet

The metering cabinet is similar to a standard Dutch cabinet mentioned in **NEN 2768 + A1 (2016)** (5.1.1) (Figure 4-1) with the following dimensions:

Height: 240 cm

Width: 77 cm

Depth: 35 cm

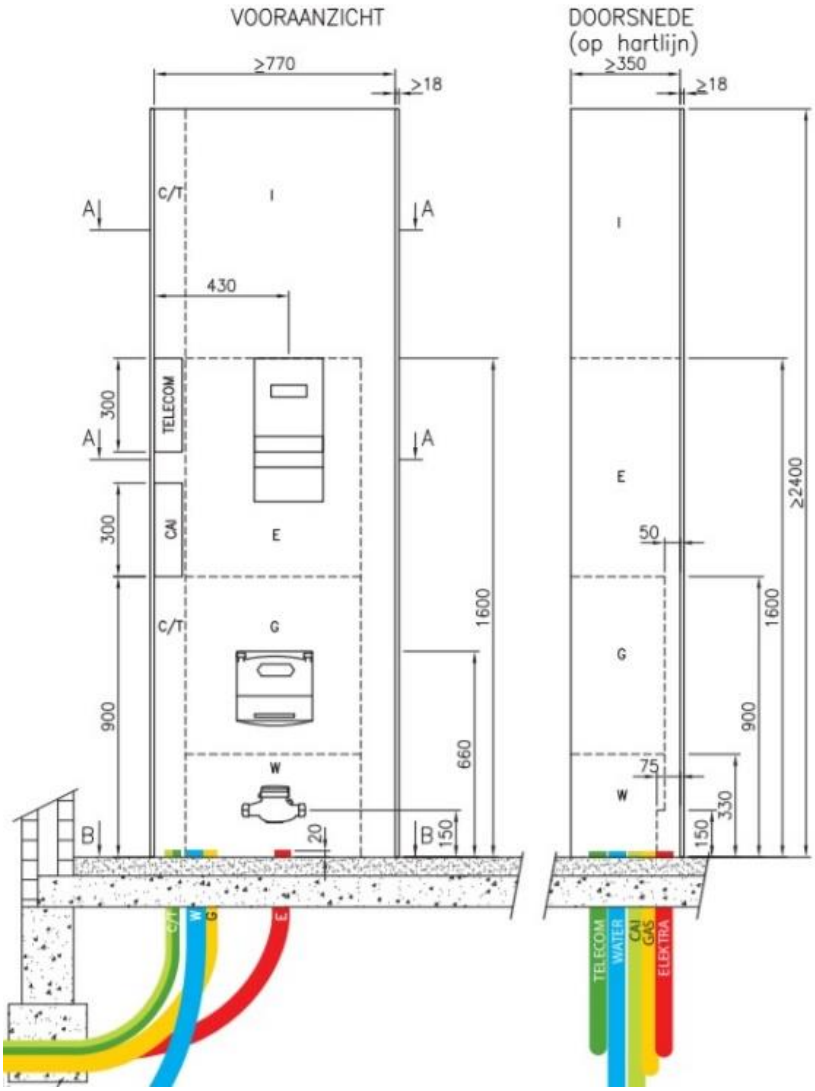

Figure 4-1: Metering cabinet dimensions according to NEN 2768+A1 [56].

The metering cabinet used for the test was a portable cabinet. It has a lower height of 200 cm which is 40 cm shorter than the one in the NEN standard, but with the same width and depth dimensions. The total volume of the metering cabinet is: 539 liters.

There were two ventilation openings embedded in the front door of the metering cabinet (ducts or grilles). One located in the upper part and one in the lower part of the metering cabinet. According to **NEN 2768 (2016)** both the openings should have an area of 200 cm^2. The width of these grilles are 40 cm and 5 cm at the small side. They are located at 4 cm from the top and bottom of the door. The ventilation grilles are equipped with a sliding door that could be completely open or closed. So, this made it possible to investigate the effect of ventilation on the development of the gas concentrations.

In every test there were at least three items present inside the metering cabinet. One is the gas meter placed at the bottom of the metering cabinet. This was a real unused gas meter. The second item is the electrical box placed at the middle of the cabinet in the center. It was a rectangular box with the same dimensions. The third one was a small box attached to the bottom of the electrical box representing a smart electricity meter. The electrical box in the center and the gas meter located at the bottom were placed at the same distance from the top similar to the standard metering cabinet according to **NEN 2768 (2016)** (Figure 4-2).

Obstacles inside the metering cabinet (such as the electricity box, the smart meter and the gas meter) might affect the flow of hydrogen and how the gas is distributed and mix with the air in the enclosure. Later in one of the study cases more obstacles were included inside the metering cabinet to identify how the obstacles change the hydrogen concentration at the locations of the sensors and how it affects the detection time.

Figure 4-2: The test-setup with the sensors positioned at the top below the ceiling and on the side of the metering cabinet.

4.2 Preliminary measurements

The first part of the measurements focused on the safety aspects and understanding how to use the test set-up. During these preliminary measurements the ventilation grilles were opened which provide air circulation and hydrogen could partially leak from the metering cabinet.

Before the supply of hydrogen was started, simulating hydrogen leakage, the supply tubes still contained air. This causes a delay in the measurements. To mitigate this issue, a small amount of hydrogen at a low leakage flow rate of 50 ml/min was supplied through the tubes for 20 seconds after which it was stopped.

The electrochemical ppm sensors appeared to be more sensitive in measuring concentrations below 1000 ppm in comparison to the catalytic (%LEL) sensors. These sensors could only measure the hydrogen concentrations when the concentration is higher than 3 %LEL (1200 ppm). One of the top sensors (sensor 3) kept showing a 0 %LEL level while at the same the electrochemical sensor showed a concentration around 500 ppm.

Afterwards, the sensors were placed at the top of the metering cabinet separately one by one. A predetermined amount of hydrogen dispersed from the bottom of the cabinet. One sensor was placed at the top and measured this hydrogen as a concentration. The time it takes to reach the concentration was measured.

When the 4 devices equipped with 2 different sensing technologies were placed at the side of the cabinet. The hydrogen concentration at different heights from the leakage at the bottom could be measured. After starting the hydrogen leakage rate, the bottom sensor showed a high concentration value (6 %LEL) close to the hydrogen leakage. All sensors from bottom to top detected hydrogen gradually.

When a measurement was nearing the end and the hydrogen supply was shut off, the set-up was not touched to see the recovery of the hydrogen concentrations measured by the sensors. This recovery time was measured before opening the door.

Based on the observation of the preliminary experiments the electrochemical sensors had a greater accuracy, but could only be used up until 1000 ppm hydrogen concentration level. Above the 1000 ppm level of hydrogen concentration, the readings of the catalytic sensors (%LEL) should be considered.

4.3 Used hydrogen sensors

4.3.1 Multi Rae Lite gas sensors

The sensors used in the measurements are Multi Rae Lite gas sensors (Figure 4-3). Eight of these sensors were available. All of the eight sensors have catalytic LEL sensors that can measure the hydrogen concentration in %LEL. This means that they measure the concentration as a percentage (%) of the LEL of hydrogen which is 4.0 vol%. Zero percent corresponds to a combustible gas-free atmosphere. A hundred percent of the lower explosive limit (100 %LEL) means a gaseous atmosphere at the lower flammable limit. Only four of the sensors include electrochemical sensors that can measure hydrogen concentration up to 1000 ppm. These are very accurate below this level.

Additionally, all 8 sensor devices also include methane detection sensor. The sensors that measure methane are infrared sensors that measure in vol% in steps of 0.1 vol%.

Figure 4-3: Multi Rae Lite sensors (source: www.gasdetectorshop.com.au/j2store/multirae)[57].

The output of the hydrogen sensors can be remotely monitored while the sensors actively measure the concentration. The measurement data of the Multi Rae sensors could be logged by a laptop that receives the data via a wireless router. The data is collected every time-step (10 s) in real-time. At the end of the measurements, the data can be processed to an Excel file format and saved to a USB for processing the data.

Back-up sensors were available if something was wrong with the main type. These Riken Keiki NP-1000 devices are hydrogen thermal conductivity detectors. These unfortunately only could be observed manually. The Riken Keiki sensors should therefore be continuously monitored.

4.3.2 Accuracy and reliability of the sensors

To test the accuracy and the reliability of the readings of the sensor devices the following check was performed. A Tedlar bag that could contain 5 liters of gas was used to supply a predetermined amount of gas to the inlets of the Multi Rae sensors as seen in Figure 4-4.

Four of the sensors with only the catalytic sensors equipped (that measure %LEL) were checked first. After first showing the right values at the start, later during the check the readings went up to 7-8 %LEL. One of the sensors checked went down to 3-4 %LEL and held value for a moment and later recovered to zero.

Figure 4-4: A bottle of hydrogen with test gas with the exact amount of 0.3 vol% hydrogen in Nitrogen. A Tedlar bag which can contain 5 liters of gas was used fill with test gas and was attached to the inlet of the sensors.

The four other sensors with both the catalytic sensors (%LEL) and the hydrogen electrochemical sensors equipped were tested next. The first LEL sensor, sensor no. 1, was already fluctuating during the beginning and eventually showed lower values and eventually decreased to zero. Sensor no. 2 showed the same behaviour as was observed earlier. First it went up and held 7 %LEL for a moment, but also decreased to 0 %LEL. Sensor no. 3 showed fluctuating values and was underestimating the %LEL. After a while, it held the value of 3 %LEL.

At the beginning of the check, sensor no. 4 did not show the correct values but overestimated the concentration up until 9 - 10 %LEL. When the hydrogen flow was stopped, the concentration value stocked on the lower %LEL values instead of zero.

With the results of the accuracy and reliability check of the sensors in mind, the conclusion was to have the hydrogen LEL sensors recalibrated. For the measurements in %LEL the best performance would be realised with a calibration of 25 %LEL hydrogen. The sensors would then have a linear slope over the desired measurement range.

4.3.3 Sensor characteristics and calibration

One full day was spent to recalibrate the accuracy of the sensors and gather more information on the Multi Rae sensors before the sensors are used to measure the hydrogen in the metering cabinet. Multi Rae devices are detection devices and not analysing devices. They are not as accurate as a gas analyser. The Multi Rae sensors are devices used in the gas industry to detect gasses at a certain range or above a certain threshold.

4.3.3.1 Characteristics

The sensors in the device are smart sensors and involve a computer chip to control the sensor (Figure 4-5). The sensor heads (one of 5 positions) do not favour a gas directly flowing over the sensor. These separate sensor heads are pressure sensitive. It is why one of the positions that would be empty always involves a dummy sensor that is turned around. This occupied sensor position then causes the gas flow to lose momentum. This way the sensor position next to that position measures the gas correctly.

Figure 4-5: View on the inside of the Multi Rae Lite sensors (source: norrscope.com/product/multirae-sensors-accessories-spares)[58].

4.3.3.2 Calibration of the Multi Rae LEL sensors

For the calibration of the LEL sensors two calibration steps were performed to calibrate the sensor. As was discussed earlier in the paper Catalytic LEL sensors could detect different combustible gases. The Multi Rae sensors provide multiple calibration profiles in the settings for different gases with methane gas as default gas.

The first calibration was performed using a bottle of methane with a 50 %LEL methane concentration. The gas bottle was fitted with a “demanded flow gas cylinder regulator”. This regulator on the gas cylinder continuously passes the same exact amount of gas through the tube towards the sensor. This amount of gas is equal to the gas demanded by the pump of the sensor.

A second calibration is done with 25% LEL of hydrogen. After the calibration, 1 vol% hydrogen was supplied to the sensors. All LEL sensors displayed the output of 25 %LEL. But when hydrogen gas was

supplied at a low concentration, by using a bottle of 1000 ppm (or 0.1 vol% / 2.5 %LEL) this amount was not detected. This is explained in the next sub-part.

Next, the electrochemical (ppm) sensors were tested with a hydrogen bottle of 200 ppm. The sensors initially measure the concentration at 200 ppm correctly. Some of the sensors showed a delay in the detection time. (The time at which 90% of the concentration of the supplied gas is reached is called the T90 value.) Sensor no. 2 indicated a bit slower reaction time in the ppm sensor than the other sensors which could explain earlier results of the sensor that showed a slower response. The calibration was confirmed by a check of the diagnostic information of the sensor. All of the calibrated sensors were well inside the limits and approved.

4.3.3.3 Dead band

Factories often apply a dead band on LEL detectors. This built-in phenomenon in the electronics of the sensor is a region where a change inside of this band produces no change in the measurement output signal of the sensor.

In Muli Rae sensors a dead band exists between 1-3 % LEL where there is an area of measurement values that is set to zero. The sensors still process a value, but the sensor display only shows a zero value in those cases. The lower range of values is not measured accurately by the LEL sensors. This was showed by supplying 1000 ppm (2,5 %LEL) hydrogen. The LEL sensor does not continuously give a value of 2-3 % LEL as it should, but instead, it remains zero. Therefore, these sensors are used for measurements of the hydrogen %LEL between 3 to 25%.

4.3.3.4 The sensors' built-in pump and retention time

The retention time of the hydrogen sensor is the time it takes for the gas to reach the sensor through the pipes and tubes configuration that is attached to the sensors. The sensors include a small pump that provides gas suction through an attached tube. The built-in pump of the sensor device has a suction capacity of 0.4-0.5 L/min. The diameter of the pipes are 4 mm and the total length of the pipe and attached tube is 90-100 cm. The retention time of the hydrogen to the sensor is estimated to be 1.69 s. Additionally, the electrochemical reactions inside the electrochemical ppm sensors and catalytic reactions inside the LEL sensors cause delays in the response of the two types of sensors.

4.3.3.5 Suction flow

During the measurements the sensors were all pumping air and gas through their tubes towards the sensors. The sensors are located outside of the metering cabinet. Thus, the combined suction flow of the sensors is equal to the suction capacity for each active sensor multiplied by the number of sensors. This amounts to 7 times the 0.5 L/min maximum suction capacity which is 3.5 L/min. The pump of the sensors does pump out a small portion of the air and measured gas. The sensors are placed outside the metering cabinet causing the gas that is pumped out to not be put back inside again.

4.4 Experimental set-up and procedure

Several important parameters need to be known before conducting the experiment. The relevant parameters are discussed in this part.

4.4.1 Sensor levels of interest

Hydrogen sensors measure the volume percentage of hydrogen gas in the metering cabinet. The volume percentage at which hydrogen will be dangerous is called the lower explosion limit or LEL or lower flammability limit LFL. For hydrogen, this level is 4,0 volume% and ranges until 75 volume % in air [59]. This is the concentration at which the gas and air will result in a flammable mixture and thus could be ignited.

In the future an alarm level needs to be determined for the hydrogen sensors to trigger and give a warning. The value of 10% of the LEL (which is 0.4 vol%) is mentioned in **Kiwa (2018)**[12] and **(Instituut Fysieke Veiligheid (2020))** [60]**.** This is a level that is currently used for natural gas as is considered a safe working environment. The minimum alarm level of the sensors at 10 % LEL should be used to trigger an alarm **(Buttner et al. (2011))** [20]. Furthermore, it could be used to activate other safety measures required to provide more safety.

For the experiments this level of 10% of the LEL is a good level to focus on. When this concentration level of 10 %LEL is not reached, another level for the hydrogen concentration becomes important. This is the 4 %LEL concentration level. The time to reach to 4 %LEL is a meaningful level for the catalytic hydrogen sensors when they first detect any hydrogen. In section 4.3.3.3 it is explained that the LEL detectors often give zero values below 3%LEL and therefore these sensors are used between 3 to 25%LEL. Thus, the important levels for the detection time were set to 4 %LEL and 10 %LEL.

The question then is: Does the hydrogen concentration reach to this level and how fast? The time it takes to reach 4 % and 10% of the LEL is checked for the different sensor positions. The detection time to reach the gas concentration levels during the measurements, indicates which sensor at which position gives the best results under the applied conditions.

To assure the safety, the measurements will be stopped if all of the top sensors surpass the maximum value of 20% of the LEL, (1.2 vol%). This way the concentration is kept below a safe value and there is still a bit of time to gather some extra results from the measurements after the values of 10% of the LEL are reached.

4.4.2 Hydrogen leakage rate

Gas flow rates are sometimes written as NL/h or Nm3/s (The N means Normal). It indicates that it was measured at standard temperature and pressure. Because the volume of gasses changes with temperature or pressure, it is necessary to specify the temperature and pressure the leakage flow rate was measured at. The standard temperature is usually 20 °C (or sometimes 0 °C is taken). The standard pressure is 1 atmosphere equal to 1013,25 hPa or 1,01325 bar. The tests in the metering cabinet were done at ambient conditions with a temperature between 15 - 25 °C and ambient pressure of around 1010-1020 hPa retrieved from Wheater Atlas [61].

Regarding the leakage flow rate, for indoor gas equipment in new buildings a maximum leakage flow rate of natural gas of 1 L/h can be present **(NEN 1078)** [62]. This is only allowed at the service line where gas enters the building. At other places in the system, the gas lines should be 100% gas tight, so meaning 0 L/h.

For currently existing older buildings, another standard **(NEN 8078)** [63] states that the acceptable limit for a leak in indoor installations should have a maximum of 5 L/h leakage rate for natural gas. Furthermore, it says that there shouldn't be dangerous concentrations of gas in the surroundings.

This value of 5 L/h is a good limit to take for the experiments as it is the highest value that is allowed. Also, to check the 5 L/h value for the safety of currently existing older buildings. As there is a big chance the indoor gas installations for hydrogen might be applied in existing older buildings in the future as was explained in the introduction (1.1).

4.4.3 Leakage flow set-up

Hydrogen is supplied by a bottle of hydrogen. This part of the system, the large gas bottle, is equipped with a pressure reducer on the top to reduce the pressure to 2,2 bar. This is the amount of pressure needed to supply the hydrogen gas to the next component in the system.

The leakage rate is regulated by a mass flow controller (MFC) to simulate the gas leakage inside the cabinet. This mass flow controller measures and regulates the mass flow rate which is set to 5 L/h (or 83.3 ml/min).

The mass flow controller, a Bronkhorst El-Flow Select, is originally calibrated for nitrogen (N_2). But with a conversion factor applied to the amount of gas it could be used for many different gasses [64]. A conversion factor of 1.01 (N_2 - H_2) was used to regulate the right amount of hydrogen with this mass flow controller.

The leak will be simulated with a round pipe (inner diameter 4 mm) that leaks hydrogen at a small leakage rate (5 L/h). It is assumed that the hydrogen gas enters the cabinet from the right side. The output opening of the pipe is located at the bottom part of the metering cabinet with the end of the round pipe at the height of the gas meter outlet (26 cm from the bottom of the metering cabinet, 26 cm from the side and 10 cm from the back of the cabinet).

Attached to the pipe will be a 90 degrees bended outlet with a nozzle to decrease the size of the opening (inner diameter of 2 mm). This way the direction of the opening can be varied. The size (diameter) of the opening is kept constant.

4.4.4 Sensor lay-out

Hydrogen might eventually build up just below the ceiling due to hydrogen being lighter than air. At the highest position on the ceiling 4 of the Multi Rae sensors will be positioned in a square as showed in Figure 4-6. These 4 sensors also have the electro-chemical sensor equipped.

The sensors work with flexible and metal tubes extending the location where exactly will be measured (Figure 4-7). The tubes go through the walls of the metering cabinet with the use of open links.

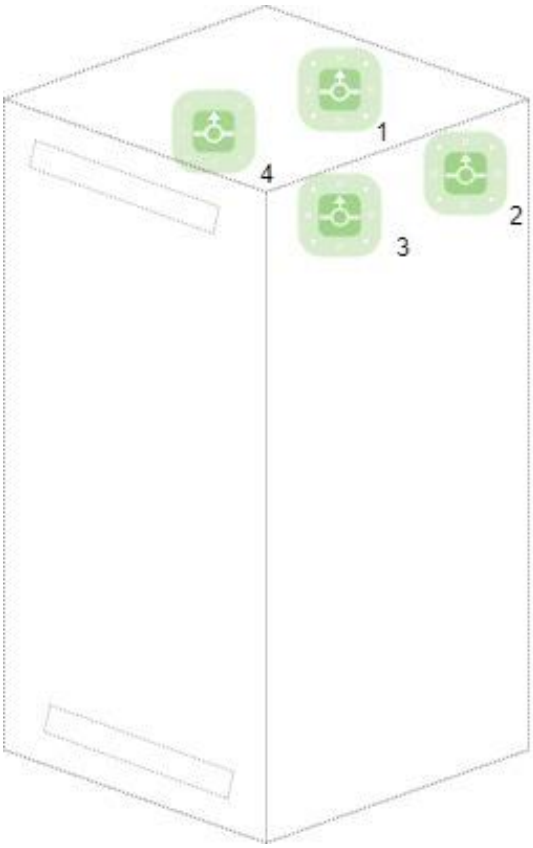

Figure 4-6: The four sensor devices at the top of the metering cabinet include two types of sensors.

Figure 4-7: The sensor inlets of the four top sensors were positioned with the use of the metal and flexible tubes.

The test was performed by setting the gas flow through the mass flow controller. The mass flow controller is controlled via a laptop. During the measurements the sensors were monitored on another laptop with a wireless connection to the sensors.

The measurement set-up and the layout of the sensors is illustrated in the schematic of Figure 4-8.

- 1. One sensor in the top section at the back of the cabinet - 195 cm from the bottom.
- 2. One hydrogen sensor at the ceiling as far as possible towards the backside corner of the enclosed space - 195 cm.
- 3. One hydrogen sensor below the ceiling of the metering cabinet at the side close to the wall - 195 cm.
- 4. One hydrogen sensor below the ceiling of the metering cabinet right above the leak position - 195 cm.
- 5. One sensor between the middle and the top section cabinet - 160 cm from the bottom.
- 6. One sensor in the middle section of the cabinet - 126.5 cm from the bottom.
- 7. One hydrogen sensor in the lower half at the gas meter - 58 cm from the bottom, close to the location of the gas leakage.
- 8. One extra sensor on the left side - 195 cm

It should be mentioned that in one case, an extra sensor was located on the left side of the metering cabinet to measure the concentration at the top when the hydrogen leakage is located at the left side. This is the side where the service line enters the house. The sensors at the other side are still there to measure if these positions would still be sufficient. So, in total, there are 7 or in one case 8 sensors positioned at different locations inside the metering cabinet.

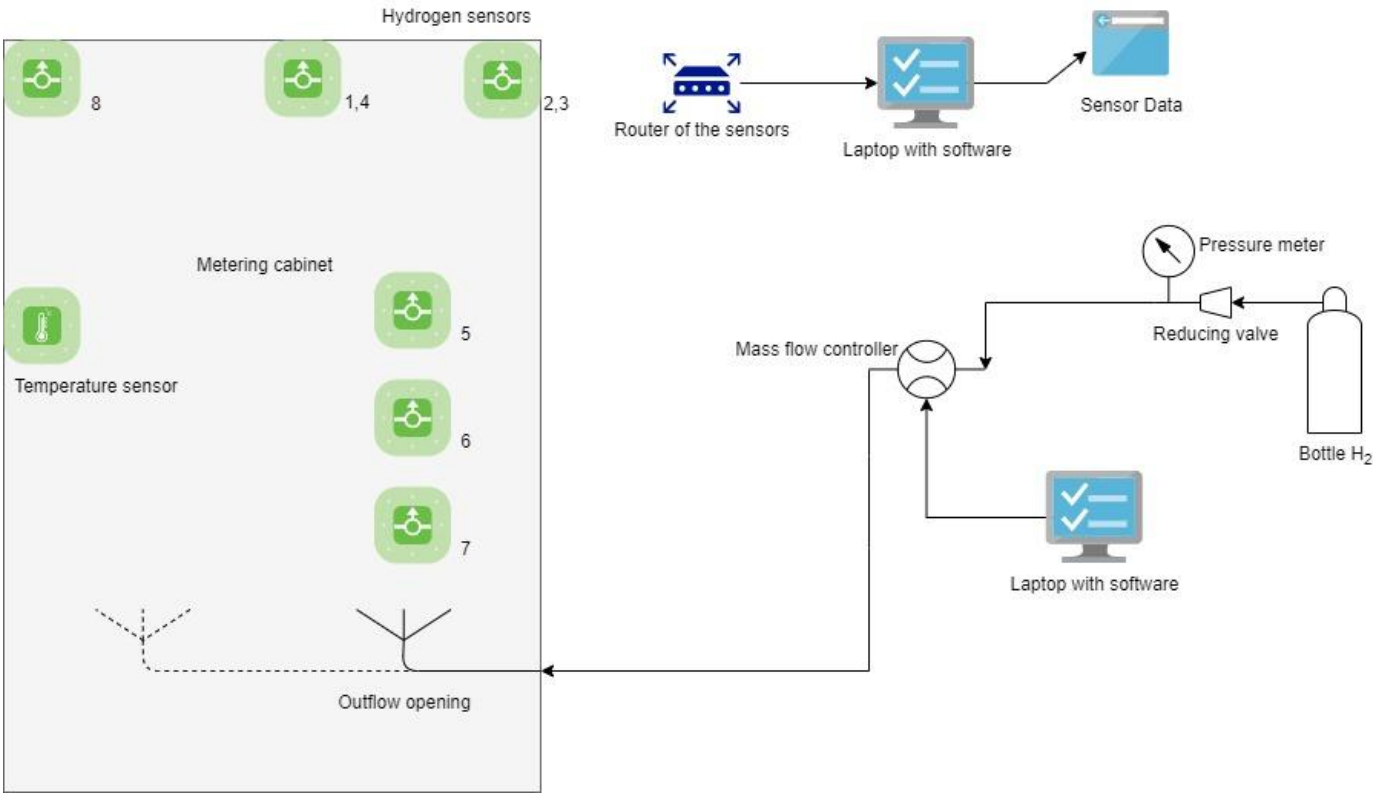

Figure 4-8: Schematic of the measurement set-up with the layout of the sensors.

4.5 Experiment overview

The initial configuration of the setup comprises seven or eight sensor positions that detect the hydrogen concentration. In the experiment hydrogen concentration was measured on these predetermined locations in the metering cabinet (Figure 4-9).

Figure 4-9: The metering cabinet including the 8 sensors and the standard items (electrical box and gas meter).

The purpose of the measurements was to investigate the effect on the hydrogen gas under different leakage conditions inside the metering cabinet. The objective of each case is to identify the sensor on the location that detects the hydrogen the fastest and to determine the (maximum) hydrogen concentration at different height levels and positions at the ceiling of the metering cabinet.

The conditions of the metering cabinet were kept the same as much as possible during the tests. This assures that the results are not accidentally showing behaviour that is related to other influences, but can be regarded as behaviour caused by the conditions of the case.

For the measurements, seven cases were considered to identify the gas behavior based on the testing conditions. Between two specific cases, a comparison between several variables of operation factors was made to see the effect of one operation factor. **Montgomery (2013)** [65] explained how to design an experimental study with different factors. These variable conditions are called factors. A factor is a controllable system input or parameter that was selected. Different cases have been selected to investigate the response of the sensors with respect to diverse circumstances. Based on these inputs (factors), the analysis of the response results from the different cases is assessed in chapter 5.

4.5.1 Test cases overview

The first two case studies have been carried out as reference tests that only differ on ventilation. In experiment case 1, the ventilation grills were closed. In experiment case 2, the sliding doors on the ventilation grills (on the top and bottom) were opened. The closed ventilation experiment is taken as a reference in the following experiment cases.

To study the impact of leakage direction, case 3 has been designed. In this case, two other directions of the outflow were studied and are divided in two parts: The direction of the leakage towards the wall (case 3-a) and the direction of the leakage towards the bottom (case 3-b). These were chosen in order to see the other possible direction of a leakage in the pipeline.

In the next case, case 4, the influence of the leakage location (at the left or right side of the gas meter) is studied. In this case the leakage was on the left side of the gas meter at the same elevation of the reference case (case 1). This is the side of the gas meter where the service line enters the house (further discussed in 4.6.5). This is done to check if similar positions of the sensors as in the previous cases, also sufficiently detect a leakage from the left side.

In the fifth case, all conditions were the same as the first case except in this case extra obstacles were positioned inside the metering cabinet. Some frequently occurring objects were chosen, including the standard gas meter, electrical box and smart meter. Moreover, two types of bags were present. Because, despite discouragements, people still use the metering cabinet for storage purposes.

In the sixth case, the changed factor was the leakage rate of hydrogen gas. In this case the leakage rate is set to 2 liters per hour which is less than the reference case (5 liters per hour). This case is designed to study the impact of smaller leakage rates, prescribed by current safety standards for natural gas.

The seventh case includes the comparison to natural gas. Thus, the factor that changed was the gas type, which was methane gas (the main component of natural gas). In this case, two conditions were conducted, where the first part involves closed ventilation grilles. The second part was a test with open ventilation grilles.

In Table 4-1 below, the factors that are varied are listed. Each time a single factor is changed. This is done to see the effect of this single factor. For a better understanding of the structure of these 7 study cases, the relation between the cases that are compared, and which factors affect the output of these experiments is further elaborated in

Table 4-2.

Table 4-1: Different measurement cases with the applied conditions (factors).

Case		Gas	Ventilation	Direction of flow	Leakage rate	Leakage side
1		H_2	Closed	Upward	5 liters/hour	Right
2		H_2	Open	Upward	5 liters/hour	Right
3	**a)**	H_2	Closed	Towards the wall	5 liters/hour	Right
	b)	H_2	Closed	Towards the bottom	5 liters/hour	Right
4		H_2	Closed	Upward	5 liters/hour	Left
5 *		H_2	Closed	Upward	5 liters/hour	Right
6		H_2	Closed	Upward	2 liters/hour	Right
7	**a)**	CH_4	Closed	Upward	2.5 liters/hour	Right
	b)	CH_4	Open	Upward	2.5 liters/hour	Right

*Extra items as extra obstacles present inside the metering cabinet

Table 4-2: Combinations of factors between the experiments and compared cases.

Factors of the cases	Compared cases
Ventilation (closed or open)	Case 1 – Case 2
Direction of the leakage (upwards, towards the wall and bottom)	Case 1 – Case 3a – Case 3b
Location of Leakage (right or left side of the gas meter)	Case 1 – Case 4
Effect of extra obstacles present in the metering cabinet	Case 1 – Case 5
Leakage rate (5 or 2 liters per hour)	Case 1 – Case 6
Other type of gas (hydrogen or methane) – ventilation closed	Case 1 – Case 7a
Other type of gas (hydrogen or methane) – ventilation open	Case 2 – Case 7b

4.5.2 CASE 1

In the following sections each of the cases will be further discussed, including the relevant response expected from the results. The objective of first case study was to identify the hydrogen gas behaviour in a standard condition without ventilation. In this case, the nozzle of the hydrogen leakage was in upward direction and both the top and bottom ventilation grilles were closed.

The recovery of the sensors in the cases and evacuating the gas from the metering cabinet was done by opening the ventilation grills and eventually also opening the door of the cabinet. The expected response of the first case might be that none of the hydrogen gas escapes. The hydrogen possibly builds up to high gas concentrations at the top section of the metering cabinet.

4.5.3 CASE 2

The objective of the second case is to identify the effect of ventilation by opening the sliding doors on the ventilation grilles on the door (Figure 4-10). The conditions applied were: The nozzle of the hydrogen leakage was in upward direction and the ventilation grilles were open.

Figure 4-10: The ventilation grilles are manually opened in the second case.

Cariteau et al. (2011) [66] conducted hydrogen experiments to study the location of the vent. It was found that for low leakage rates a higher placed vent is very effective to delay the formation of any high flammable concentrations of hydrogen. There was evidence that the highest vent position should lead to the lowest flammable volume of hydrogen in the compartment. The ambient air enters at the lower vent and hydrogen mixed with air exits on the top ventilation opening. The expected response

of the open ventilation case therefore would be the presence of lower concentrations of gas in the top part of the metering cabinet. The ventilation is an important factor that should have a big effect on the response in this experiment.

In tests with open ventilation, after the hydrogen supply was stopped, the recovery to zero of the gas concentration read by the sensors could give more understanding of the situation and is therefore also included in the results.

4.5.4 CASE 3

Next, the influence of leakage flow direction on the hydrogen leakage and the resulting concentrations was studied in the third case. These are two other directions that occur from having a leakage in the gas pipeline. Apart from a leakage at the top of the pipe the gas can also leak from the side or the bottom of the pipe. The nozzle attached to the pipe configuration of the gas supply could be directed the other way (Figure 4-11).

The expected response of one of the other directions might be the change in concentration build-up in the lower part of the metering cabinet caused by the side and bottom walls. This might cause changes in response time of the sensors on the various height levels.

This case is split in two parts:

a) Where the influence of a leak direction towards the side of the metering cabinet is determined.
b) Where the influence of a leak direction towards the bottom of the metering cabinet is investigated.

(a)

(b)

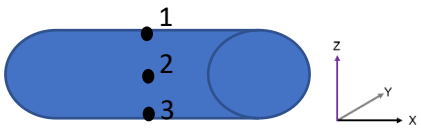

(c)

Figure 4-11: Leakage direction (a) outflow nozzle in Y direction, sideways towards the wall (position 2 in (c)) and (b) outflow nozzle in -Z direction, towards the bottom (position 3 in (c)).

4.5.5 CASE 4

In this fourth case the leakage was located at the left side of the metering cabinet. At this side of the gas meter the service line enters the house. This is the pipeline that transports gas from the gas network to the building (Figure 4-12). The leakage was positioned at the left gas meter connection, 26 cm from the bottom of the metering cabinet.

(a) (b)

Figure 4-12: Outflow on the left side of the metering cabinet: (a) This is the side of the gas meter where the service line (big yellow pipe) enters the building. (b) The change in configuration of the metering cabinet (sensor no. 8 located at the circle).

In this case, the important response is found at the sensors on the ceiling. An extra sensor (sensor no. 8) was positioned at the ceiling at the left side above the gas leak. This sensor was put there to see if this position would be a better position to measure the hydrogen concentration in this case. The other sensors are still in place as well.

4.5.6 CASE 5

The fifth case aims to identify the impact of having extra obstacles inside the metering cabinet. The response that is expected would be that these objects alter the leakage gas flow. The most interesting part of the response was the gas concentration on the different height levels.

Different items will be put left and right of the cabinet. As is seen in Figure 4-13, the following objects were included:

- The standard gas meter and the electrical box with smart meter below (present in the previous cases)
- Tennis bag
- Shoulder bag
- Internet router (Positioned at the left side at the correct height according to **NEN 2768 (2016)**)

Figure 4-13: The metering cabinet with some frequently occurring objects as extra obstacles inside.

4.5.7 CASE 6

In this sixth case the influence of a lower leakage flow rate is studied. The leakage rate in this case was set to 2 liters per hour with the nozzle of the hydrogen leakage pointed in upward direction. In safety regulations for new-built residential buildings, the required standards **(NEN 1078)** [62] sets a maximum leakage rate of 1 L/h for natural gas to ensure a safe living condition. It should be tested if this leakage rate could also be used for hydrogen when concerning the recent guidelines about residential gas safety. A study by **Caanen (Kiwa) (2019)** [16] showed the difference in the outflow of hydrogen with respect to natural gas with the same leak size in pressurized pipe lines. It is done for the two pressures occurring in the Dutch gas network: 25 and 100 mbar.

The difference between natural gas and hydrogen gas could be factored in by including the factor 1.64. At the end of the above-mentioned paper of Kiwa, it was recommended to assume the factor 2 for safety reasons.

This experiment case with a small leakage rate of hydrogen would therefore require a leakage rate of 2 L/h hydrogen which is equal to 34 ml/min. This is very close to the lower limit set-point for the mass flow controller. Consequently, the mentioned leakage rate could not be smaller than 2 L/h.

The response that is expected in this case with smaller leakage rate, is a lower concentration. But in some parts of the metering cabinet there might be build-up of gases. Also, the difference between the top of the cabinet and the location close to the leakage is interesting.

4.5.8 CASE 7

Additionally, two tests with natural gas (methane) have been conducted. The objective of the seventh case is to identify the concentration differences between hydrogen and methane. The conditions applied were similar to the hydrogen experiments. This experiment case was further split into two parts:

a) The ventilation grilles closed.
b) The ventilation grilles opened.

To add to the analysis and compare the difference between natural gas and hydrogen leakage behaviour, two sensors of the hydrogen case and two sensors of a natural gas (methane) case were compared.

In the measurements to investigate the difference, pure methane was used instead of natural gas. The leakage rate of methane was set in the right amount equal to the presence of methane in natural gas. This case represents a situation where the natural gas pipeline network is used for hydrogen distribution. It is assumed that the leakage size for natural gas is the same as the hydrogen leakage. The size of the opening (nozzle) is constant. But, due to a bigger CH4 molecule, the leakage rate of methane would be less. The leakage rate depends on the difference in flow between hydrogen and natural gas.

From the literature it was found that when small leaks are present with the same pressure and the same leak size, hydrogen is leaking about 1.6 to 3 times more in volume than natural gas would be leaking. Or the leakage rate of natural gas is 1.6 to 3 times less than hydrogen. The factor from 1.6 is valid for minor cracks in a 100 mbar pipeline. The factor of 3 is valid for major pipeline damages [16], [67].

Based on the research paper of **Caanen (Kiwa) (2019)** [16] to account for the ratio between hydrogen and natural gas, the factor 1.64 was used. The second factor that was used for the leakage rate of methane is the correction for the amount of methane fraction in natural gas which amounts to 82% (0.82) [15].

In case of hydrogen the leakage rate was equal to 83,3 ml/min (5 L/h). The corrected methane leakage rate, calculated from the hydrogen leakage rate based on the two mentioned factors, was found to be 41,65 ml/min (2,5 L/h). The conversion factor of 0.72 (N_2 to CH_4) was further needed to regulate the right amount of methane with this mass flow controller.

5

Results and discussion

5 Results and discussion

In this next chapter the results are discussed. Starting with two sections of extra tests on the response of the electrochemical sensors and influence of the environment temperature on the measurements. In the third section the experiments of the 7 case studies are discussed with the interpretations of the figures. Ending with a section that gives an overview of sensors that are ranked on the detection time.

5.1 Response correction of the ppm electrochemical sensors

5.1.1 Response correction measurements

Prior to commencing the main measurements, the 4 top electrochemical sensors were analysed to obtain more information about their response to the same hydrogen concentration. The data of these electrochemical sensors has been collected in a separate evaluation of their response (Figure 5-2).

These differences found in the sensors' response could be due to several factors related to the operation of the sensors. The suction flow rate of the sensor could differ in amount of gas that the sensors pump. The lengths of the tubes attached to the sensors vary in length depending on the application of an additional metal tube. The hydrogen gas may take longer to reach the sensor heads.

The differences in the electrochemical sensors can also be a result of the difference in the electrochemical reaction of hydrogen on the sensor active area. The electrochemical reactions in each sensor that cause the transport of electrons that gives the output signal could be different. This method helps to identify the delay of the electrochemical reaction of the sensors.

By supplying the same 5 L/h leakage rate of hydrogen and keeping other measurement parameters constant for every sensor, the output of the sensors indicates a difference in the electrochemical sensors (measuring ppm).

The experiment was run by having the 4 sensors placed at the top center of the metering cabinet with the tubes all together located at the same spot (Figure 5-1). Two tests were done with increasing hydrogen concentration ([H2]) found in Figure 5-3 and Figure 5-4. One test was done with decreasing hydrogen concentration (recovery) found in Figure 5-5. If there is one sensor that has a delay, this will show from the measurement results. A correction factor could later be applied to the one that has a varying response.

Figure 5-1 Inlets of the 4 (electrochemical) sensors positioned together in one spot in the top center of the metering cabinet.

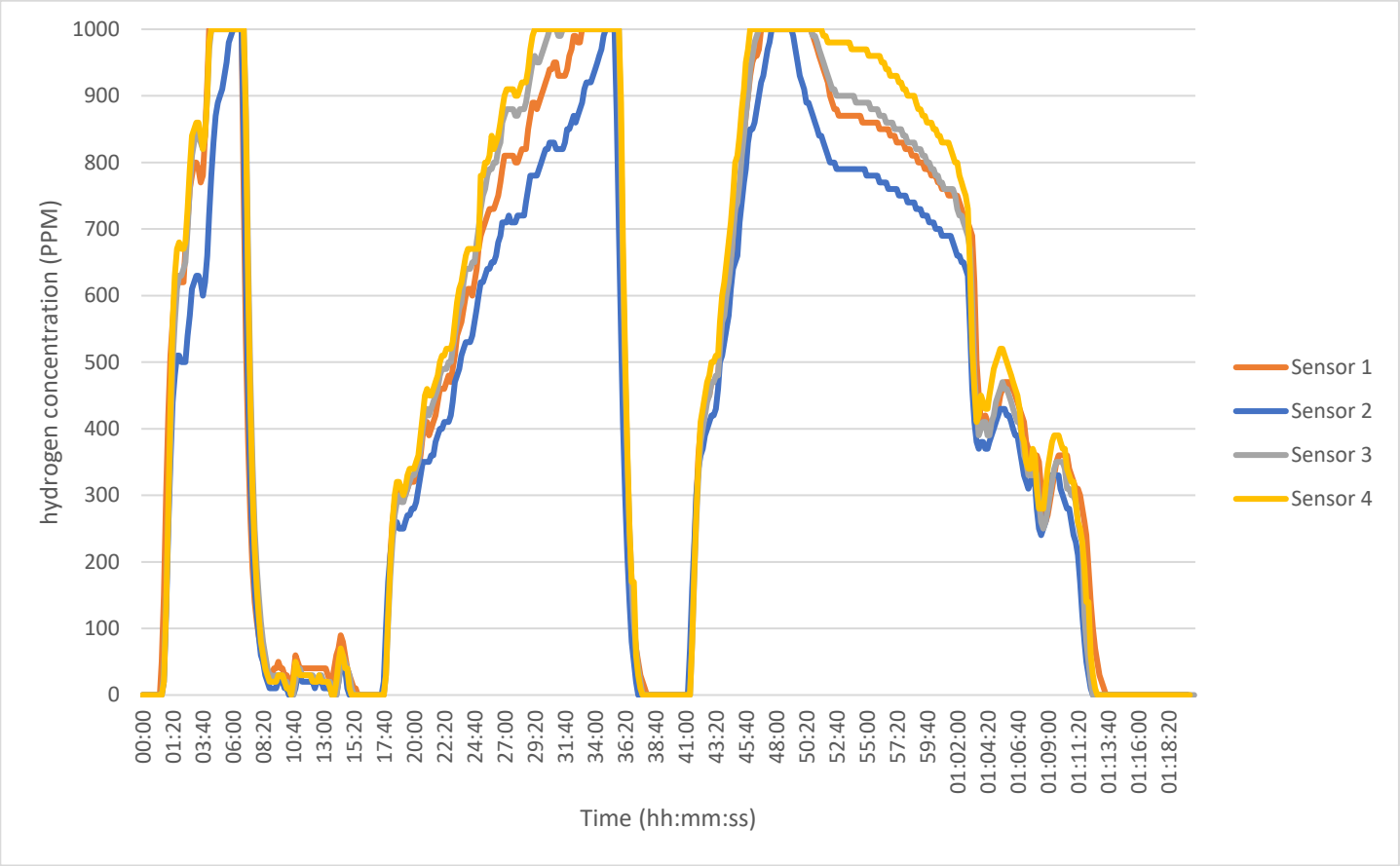

Figure 5-2: Test on the response time of the electrochemical sensors. The results of 4 sensors placed at the top of the metering cabinet with the tubes all together located at the same spot.

5.1.2 Correction factor

By comparing the response of each of the 4 electrochemical sensors (when they are placed in the same position), a correction factor can be defined to cancel the differences in concentration and delays (Table 5-1).

Sensor no. 1 is assigned to have a reference value meaning a correction factor of 1 is given to this sensor. Based on the measured data of the other 3 sensors, a correction factor of these 3 could be determined. During the sensor 3 showed comparable results and therefore got a correction factor of 1. Sensor 2 showed lower the values of the hydrogen concentrations in comparison to sensor 1 and needed a positive correction factor. Sensor 4 slightly showed a higher hydrogen concentration, especially in the upper range. Therefore, a correction factor below 1 is considered to correct it.

Table 5-1: Correction factors to cancel the differences in concentration measurements and delays.

	Correction factor
Sensor 1	**1**
Sensor 2	**1.15**
Sensor 3	**1**
Sensor 4	**0.93**

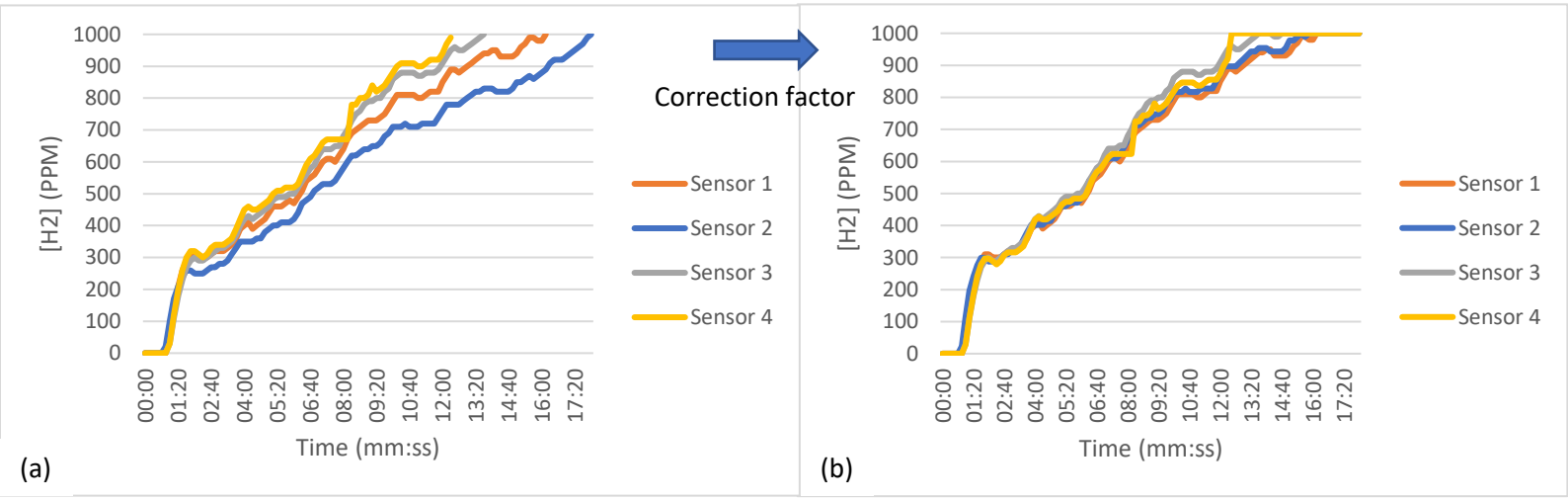

Figure 5-3: (a) Response correction test of increasing hydrogen concentration for the 4 electrochemical ppm-sensors. And (b) after applying the correction factor results in minor differences in the readings of the sensors.

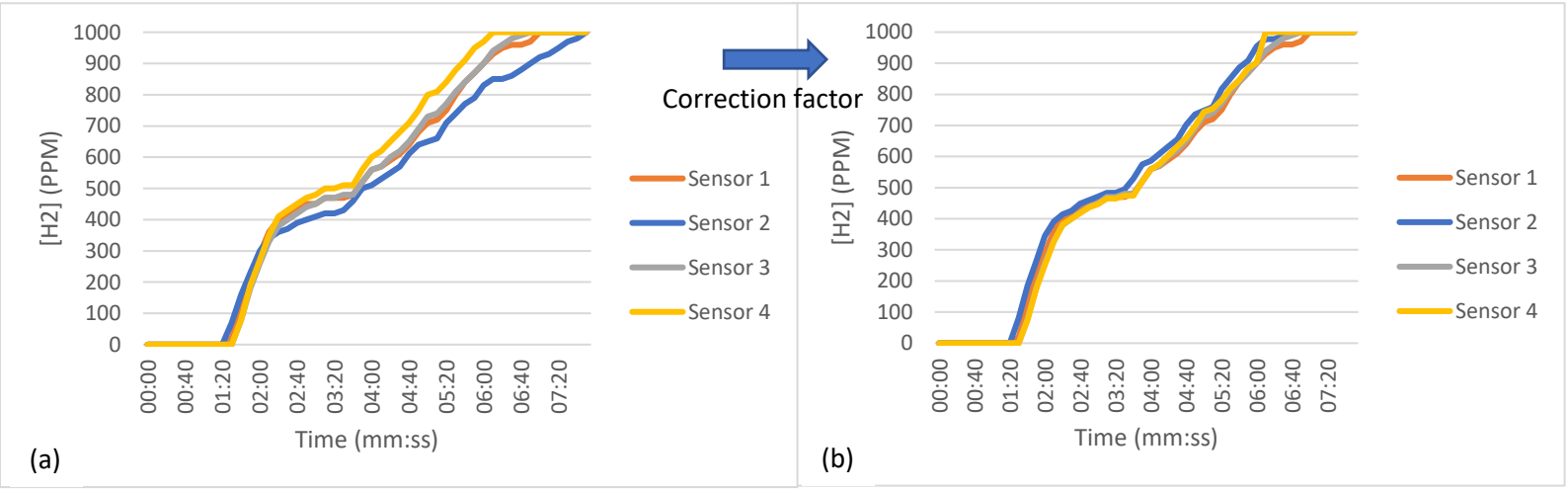

Figure 5-4: (a) Second response correction test of increasing hydrogen concentration for the 4 electrochemical ppm-sensors. And (b) after applying the correction factor results in minor differences in the readings of the sensors.

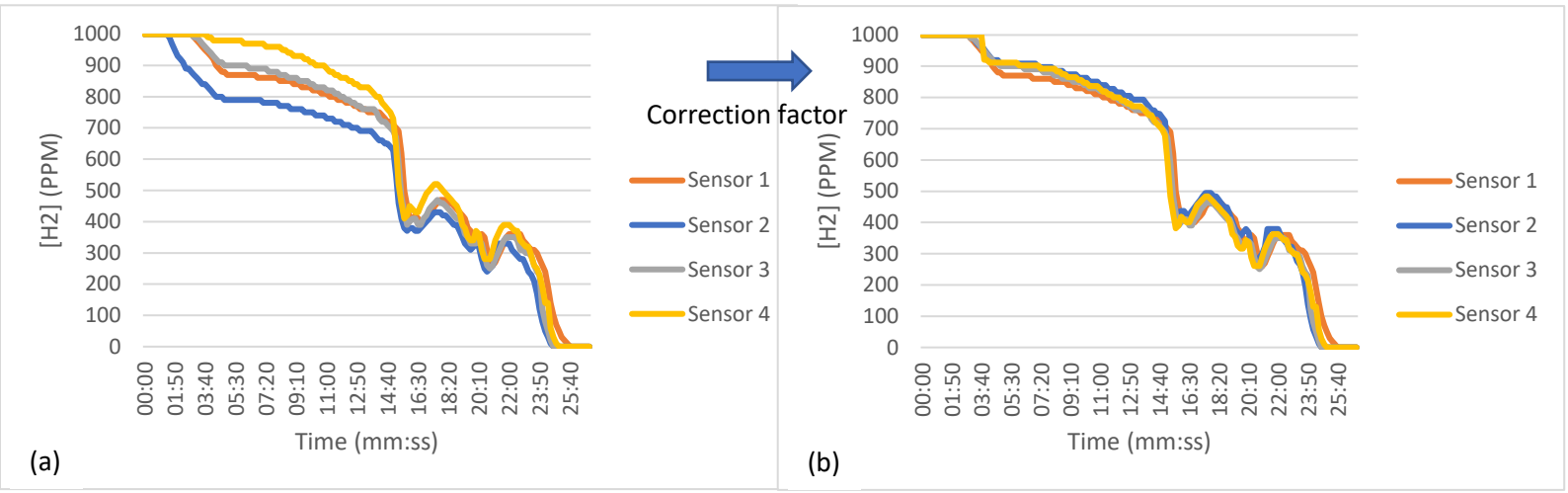

Figure 5-5: (a) Third response correction test of decreasing hydrogen concentration (recovery) for the 4 electrochemical ppm-sensors. And (b) after applying the correction factor results in minor differences in the readings of the sensors.

5.2 Influence of environment temperature on measurements

To establish whether temperature has an influence on the hydrogen detection the results of two tests have been investigated for the 4 more sensitive electrochemical sensors at the top of the metering cabinet.

The ventilation was kept open and there were no obstacles inside the metering cabinet. The outflow of hydrogen was set to 5 liters per hour. The lowest measured temperature (inside the metering cabinet) in the morning was 17.0 °C resulted in a hydrogen concentration of 740 ppm at the ceiling (Figure 5-6). The highest measured temperature in the afternoon was 22.3 °C resulted in a higher hydrogen concentration with a maximum of 1000 ppm (Figure 5-7).

The temperature is generally higher in the afternoon and this causes a higher hydrogen concentration accumulated at the top of the metering cabinet. Room temperature hydrogen will rise to the ceiling and partly exits through the top ventilation grill.

The effect of thermocirculation opposes the ventilation caused by the buoyancy of hydrogen [68]. This effect may occur on a hot day. The outdoor air temperature here is higher than the temperature inside the metering cabinet. While hydrogen accumulates near the ceiling, the warmer air enters the top ventilation grille. This hydrogen near the ceiling could not go out through the top vent. This results in a concentration of hydrogen that is significantly higher in the afternoon than in case of lower morning temperatures.

Other factors could influence the rising velocity of hydrogen. Not only the positively buoyant forces that act on the gas are the only factor. Also density difference, fluid dynamics and atmospheric turbulence due to ventilation influence the rising behaviour of the gas. Furthermore, at afternoon temperatures there is a larger rate of diffusion, because the gas molecules have greater kinetic energy [69].

A situation with large differences in temperature could therefore have some influence on the measurements. Although the measurements were conducted in summer, the weather on days of the measurements was very constant. No days with extreme values of temperature occurred. The days all had temperatures below 25 °C.

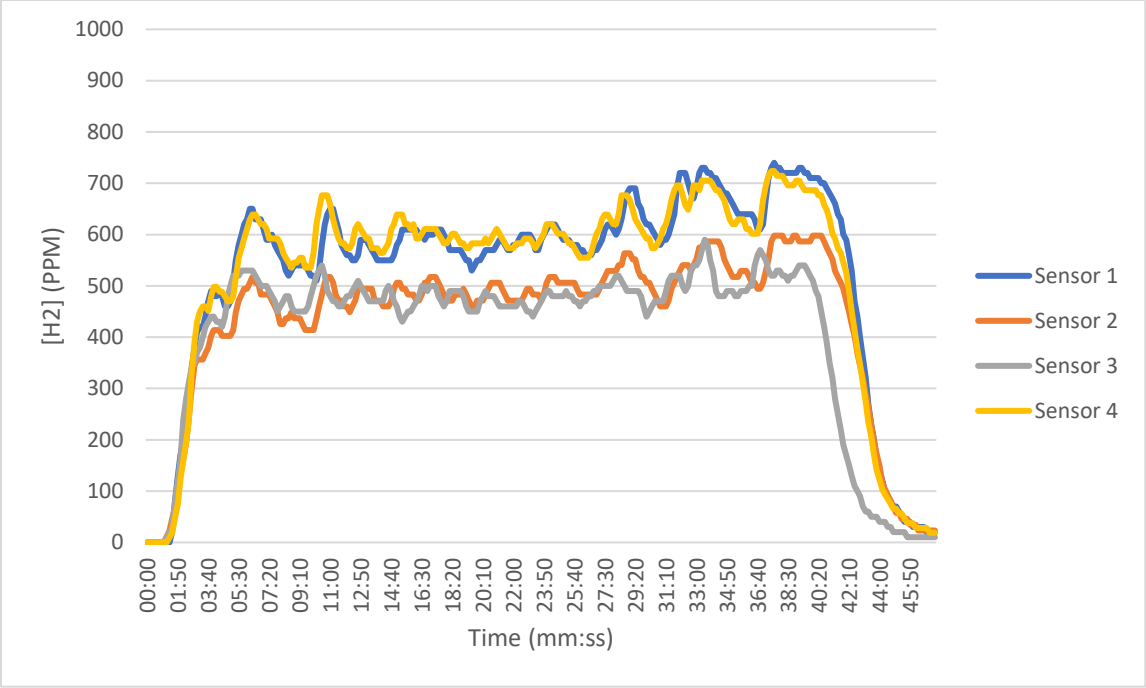

Figure 5-6: Top sensors measuring the ppm concentration levels in a test at a temperature of 17.0 °C in the morning.

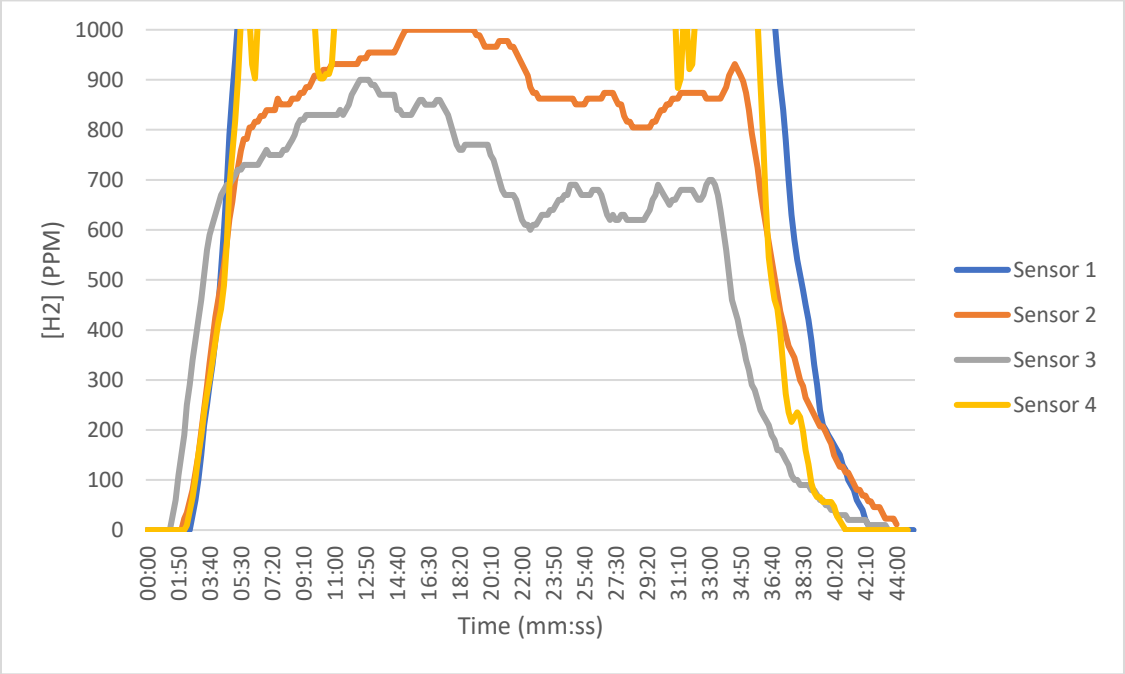

Figure 5-7: Top sensors measuring the ppm concentration levels in a test at a temperature of 22.3 °C in the afternoon.

5.3 Experiments of the 7 case studies

As discussed in the previous section, there has been a focus on 7 case studies under different applied conditions. Inside the metering cabinet the standard items (electrical box and gas meter) were present.

In this study, a total of 7 different conditions (7 cases) are considered. The different conditions applied to every case are clearly shown in Table 4-1 that contains an overview of all the applied conditions per case. By default (case 1 to 5), the leakage rate of 5 L/h hydrogen is used. Case 6 involves a leakage with a lower leakage rate. In case 7 a leakage with natural gas (methane) is simulated.

This results section will continue with a more elaborate discussion of each case with the help of figures representing the measured data. The first two tests with open and closed ventilation are used as references for the rest of the tests to compare the different conditions.

Furthermore, for every test, the detection of the sensors to trigger at a specific hydrogen concentration is tabulated in Table 5-2 until Table 5-12. The detection times of the sensors were determined through inspection of the data. For consistency the retention time is taken into account of the gas transport from the inlet through the sensor tubes.

The next part covers the results from the main experiments. The results in this chapter indicate the behaviour of the gas leakage in 7 different cases. First, the four electrochemical sensors at the ceiling were considered. The attention goes to these accurate sensors in the beginning of each experiment. As discussed, these sensors could only be used up until 1000 ppm hydrogen concentration level. Secondly, above the 1000 ppm level of hydrogen concentration, the readings of the catalytic sensors (%LEL) should be considered. These sensors predict the hydrogen concentrations well above the 3 %LEL concentration level.

5.3.1 Case 1: Closed ventilation

The first case is an evaluation of a gas leakage in the metering cabinet with no ventilation. A leakage of hydrogen of 5 liters per hour was simulated in upward direction.

Starting with the results of the electrochemical sensors in Figure 5-8: While the ventilation of the metering cabinet is closed, the hydrogen gas increased very fast at the beginning of the test. Sensors 1 and 4 in the top middle of the cabinet were the sensors that reached 200 ppm the fastest within 01:48 min. Sensor 1 at the middle-back was the first sensor to reach the 1000 ppm limit (0.1 vol%) at 2:40 min.

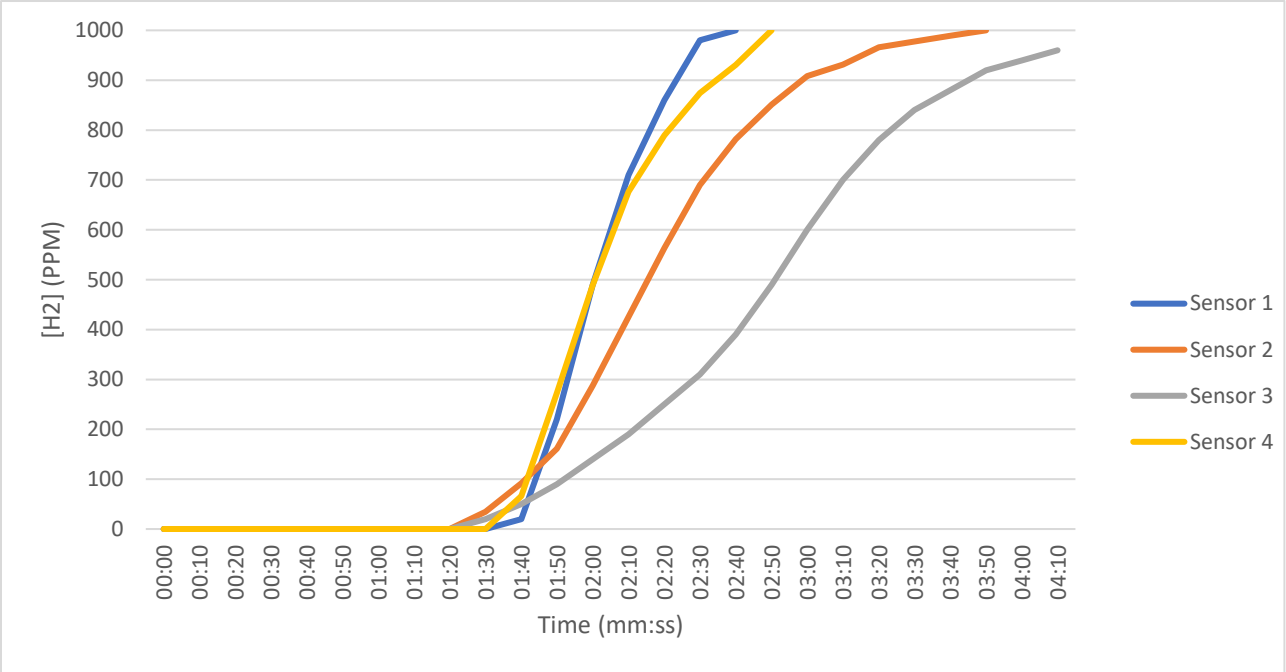

Figure 5-8: Top 4 sensors measuring ppm concentration levels. With 5 L/h upward hydrogen gas outflow and closed ventilation.

Then, the analysis continues with an evaluation of the higher concentrations measured by the catalytic (%LEL) sensors. The results from the top sensors can be seen in Figure 5-9 and from the sensors on the side in Figure 5-10. Results that stand out are the following: Sensors no. 5, 6 and 7 on the side close to the leakage detected 4 %LEL (equal to 1600 ppm) of hydrogen concentration the fastest in 00:58 min (sensor 6) and in 01:28 min (sensor 5 and 7). From the sensors at the ceiling the fastest detection time was 01:48 min by sensor no. 1.

Regarding the side sensors, the first sensor that reached to 10 %LEL was sensor no. 6 in the middle section after 14:08 min. From the top sensors, the detection time to reach this concentration was shortest for sensor no. 1 after 18:58 min.

Sensor no. 6, the sensor mounted on the side just above the middle section (Figure 4-8), showed the highest concentration of hydrogen of 19% LEL after 43:48 min. The electrical box in the middle of the metering cabinet influenced the direction of the gas flow towards this middle sensor.

There was a constant increase in hydrogen concentration levels that kept increasing. The detected maximum was 19% LEL in less than 44 min. The final concentration could have been a higher value than reported and depends on the time of hydrogen leakage into the confined space of a metering cabinet. Without ventilation the concentration continues to increase when a constant flow of hydrogen enters. Therefore, there is a risk to eventually reach the LEL of 4 vol% (100 %LEL) and the present concentrations have a chance to ignite. In this experiment the LEL was not reached as the hydrogen supply was stopped after 46:00 min. The metering cabinet is also not completely airtight which could prevent too high concentrations.

The gas flow into the metering cabinet and the distribution of the gas resulted in a homogeneous distribution of hydrogen gas at the mounted sensor levels. The difference between the sensors was less than 2 %LEL. After 42:00 min the hydrogen gas was homogeneously distributed in the metering cabinet measuring 16 %LEL which is a similar finding as was mentioned in the paper of **M. De Stefano (2019)**[50].

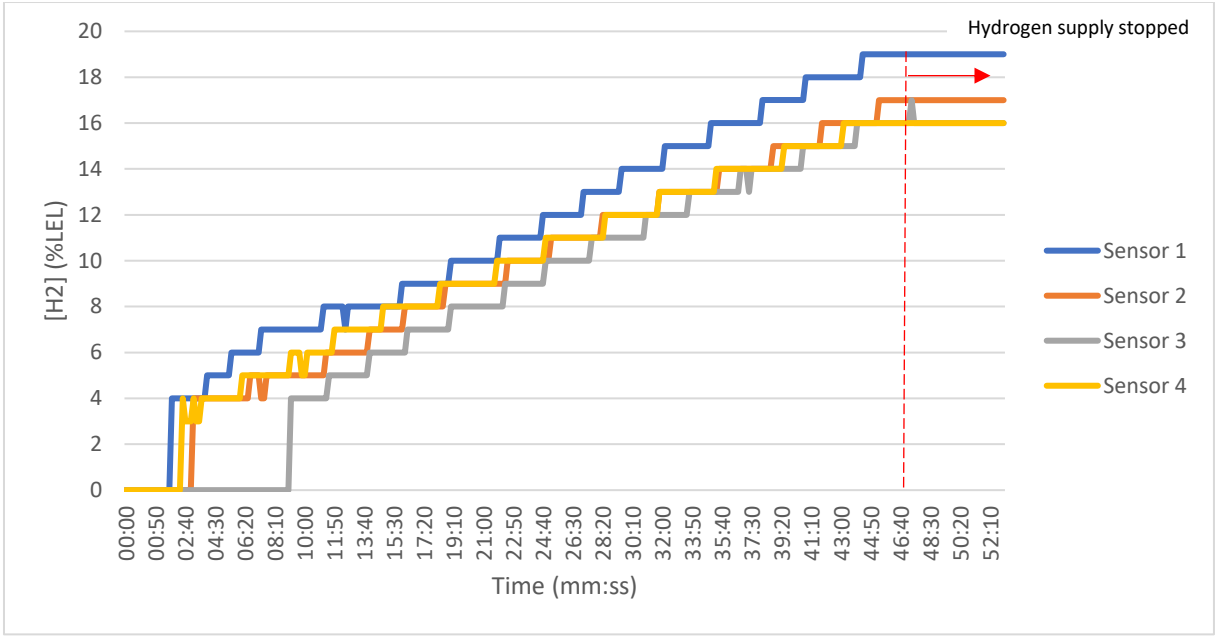

Figure 5-9: Top 4 sensors measuring %LEL concentration levels. With 5 L/h upward hydrogen gas outflow and closed ventilation.

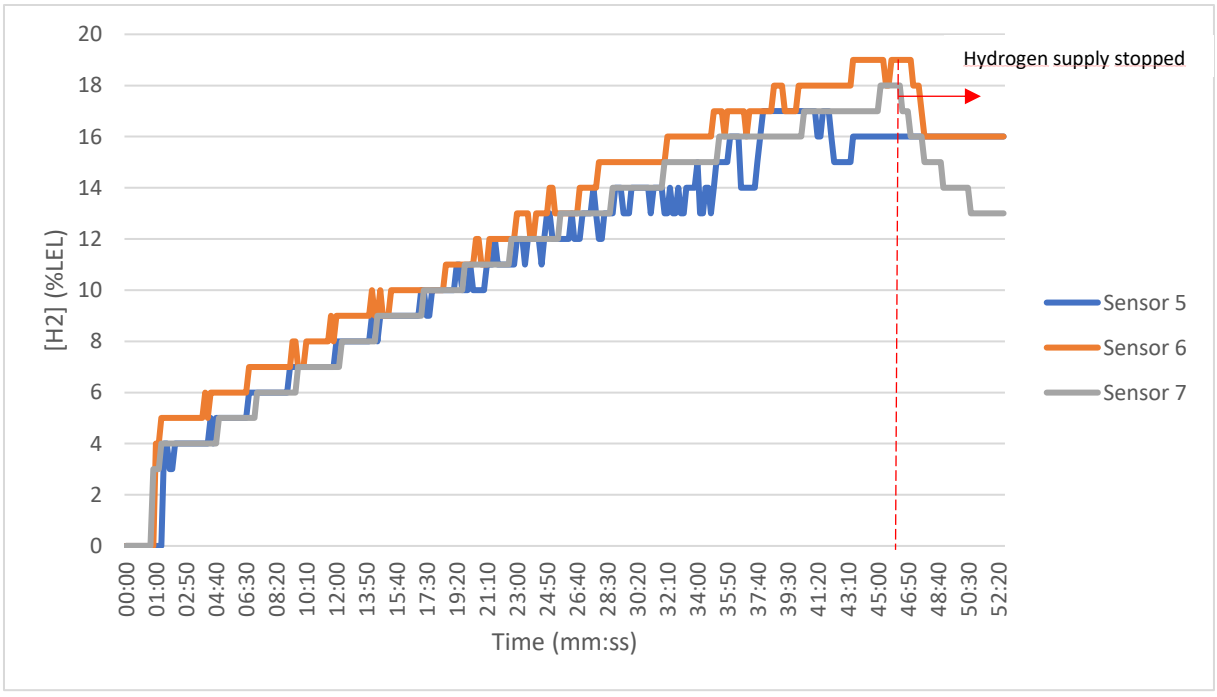

Figure 5-10: Sensors on the side measuring %LEL concentration levels. With 5 L/h upward hydrogen gas outflow and closed ventilation.

Table 5-2: Detection time and maximum concentration per sensor of Case 1: closed ventilation.

Case	sensor	Detection time 200 ppm (mm:ss)	Detection time 4 %LEL (mm:ss)	Detection time 10 %LEL (mm:ss)	Max. concentration (%LEL)
1	1	01:48	01:48	18:58	19
	2	02:08	03:18	22:38	17
	3	02:13	09:08	24:48	17
	4	01:48	02:28	21:48	16
	5		01:28	17:08	17
	6		00:58	14:08	19
	7		01:28	17:28	18

5.3.2 Case 2: open ventilation

In the second case the situation is evaluated of a gas leakage in the metering cabinet with open ventilation. The leakage of hydrogen of 5 liters per hour was simulated in upward direction. The ventilation can be manually opened or closed by opening or closing the doors as seen in Figure 5-11.

Figure 5-11: The ventilation grilles are manually opened in the case of open ventilation.

In the open ventilation case, the ventilation caused fluctuation in the sensor readings (Figure 5-12). When comparing the data of the open ventilation case with the closed ventilation case (Figure 5-8) the detection times to reach to lower concentrations were comparable. But at concentration higher than 850 ppm, the concentration oscillated around this level. The results of the electrochemical sensors showed that sensor no. 3 detected a lower concentration than the other sensors at the cabinet ceiling.

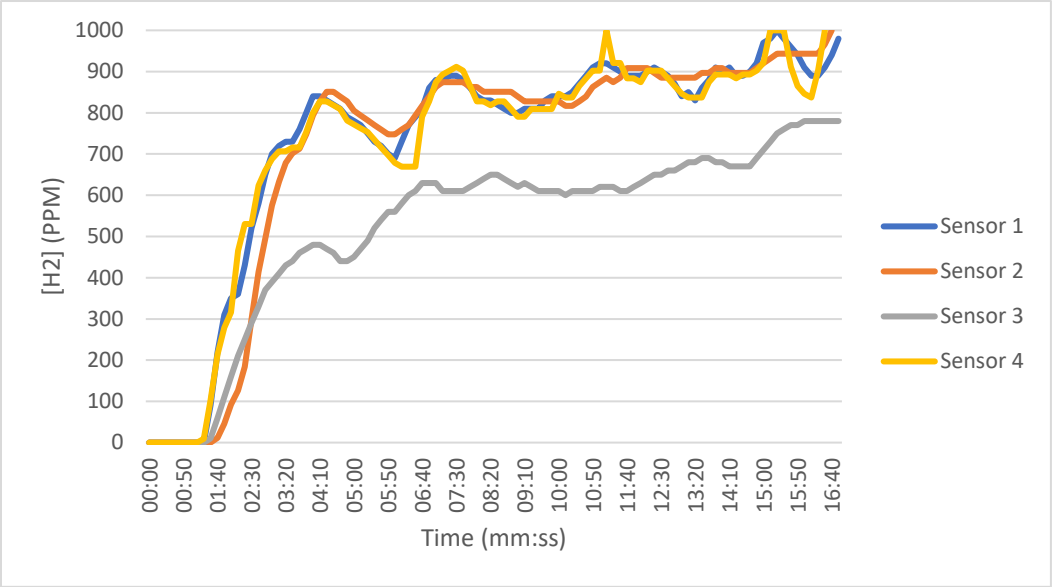

Figure 5-12: Top 4 sensors measuring ppm concentration levels. With 5 L/h upward hydrogen gas outflow and open ventilation.

Then, regarding the catalytic (%LEL) sensors that measured up until larger concentrations. The results from the top sensors can be seen in Figure 5-13 and from the sensors on the side in Figure 5-14. Sensor no. 4 on the ceiling was the sensor with the fastest detection time that reached 4 %LEL after 03:28 min. From the sensors at the side, first sensor no. 7 reached this level after 02:18 min, sensor no. 6 shortly after that (02:28 min), then sensor no. 5 after 02:38 min. The level of 10 %LEL was not reached for all sensor positions in this experiment case.

What is striking from the data in the figures and the Table 5-3 is that a clear fluctuation of the hydrogen concentration can be observed. Furthermore, a maximum concentration of 6 %LEL was observed during the test. None of the sensors reached the 10 %LEL level. After the peaks of 6 %LEL, the concentration level was stable or slightly declined.

The results of the test illustrated that the sensors right above the hydrogen leak at the back of the enclosure detected the highest concentrations. Close to the leak where the bottom sensors were installed (sensor no. 6 and 7), the sensors had a quick response and showed a peak at the beginning of the test and fluctuated during the rest of the test.

The effect of ventilation on the hydrogen concentration results is significant as is obviously seen in Figure 5-13 and Figure 5-14. The build-up of hydrogen concentration was reduced by the extra ventilation causing the concentration levels to drop.

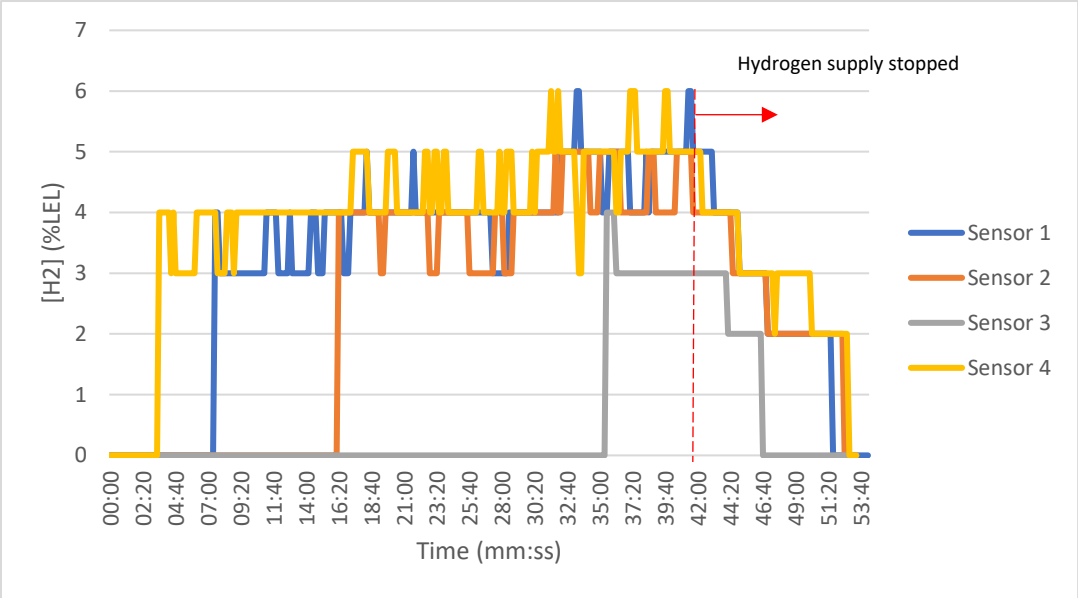

Figure 5-13: Top 4 sensors measuring %LEL concentration levels. With 5 L/h upward hydrogen gas outflow and open ventilation.

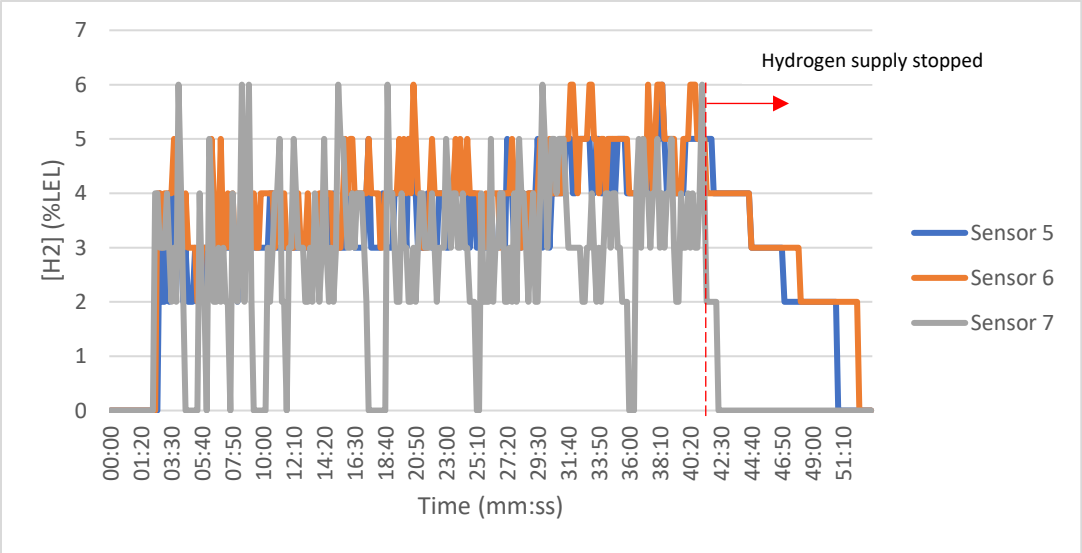

Figure 5-14: Sensors on the side measuring %LEL concentration levels. With 5 L/h upward hydrogen gas outflow and open ventilation.

Table 5-3: Detection time and maximum concentration per sensor of Case 2: open ventilation.

Case	sensor	Detection time 200 ppm (mm:ss)	Detection time 4 %LEL (mm:ss)	Detection time 10 %LEL (mm:ss)	Max. concentration (%LEL)
2	1	01:38	06:38	not reached	6
	2	02:23	16:28	not reached	5
	3	02:08	35:08	not reached	4
	4	01:38	03:28	not reached	6
	5		02:38	not reached	5
	6		02:28	not reached	6
	7		02:18	not reached	6

According to a report paper of **DNV (2020)** [70], that did a similar test in a metering cabinet with ventilation, also fluctuating hydrogen concentrations were observed. The paper describes it as a sinusoidal movement in the figures of the sensors' response.

The situation of the hydrogen-air mixture was explained as being similar to the chimney effect. Inside the chimney of a fireplace the density of the heated air decreases. The gas with lower density and therefore lighter gas rises. Instead, now the addition of hydrogen with a lower density than air causes the lower density of the gas mixture.

Ventilation has a larger influence on the lighter gas and causes a lower hydrogen concentration. When the concentration is lower, this causes the influence of ventilation to decrease. As the inflow of hydrogen continues, the hydrogen concentration increases again and the process repeats.

The risk of the hydrogen leakage is reduced by having open ventilation. The hydrogen mixed with air escaped through the ventilation grilles. Ventilation causes changes in the distribution mechanism, resulting in better mixing of the hydrogen. This hydrogen-air mixture is better distributed and reduces hydrogen concentrations. The concentration fluctuated with a maximum value reached of 6 %LEL.

The paper of **DNV (2020)** [70] also indicated results of maximum concentration for the larger leakage rates of hydrogen and methane. Their extra tests were carried out with permitted leakage rates of 10, 15, 20 and 25 L/h. These last three leakage rates represent inadmissible leakage rates and could give an indication on a worst-case scenario situation. The experiment was done over a longer period of around 7 hours.

The results of the maximum hydrogen concentration reached (in vol%) are shown in Appendix F (Figure F1) for the ventilated metering cabinet. Unfortunately, the maximum concentration for the 5 L/h leakage rate deviates from the rest of the measurements and is lower than the measured maximum concentration of the 3 L/h leakage flow rate.

5.3.3 Case 3: Influence of leak direction

In the next experiment case, the direction of the hydrogen leakage is different than the cases before. First in a) the direction of the leakage with a leakage rate of 5 liters per hour is pointed towards the wall. In the second experiment in b) the hydrogen leakage is pointed towards the bottom.

a) Towards the wall

In the first part of this case, the nozzle of the outflow of hydrogen pointed towards the back wall of the metering cabinet. This is shown in Figure 5-15 below.

Figure 5-15: Flow direction towards the back wall of the metering cabinet (y direction in Figure 4-11 (c)).

Starting with the results of the accurate electrochemical sensors in Figure 5-16: The sensors no. 1 and 2 which were placed at the backside of the metering cabinet showed higher hydrogen concentration levels in comparison with the top sensors. Sensor no. 4 had a slightly longer time of the detection of these levels. Sensor no. 3 showed a lower measured concentration in this case. In the reference test (case 1) with upward outflow and closed ventilation these lower readings of sensor 3 were also observed.

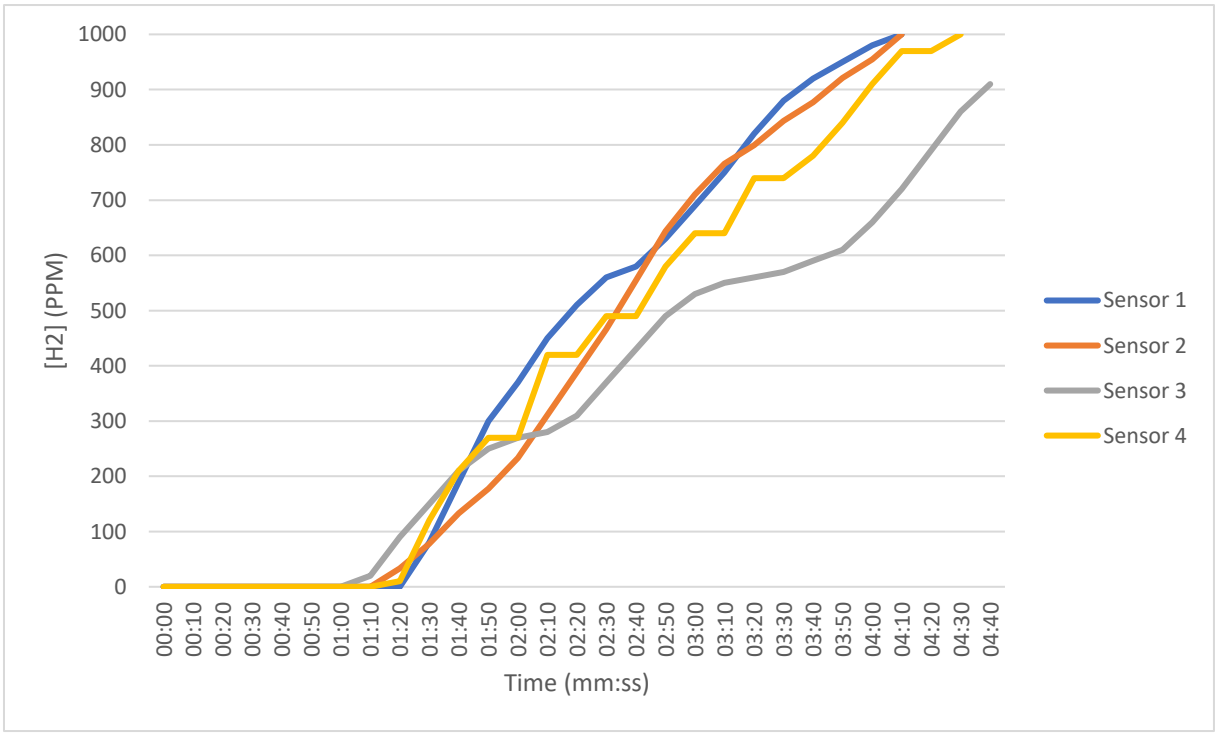

Figure 5-16: Top 4 sensors measuring ppm concentration levels. With 5 L/h hydrogen gas outflow towards the wall and closed ventilation.

Together with these results, the results of the higher concentrations by the catalytic (%LEL) sensors were evaluated. The figure from top sensors' data is seen in Figure 5-17 and the figure from the sensors on the side in Figure 5-18. The fastest detection time to reach 4 %LEL of the side sensors was attained by sensor no. 7. It showed values above 4 %LEL and 10 %LEL after 00:18 min. At the ceiling of the cabinet sensor no. 1 showed a hydrogen concentration of 4 %LEL after 03:08 min.

Sensor no. 7 on the side which was closest to the outflow opening showed a high pike of 19 %LEL after the start. The increased hydrogen concentration was maintained during the whole test and reached a maximum of 20 %LEL. This is explained because the sensor inlets were positioned at the backside of the metering cabinet. The nozzle of the hydrogen leakage was pointed towards the wall and caused the gas to immediately flow into the inlets of the tubes of the sensors. Therefore, the sensor closest to the hydrogen leakage had a peak in concentration readings.

The concentration level of 10 %LEL was reached by sensor no. 1 after 12:58 min. Except from the high reading of sensor no. 7, sensor no. 1 had the second-best detection time and reached the maximum concentration of 12 %LEL. Regarding the other sensors, most of them reached 10% LEL after 16:48 min, except sensor no. 3.

The risk of the build-up of the hydrogen concentration in the lower section of the cabinet is high due to blockage of the flow by the back wall. In this case, the hydrogen gas keeps being added at the position of the lowest sensor.

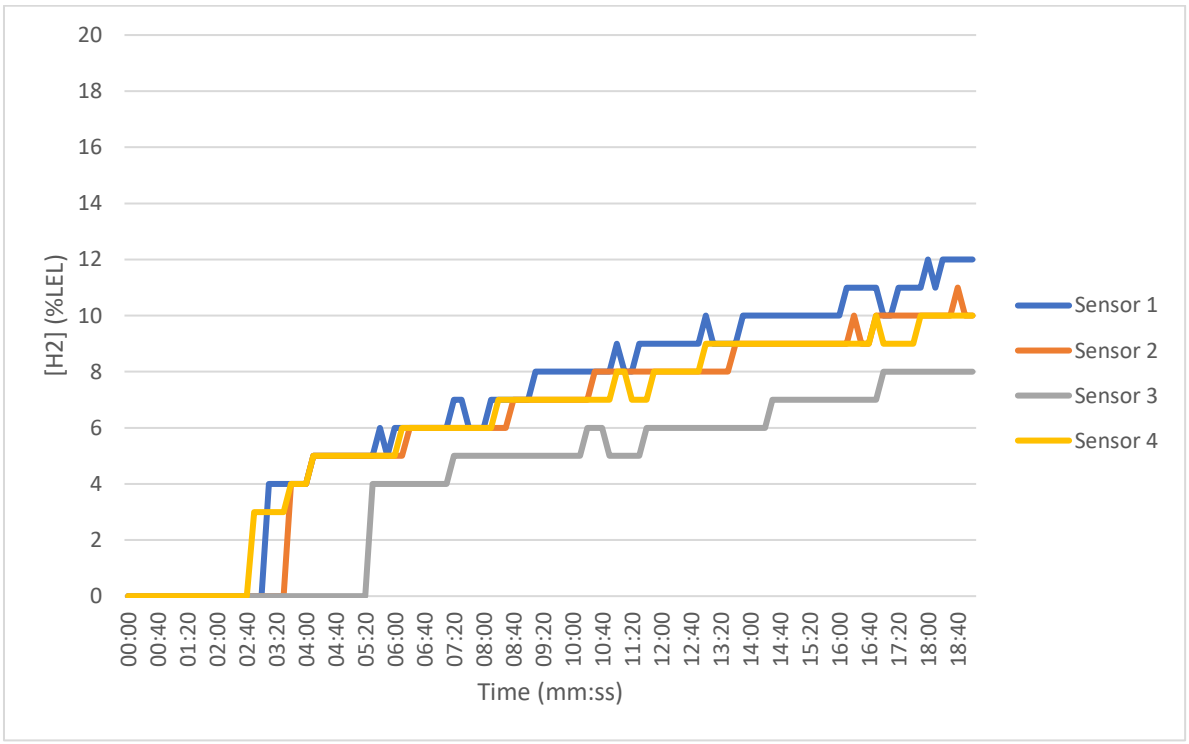

Figure 5-17: Top sensors measuring %LEL concentration levels. With 5 L/h hydrogen gas outflow towards the wall and closed ventilation.

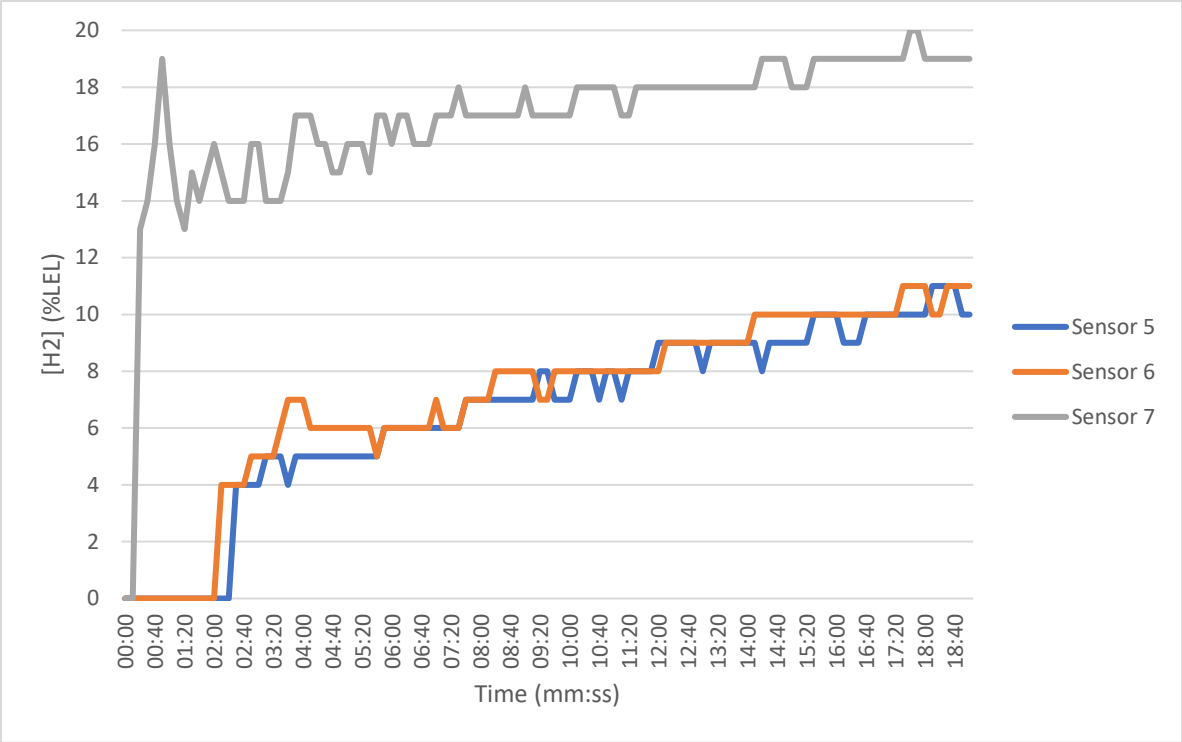

Figure 5-18: Sensors on the side measuring %LEL concentration levels. With 5 L/h hydrogen gas outflow towards the wall and closed ventilation.

Table 5-4: Detection time and maximum concentration per sensor of Case 3-a: Towards the wall.

Case	sensor	Detection time 200 ppm (mm:ss)	Detection time 4 %LEL (mm:ss)	Detection time 10 %LEL (mm:ss)	Max. concentration (%LEL)
3 - a	1	01:43	03:08	12:58	12
	2	02:27	03:58	16:18	11
	3	01:47	05:58	not reached	8
	4	01:38	03:38	16:48	10
	5		03:26	15:28	11
	6		02:08	14:08	11
	7		00:18	00:18	20

b) Towards the bottom

In the next part of this experiment case, the direction of the nozzle of the gas outflow is pointed towards the bottom as is illustrated with Figure 5-19**.** The hydrogen leakage rate of 5 liters per hour is still maintained.

Figure 5-19: Flow direction towards the bottom of the metering cabinet (-z-direction in Figure 4-11 (c)).

The results of the electrochemical sensors are found in Figure 5-20: Sensors no. 1,2 and 4 showed the same levels of concentrations. These sensors steadily reached the 1000 ppm level around the same time (less than 20 second difference). Sensor no. 3 showed a lower concentration around 600 ppm at the same leakage period.

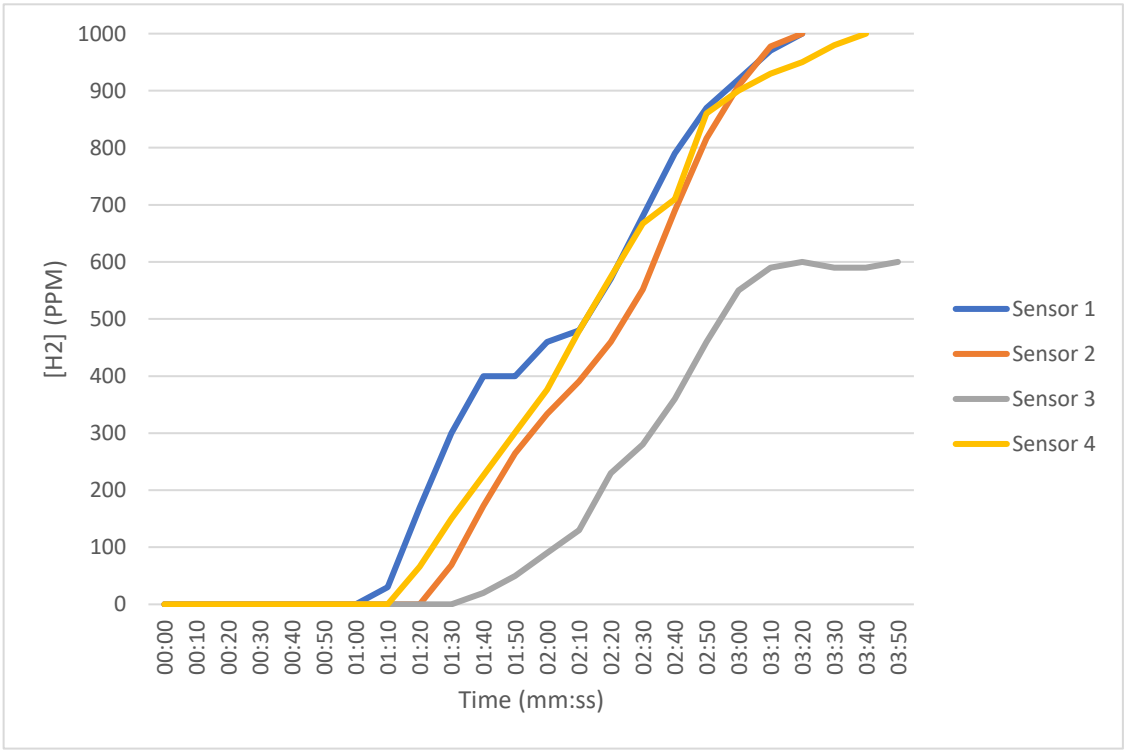

Figure 5-20: Top sensors measuring ppm concentration levels. With 5 L/h hydrogen gas outflow towards the bottom and closed ventilation.

The results of the higher concentrations by the catalytic (%LEL) sensors were evaluated. The data from top sensors are illustrated in Figure 5-21 and data from the sensors on the side in Figure 5-22. In this case the four positions of the sensors at the ceiling are very similar to when 4 %LEL was detected.

In this case the four positions of the sensors at the ceiling are very similar to when 4 %LEL (equal to 1600 ppm) was detected. Sensor no. 4 was the first sensor to detect 4 %LEL and showed a detection

time of 02:08 min and sensors no. 1 and 2 reached 4 %LEL after 02:28 min. Sensor no. 3 detected the same concentration in 08:28 min. The order of hydrogen detection was similar to the results of ppm sensors. The first sensor that reached 10 %LEL hydrogen concentration was sensor no. 1 which detected this concentration within 16:28 min.

From the side sensors, sensor no. 6 (located in the middle height of the cabinet) showed the fastest detection time of 00:48 min to reach 4 %LEL. Sensor no. 6, also reached the 10 %LEL level shortly after that (16:38 min).

Comparing the results of figures of the top and side sensors, the sensors on the ceiling and on the side showed very similar increasing levels of concentration from 5:00 min until 18:00 min. The nozzle with the outflow of hydrogen pointed towards the bottom made the gas spread very evenly throughout the metering cabinet. Both the top sensors and the side sensors reached the same 10 % LEL level all after 19:28 min except for sensor no. 3.

The risk of high hydrogen concentrations involved with outflow towards the bottom is less than the upward outflow. It caused a better mixture of hydrogen in the air and let the gas disperse more homogeneously in the compartment.

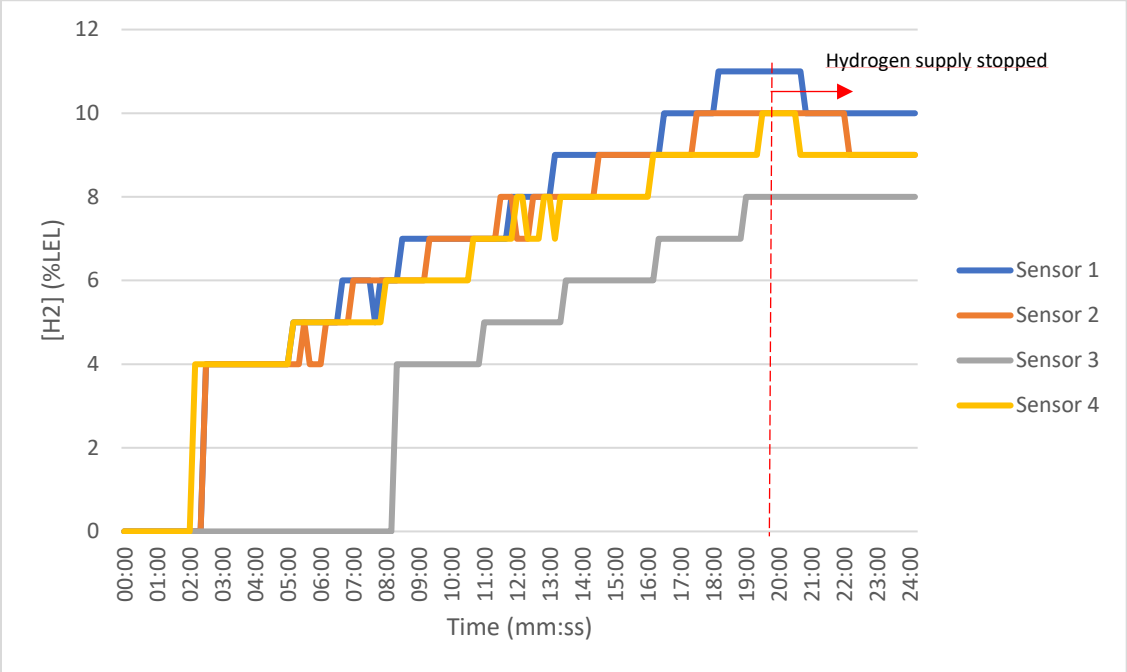

Figure 5-21: Top sensors measuring %LEL concentration levels. With 5 L/h hydrogen gas outflow towards the bottom and closed ventilation.

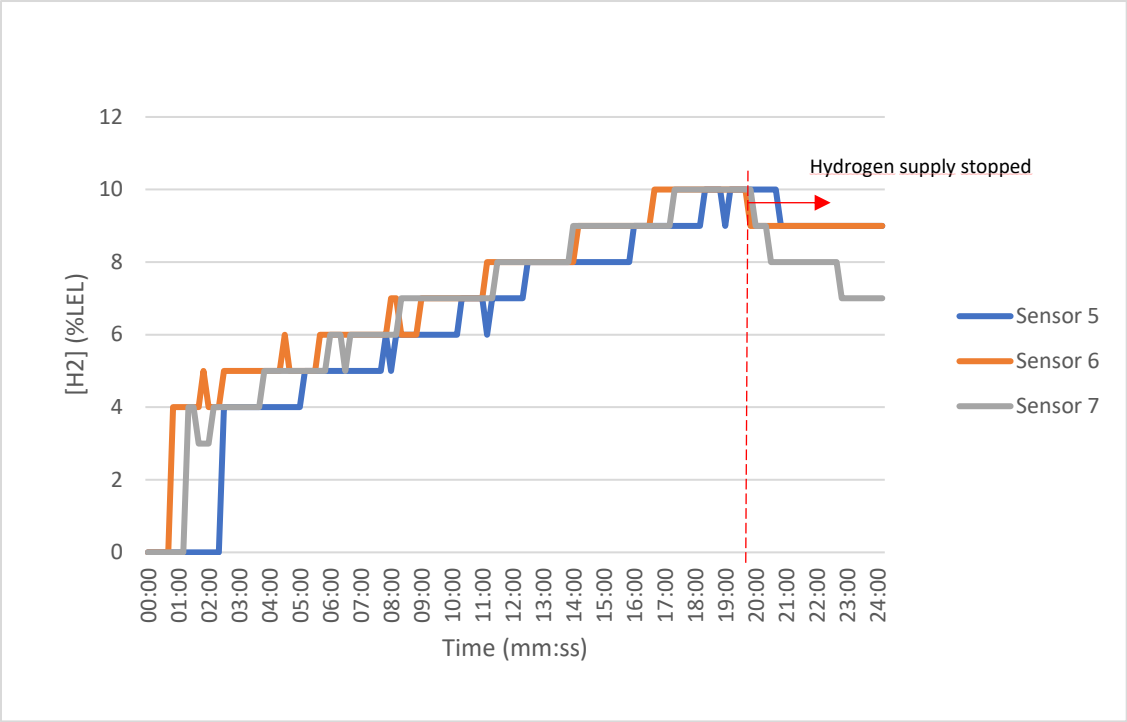

Figure 5-22: Sensors on the side measuring %LEL concentration levels. With 5 L/h hydrogen gas outflow towards the bottom and closed ventilation.

Table 5-5: Detection time and maximum concentration per sensor of Case 3-b: Towards the bottom.

Case	sensor	Detection time 200 ppm (mm:ss)	Detection time 4 %LEL (mm:ss)	Detection time 10 %LEL (mm:ss)	Max. concentration (%LEL)
3 – b	1	01:23	02:28	16:28	11
	2	02:43	02:28	17:28	10
	3	03:28	08:28	not reached	8
	4	02:38	02:08	19:28	10
	5		02:18	18:18	10
	6		00:48	16:38	10
	7		01:18	17:18	10

In summary, the direction of the nozzle of the leakage pointed towards the wall caused the gas to immediately flow into the inlets of the tubes of the sensors positioned at the backside of the metering cabinet. This is why the sensor closest to the hydrogen leakage had a peak in concentration readings. The behaviour of the hydrogen concentration measured at the sensors at the ceiling of the cabinet was comparable with the case with closed ventilation (case 1).

The direction of the nozzle pointed towards the bottom made the gas spread very evenly throughout the metering cabinet. It showed only small differences between the concentrations measured by the sensors.

5.3.4 Case 4: Leakage on the Left side of the metering cabinet

In the next experiment case, the side of the hydrogen leakage was assumed to be at the left side of the metering cabinet (Figure 4-12). An extra sensor was located on the top left side of the metering cabinet (sensor no. 8) to measure the hydrogen concentration. This is the side where the service line enters the house.

Figure 5-23 shows the results of the sensors positioned at the ceiling. The left side sensor (sensor no. 8 in this case) was the first one that detected hydrogen (200 ppm) after 38 seconds. Sensor no. 1 at the middle back was the first one that showed the highest reading (1000 ppm).

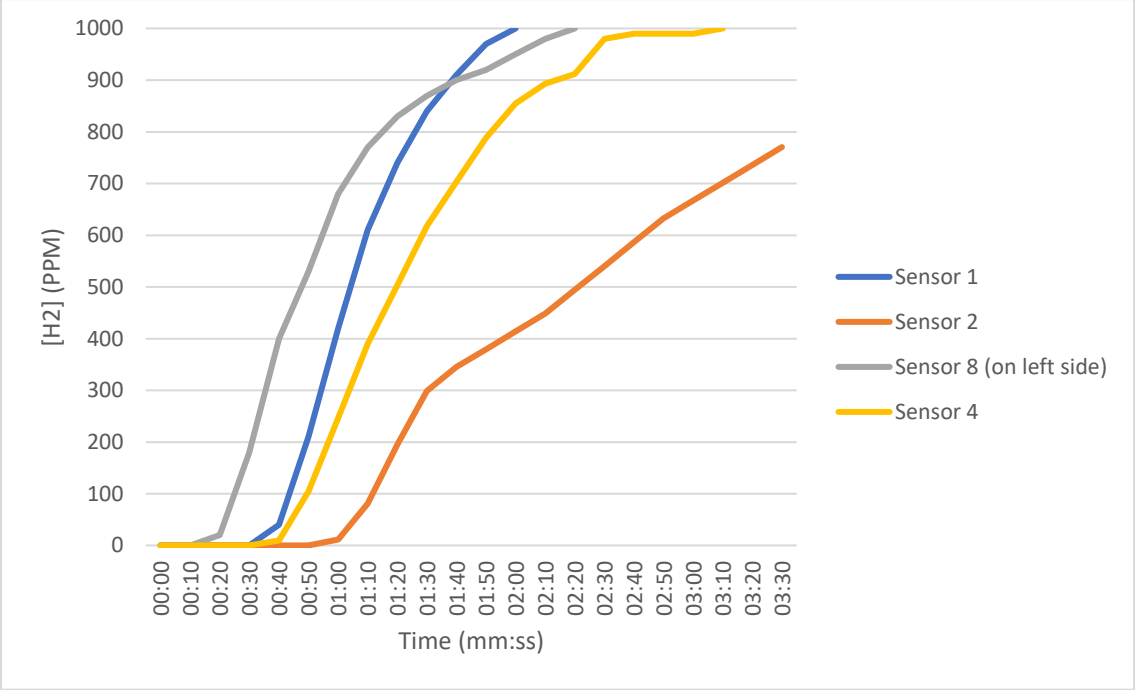

Figure 5-23: Top sensors measuring ppm concentration levels. With 5 L/h upward hydrogen gas outflow on the left side of the metering cabinet and closed ventilation.

With regard to the LEL sensors, the data from top sensors and the sensors on the side are seen in Figure 5-24 and Figure 5-25, respectively. The test showed similar detection times for the top sensors compared to the other cases before this test. Sensor no. 1 at the ceiling reached 4 %LEL after the shortest time: 01:08 min. Sensor no. 4 (also in the middle of the ceiling) reached to 4 %LEL after sensor no. 1 with a detection time of 01:38 min.

In contrast to the ppm sensors results, the sensor no. 8 at the left side was not the first sensor that reached to 4 %LEL. Sensor no. 1 in the top middle was the one that measured the highest concentration and reached to 10 %LEL after 14:48 min.

By looking at the results of the side sensors, a variation in the concentration distribution is noticed. Here, the top sensor on the side, sensor no. 5, was the first that measured any hydrogen concentration. The bottom two sensors sensor no. 6 and sensor no. 7 measured the hydrogen concentration after sensor no. 5. This is because the gas flow during this test ascended to the ceiling of the metering cabinet from the left side and then came down from the top to the bottom at the right side of the cabinet.

The same as Case 1 (with the leakage in the right side), a leakage on the left side caused highest hydrogen concentrations in the top-center of the metering cabinet. After a period of 5 min. of leakage the sensor in the top-center (sensor no. 1) is reading higher concentrations than the sensor on the left side (sensor no. 8). This is an equal finding compared to the results on the right side. The risk of having a leakage on the left side is therefore similar to a leakage on the right. However, in reality the pressure in the service line is higher. This influences the leakage rate and therefore the maximum concentrations that could be reached.

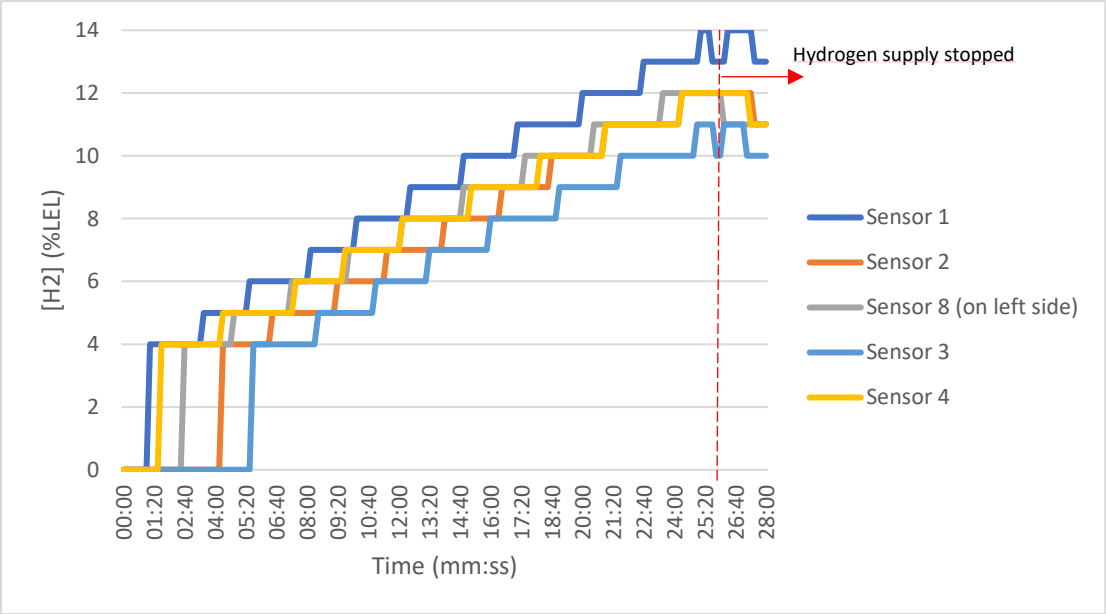

Figure 5-24: Top sensors measuring %LEL concentration levels. With 5 L/h upward hydrogen gas outflow on the left side of the metering cabinet and closed ventilation.

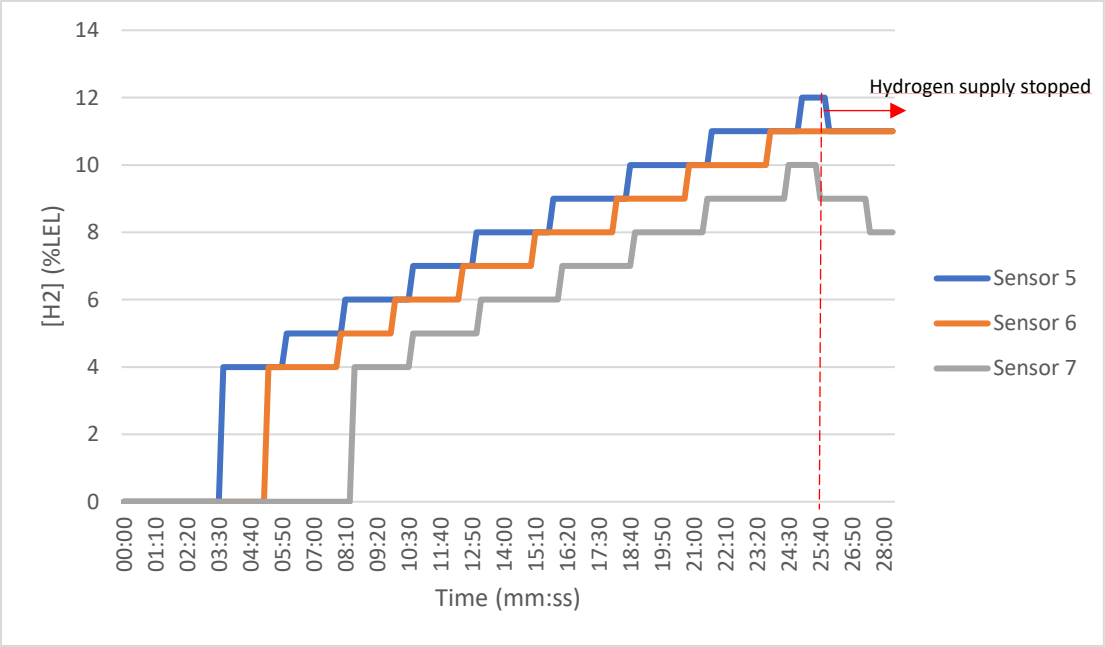

Figure 5-25: Sensors on the side measuring %LEL concentration levels. With 5 L/h upward hydrogen gas outflow on the left side of the metering cabinet and closed ventilation.

Table 5-6: Detection time and maximum concentration per sensor of Case 4: Leakage on the left side.

Case	sensor	Detection time 200 ppm (mm:ss)	Detection time 4 %LEL (mm:ss)	Detection time 10 %LEL (mm:ss)	Max. concentration (%LEL)
4	1	00:48	01:08	14:48	14
	2	01:13	04:18	18:38	12
	3		05:58	17:28	11
	4	00:53	01:38	18:08	12
	5		03:58	18:38	12
	6		05:18	20:48	11
	7		08:48	24:28	10
	8	00:38	03:08	21:38	12

5.3.5 Case 5: Extra obstacles present in the metering cabinet

In the next case a number of items were put as extra obstacles inside the metering cabinet. These objects are commonly seen inside the metering cabinet. The extra obstacles were positioned at the right side of the metering cabinet, the same side of the hydrogen leakage. By putting objects in the metering cabinet, it might cause changes in the air flow circulation. The objects that were included could be found in Figure 4-13.

With extra obstacles present, as seen in Figure 5-26: The hydrogen gas concentration at the top sensors increased in a similar way. The applied conditions caused an even distribution of the concentration read by the top sensors. This could be because of the hydrogen flow blockage by the extra obstacles, the disturbances in the flow made the gas slowly move upwards. Also, the time it took to reach 1000 ppm is longer than the tests before (case 1 and 3).

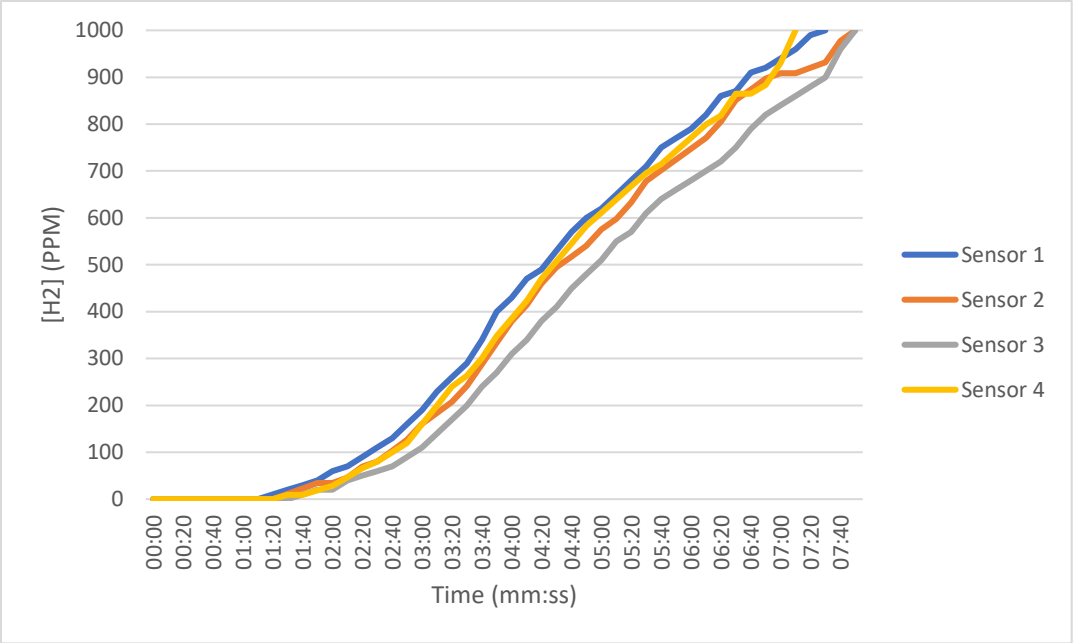

Figure 5-26: Top sensors measuring ppm concentration levels. With 5 L/h upward outflow and closed ventilation. Extra obstacles were present inside the metering cabinet.

The results from top sensors and the sensors on the side are shown in Figure 5-27 and Figure 5-28, respectively. The fastest detection time of 4 %LEL was achieved by sensor no. 1 within 07:08 min. Regarding the side sensors, sensor no. 7 showed the quickest response in 00:38 min.

Moreover, the concentration level of 10 %LEL was observed after 15:38 min by sensor no. 2 which was the fastest detection time. In the top of the metering cabinet sensors no. 1 and 2 reached the highest concentrations (13 and 12 %LEL respectively).

The same rising concentration levels were observed in Figure 5-28. A small early peak in hydrogen concentration is seen where the bottom sensors no. 6 and 7 reached 5 %LEL. The lowest sensor (sensor no. 7) closest to the leakage showed this level after 38 seconds in the beginning of the test. This could occur because of the blockage of the hydrogen gas caused by the extra obstacles at the right side close to the leakage. The high hydrogen concentration near the leakage location is therefore larger at the start of the experiment, with the presence of extra obstacles. However, dangerous concentrations (above 20 %LEL) were not reached. The highest concentration that was reached, was 13 %LEL in the top-center of the metering cabinet.

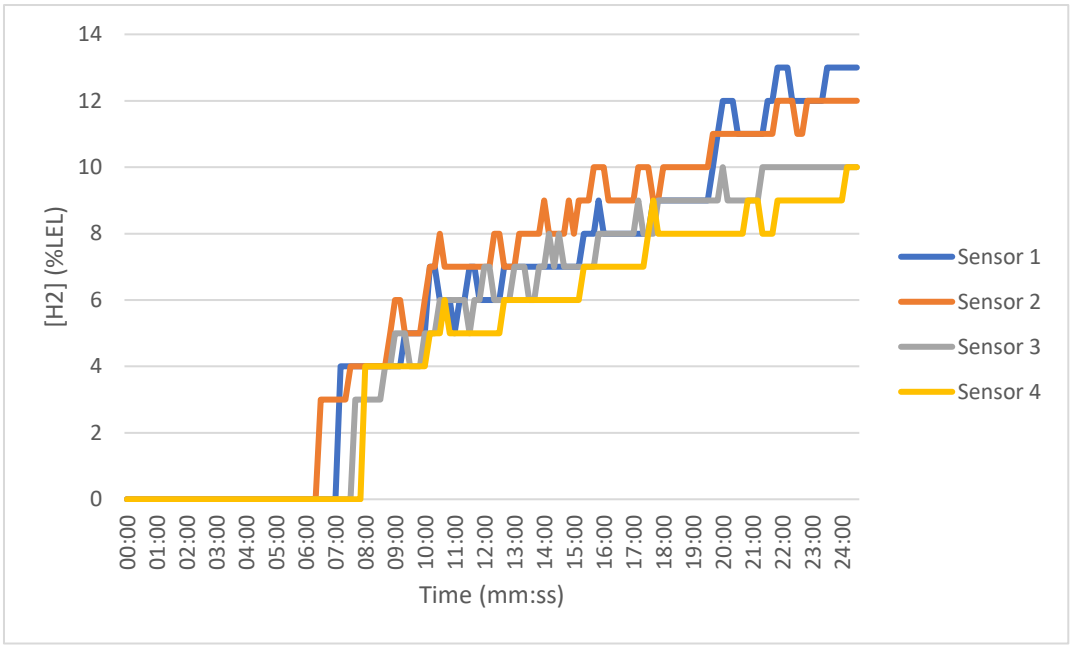

Figure 5-27: Top sensors measuring %LEL concentration levels. With 5 L/h upward outflow and closed ventilation. Extra obstacles were present inside the metering cabinet.

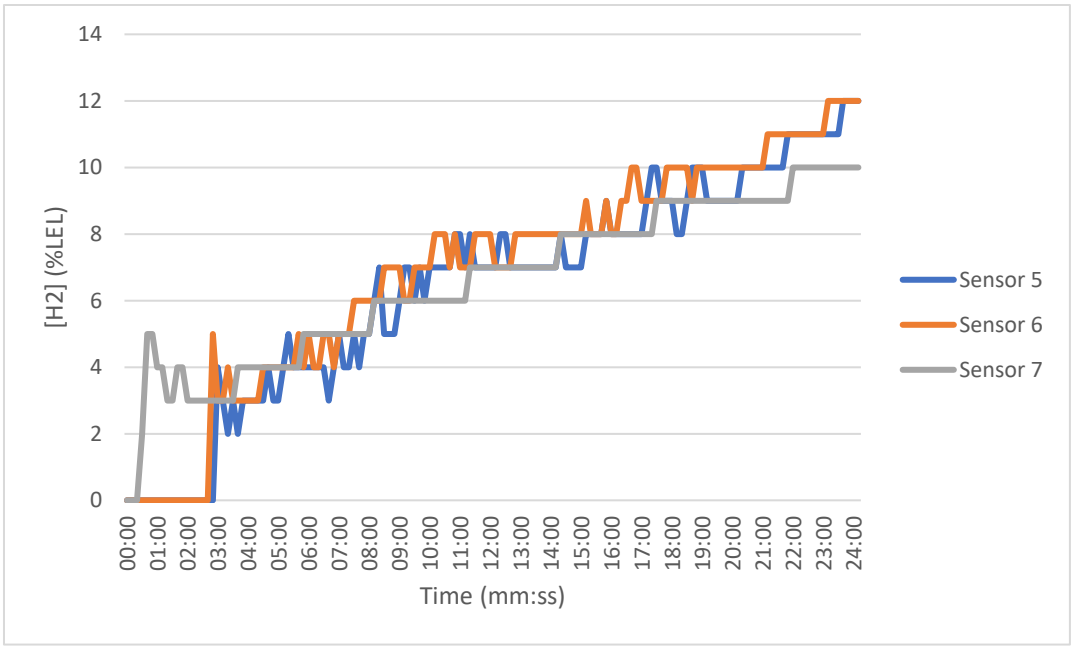

Figure 5-28: Sensors on the side measuring %LEL concentration levels. With 5 L/h upward outflow and closed ventilation. Extra obstacles were present inside the metering cabinet.

Table 5-7: Detection time and maximum concentration per sensor of Case 5: Extra obstacles present.

Case	sensor	Detection time 200 ppm (mm:ss)	Detection time 4 %LEL (mm:ss)	Detection time 10 %LEL (mm:ss)	Max. concentration (%LEL)
5	1	03:08	07:08	19:38	13
	2	03:28	07:38	15:38	12
	3	03:38	08:48	19:58	11
	4	03:08	08:08	23:28	10
	5		02:58	17:18	12
	6		02:48	16:38	12
	7		00:38	22:18	10

The time to reach the same concentration levels at the ceiling in the case without the extra obstacles (case 1) was comparable to the case with extra obstacles (case 5). Results showed that the hydrogen distributed evenly towards the top during the first part of the test. An explanation for this is found in the research performed by **M. De Stefano (2019)**[50]. The paper investigates that in case of laminar behaviour, the distribution of hydrogen does not change and after the first phase of injecting hydrogen, the concentration is comparable to that of an enclosure without the extra obstacles. However, in the case of a hydrogen leakage with more energy or closer to the location of the leakage, this report states that the flow of the hydrogen gas leakage will lose its kinetic energy when it impacts the obstacle. Because of the obstacles, there were significant differences in the concentration of hydrogen that diffuses horizontally across the cabinet.

5.3.6 Case 6: Test with a lower leakage rate of hydrogen (2 liters per hour)

In the following experiment case, the leakage rate of the hydrogen leakage is set to 2 liters per hour instead of 5 liters per hour with the hydrogen leakage nozzle pointed in upward direction and closed ventilation. The size of the nozzle opening was kept the same and only the velocity of the flow was changed. A more elaborate explanation of this case number could be found in the experiment overview in section 4.5.

The test with the small leakage rate resulted in substantial difference in the hydrogen detection to the higher leakage rate. As seen in the achieved data from the electrochemical sensors in Figure 5-29, the time to detect any concentration above 200 ppm was 2,5 times longer than it took for hydrogen with the 5 liters per hour leakage rate. The first sensor that showed 200 ppm was sensor no. 4 within 04:38 min.

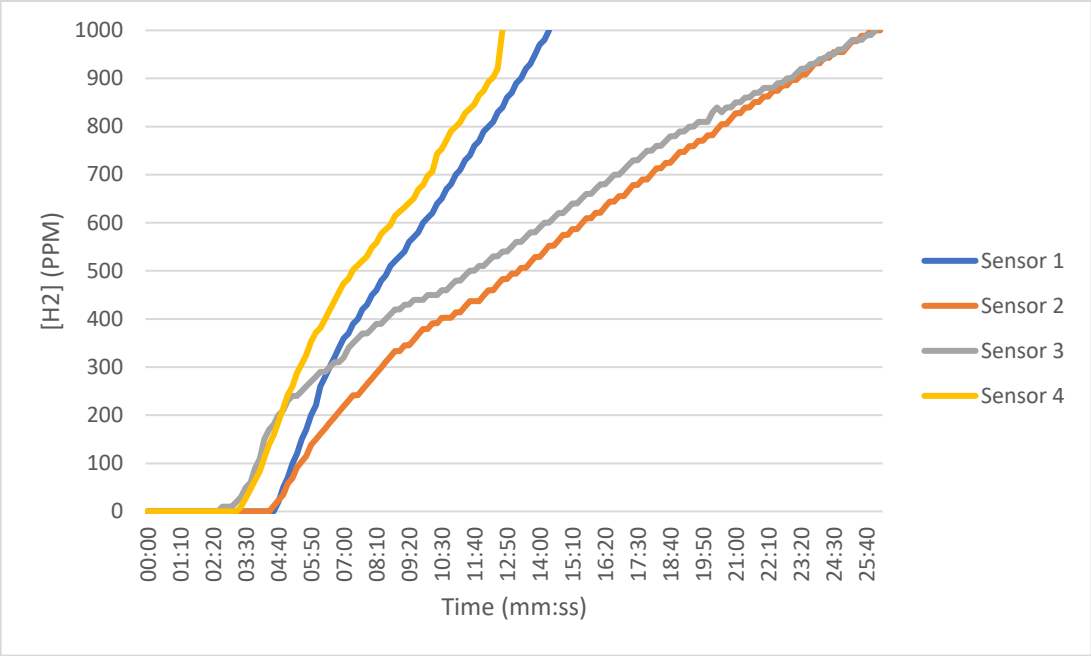

Figure 5-29: Top sensors measuring ppm concentration levels. With a lower leakage rate of 2 L/h in upward direction and closed ventilation.

Results of the hydrogen concentrations above 1000 ppm measured by the catalytic (%LEL) sensors are shown in Figure 5-30 and Figure 5-31. On the side of the metering cabinet, the closest one to the leakage, sensor no. 7 reached the 4 %LEL level only after 00:28 min. Sensor no. 1 at the ceiling had the second fastest 4% LEL detection time after 25:38 min.

The hydrogen concentration level of 10 %LEL was not reached anywhere in the cabinet compartment and was therefore not detected. With the lower leakage rate of 2 L/h, the concentration of hydrogen close to the ventilation opening was also significantly lower compared to the higher leakage rate (5 L/h) tests. This might be caused by more air inflow from ventilation compared to incoming hydrogen gas.

After setting the hydrogen leakage rate, the closest sensor to the leak location (sensor no.7), detected the hydrogen immediately. It is also the only sensor that reached above the 6 %LEL. This result may be explained by the fact that sensor no. 7 was closest to the nozzle where extra hydrogen was entering the cabinet. Because the leakage rate was low, only the closest sensor measured this higher concentration level of 8 %LEL. Other sensors on the top and on the side showed significant concentration levels above 4 %LEL from 25:38 min.

Overall, in the test with the lower leakage rate (2 L/h), there was less risk involved compared to the reference test (5 L/h). The period until significant concentrations were reached was longer (Table 5-8).

Table 5-8: The detection times from sensor 1 and sensor 4 for low (2 L/h) and higher leakage rate (5 L/h).

	Detection time 4 %LEL Sensor 1 (mm:ss)	**Detection time 4 %LEL Sensor 4 (mm:ss)**
Low leakage rate (2 L/h)	25:38	27:58
High leakage rate (5 L/h)	01:48	02:28

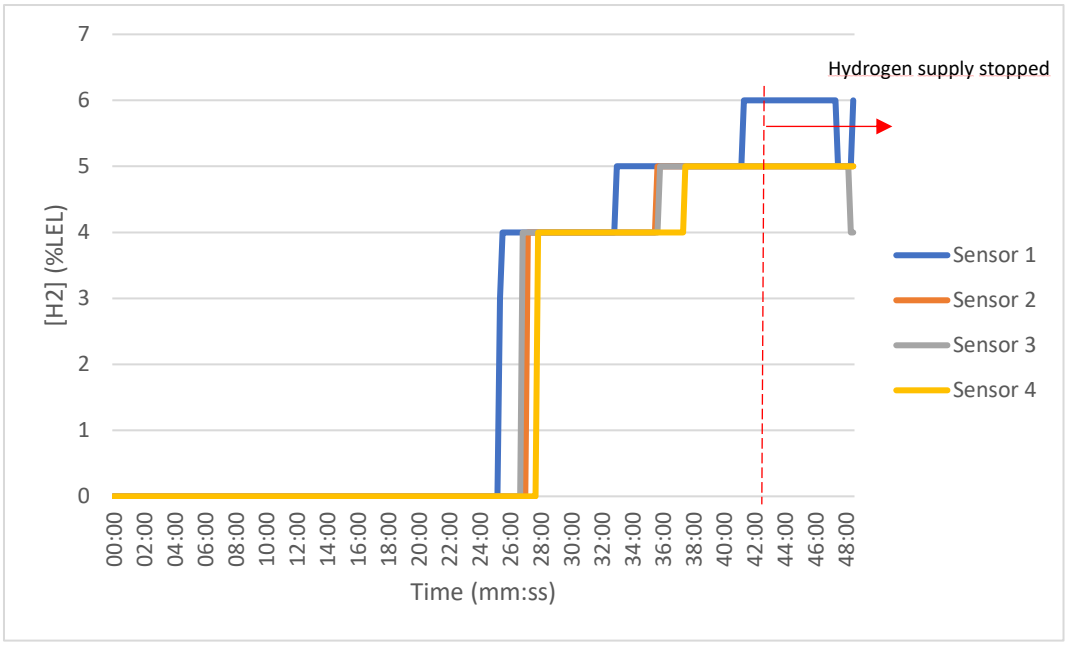

Figure 5-30: Top sensors measuring %LEL concentration levels. With a lower leakage rate of 2 L/h with upward direction and closed ventilation.

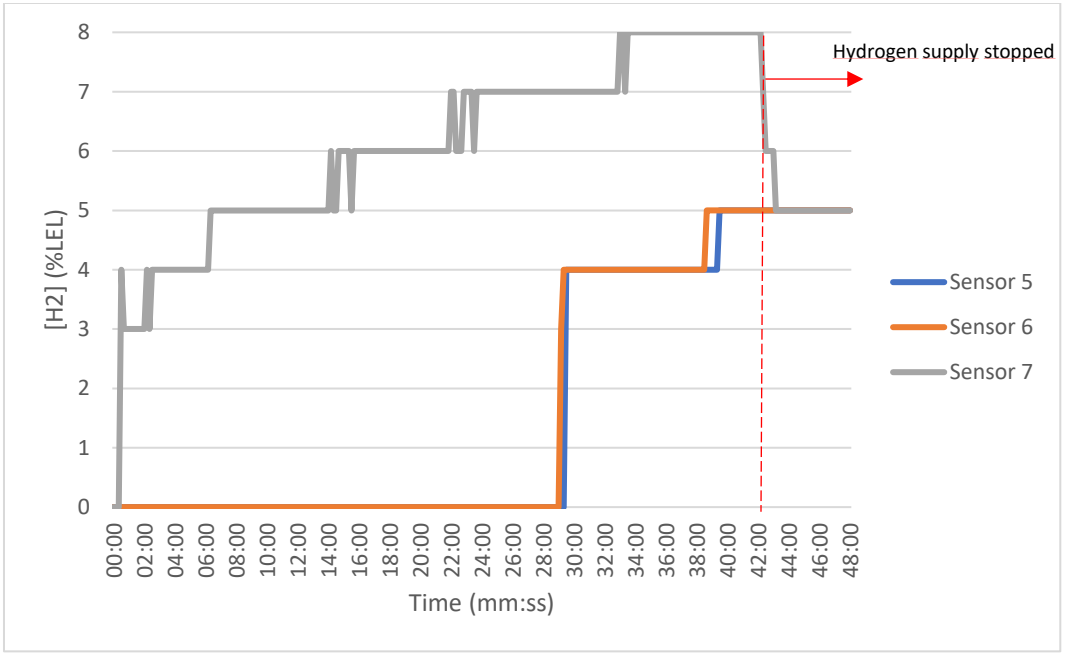

Figure 5-31: Sensors on the side measuring %LEL concentration levels. With a lower leakage rate of 2 L/h with upward direction and closed ventilation.

Table 5-9: Detection time and maximum concentration per sensor of Case 6: Lower hydrogen leakage rate.

Case	sensor	Detection time 200 ppm (mm:ss)	Detection time 4 %LEL (mm:ss)	Detection time 10 %LEL (mm:ss)	Max. concentration (%LEL)
6	1	05:48	25:38	not reached	6
	2	06:58	27:08	not reached	5
	3	05:08	27:18	not reached	5
	4	04:38	27:58	not reached	5
	5		29:28	not reached	5
	6		28:58	not reached	5
	7		00:28	not reached	8

5.3.7 Case 7: Natural gas (methane) leakage

Additionally, two tests with natural gas (methane) have been conducted. The goal was to investigate the difference between natural gas and hydrogen leakage behaviour inside a closed compartment. In these measurements, pure methane was used instead of natural gas. Natural gas contains 82% of methane. The methane leakage rate is therefore corrected considering the methane fraction in natural gas.

This case represents a situation where the natural gas pipeline network is used for hydrogen distribution. It is assumed that the leakage size for natural gas is the same as the hydrogen leakage. The size of the opening (nozzle) is constant. But, due to a bigger CH4 molecule, the leakage flow rate of methane needs correction for the difference in the leakage rate between hydrogen and natural gas [16], [67]. As found in the experiment overview in section 4.5, the corrected methane leakage rate calculated from the hydrogen leakage rate was 41,65 ml/min.

The used sensors for methane measurements were infrared sensors. These sensors measure methane vol% in steps of 0.1 vol%. To convert the volume % to %LEL of methane (LEL of methane (5.0 vol%)), a factor of 20 is used. Therefore, 0.1 volume % is equal to 2 %LEL. The conversion rates are shown in the following Table 5-10.

Table 5-10: Units of the methane concentration.

Unit	Methane concentration
vol%	0.1
ppm	1000
%LEL	2

a) Methane leakage inside a cabinet with closed ventilation

In the first part (a) of the case, the methane concentration is measured in the metering cabinet with the nozzle in an upward direction and closed ventilation. The results of this case are illustrated in Figure 5-32 and Figure 5-33. The results showed that the time required for the methane gas to reach the top sensors at the ceiling was three times longer than the hydrogen leakage.

During the first 10 min of the test, the side sensors measured a higher concentration of methane in comparison to the top sensors. The methane gas was still at the bottom half of the metering cabinet. The sensors at the side of the metering cabinet measured 4 %LEL at sensor no. 6 and sensor no. 5 after 1:48 min and 3:38 min, respectively.

Regarding the maximum concentration, the sensors at the back of the ceiling (sensors no. 1 and 2) were the sensors with the highest readings (14 %LEL). For sensor no. 1 in the top-middle, the 10%LEL detection time was 24:28 min. Then, sensor no. 2 showed 10 %LEL after 24:48 min. Four of the sensors (sensors no. 3, 4, 6 and 7) did not reach the 10 %LEL concentration level.

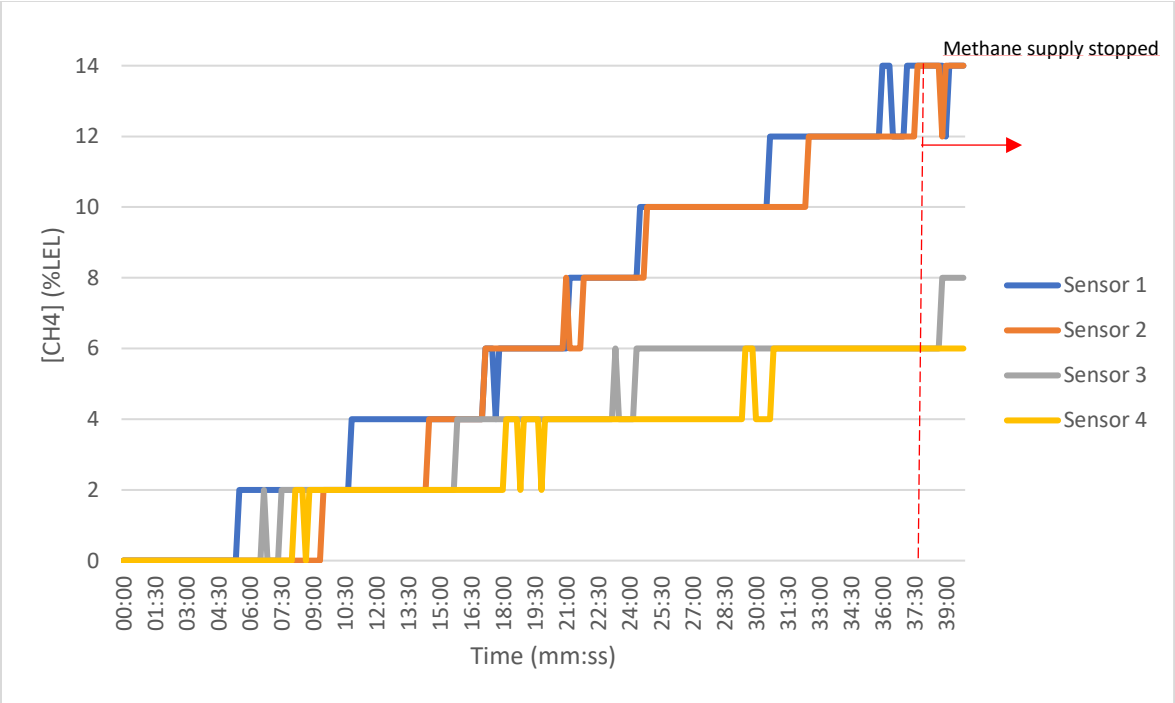

Figure 5-32: Top sensors measuring %LEL methane concentration levels. With flow in upward direction and closed ventilation.

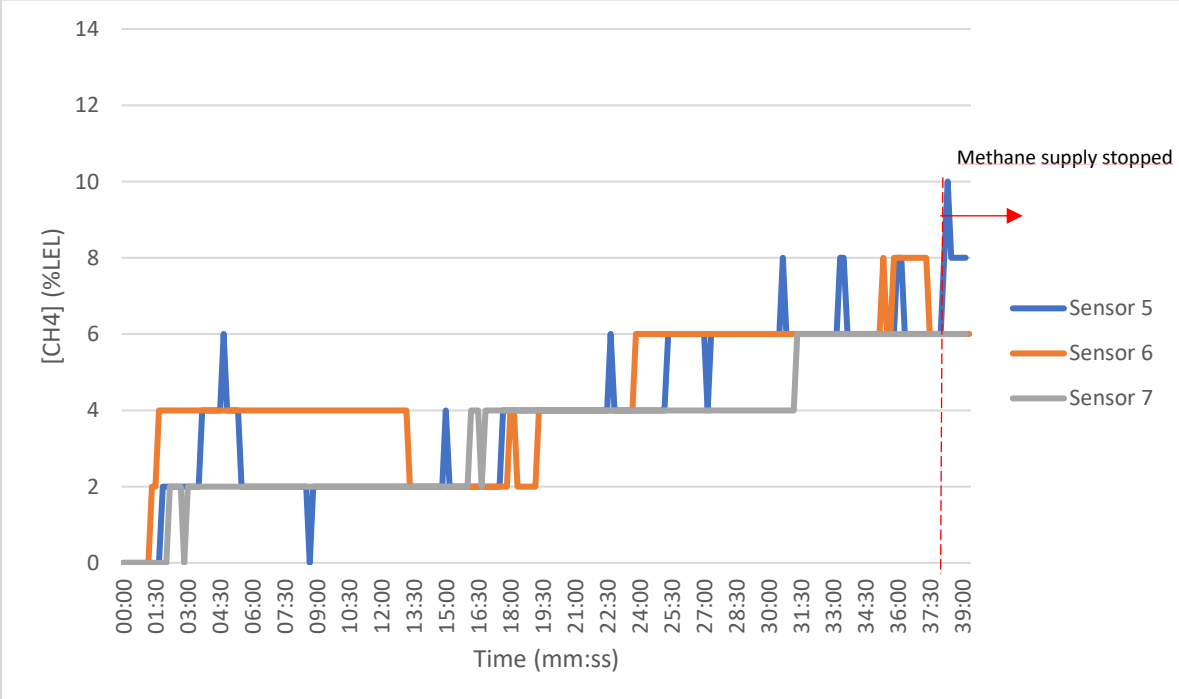

Figure 5-33: Sensors at the side measuring %LEL methane concentration levels. With flow in upward direction and closed ventilation.

Table 5-11: Detection time and maximum concentration per sensor of Case 7-a: CH4 leakage with closed ventilation.

Case	sensor	Detection time 4 %LEL (mm:ss)	Detection time 10 %LEL (mm:ss)	Max. concentration (%LEL)
7 - a	1	10:48	24:28	14
	2	14:28	24:48	14
	3	15:48	not reached	8
	4	18:08	not reached	6
	5	03:38	38:18	10
	6	01:48	not reached	8
	7	16:08	not reached	6

A comparison the results of the hydrogen and the natural gas (methane) leakage is shown in Figure 5-34. The first detection at the ceiling of the metering cabinet was longer for methane than hydrogen. The different detection times for both gases to reach 4 %LEL at sensor no. 1 were 1:48 min and 10:48 min for hydrogen and methane, respectively.

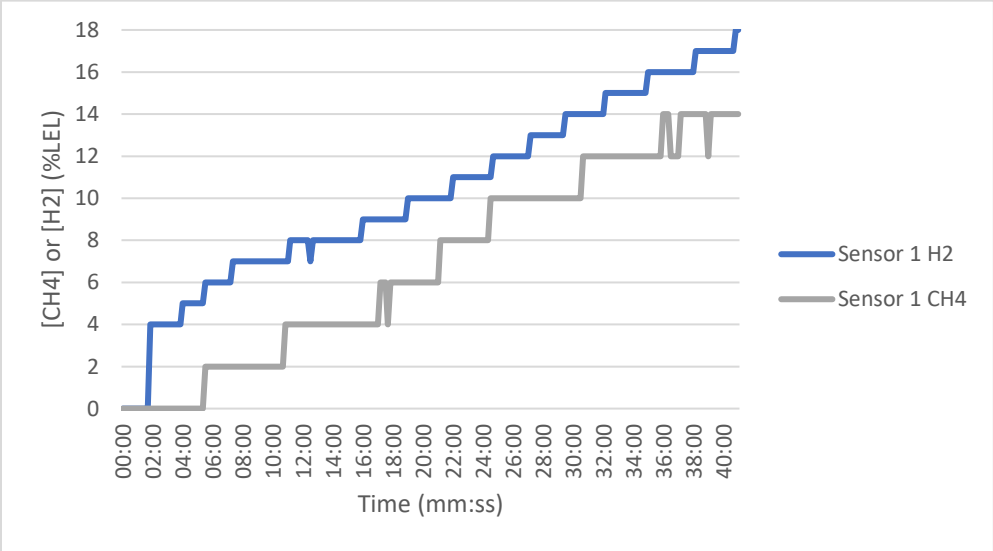

Figure 5-34: Comparison between the sensors no. 1 on the ceiling (One hydrogen sensor and one methane sensor). In both cases the ventilation was closed.

Then, regarding the results of the hydrogen and the natural gas (methane) case with closed ventilation for sensor no. 5 (Figure 5-35), a peak at 4:38 is observed for the CH_4 sensor no. 5 (located at the side of the cabinet). This observed high concentration could be because of methane gas slowing down at this height because of the electrical box. Sensor 5 was at the position between side and the ceiling sensors at two third of the height of the cabinet. The methane also did not rise as fast to the ceiling as the hydrogen did. In the discussion of Case 1 also the influence of the electrical box obstacle on the gas flow in the middle of the metering cabinet was discussed. This object influenced the direction of the gas flow towards the middle sensors on the side. As is seen in Figure 5-33 for the first 13:00 min, sensor no. 6 showed increased concentrations as well.

Overall, these results indicate that the hydrogen concentrations at these sensors were higher in %LEL than methane leakage case with the same leakage period. In closed ventilation condition, the risk of having an explosive gasmixture is higher in the case of hydrogen leakage.

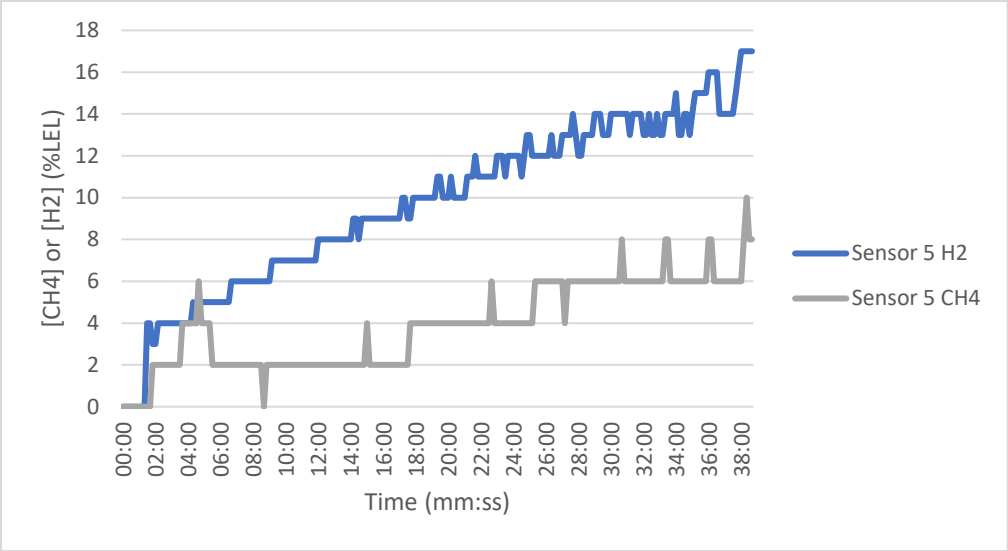

Figure 5-35: Comparison between the sensors no. 5 on the side (One hydrogen sensor and one methane sensor). In both cases the ventilation was closed.

b) Methane leakage inside the metering cabinet with open ventilation

In the second part (b) of this case, the methane concentration is measured in the metering cabinet with the nozzle in an upward direction and open ventilation. Then, for the evaluation of the methane concentrations measured by methane sensors, the results are illustrated in Figure 5-36 and Figure 5-37. In the open ventilation case of the methane leakage, the concentrations were also lower than in the closed ventilation case 7-a and the CH_4 concentration is more fluctuating in comparison to the case of the hydrogen leakage. The maximum concentration value was 4 % LEL.

Apart from sensor no. 7 that reached 4 %LEL within 1:28 min, the other sensors had a longer detection time to reach to 4 %LEL. Three sensors did not detect the 4 %LEL level and none of them reached the 10 %LEL level in the case with open ventilation.

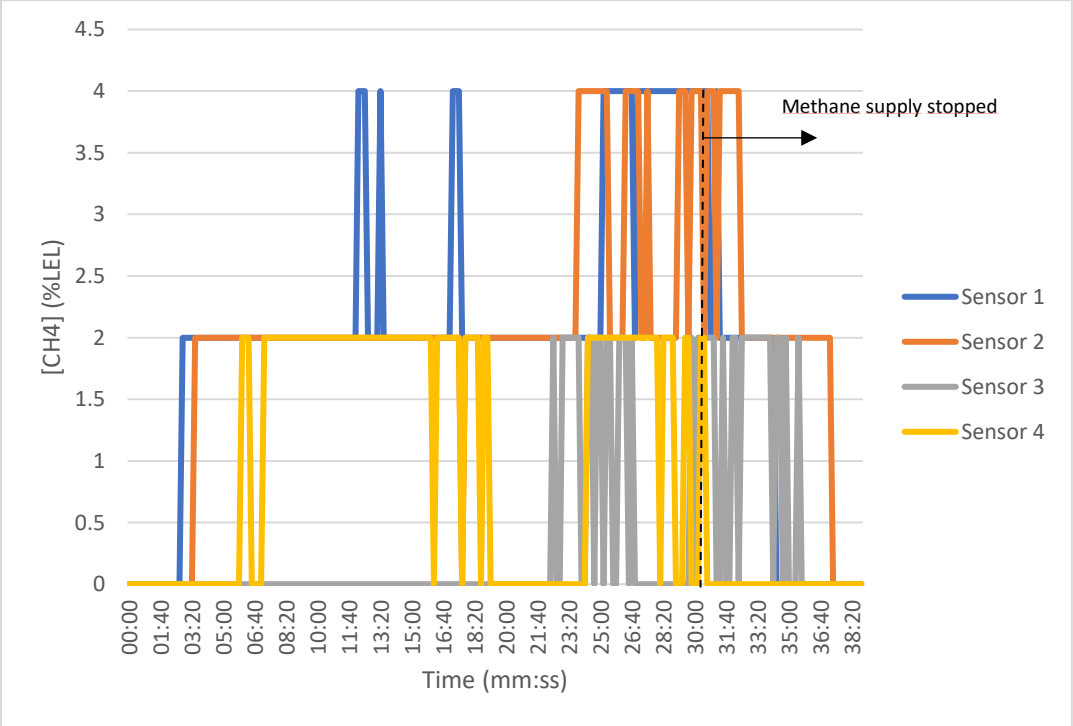

Figure 5-36: Top sensors measuring %LEL methane concentration levels. With flow in upward direction and open ventilation.

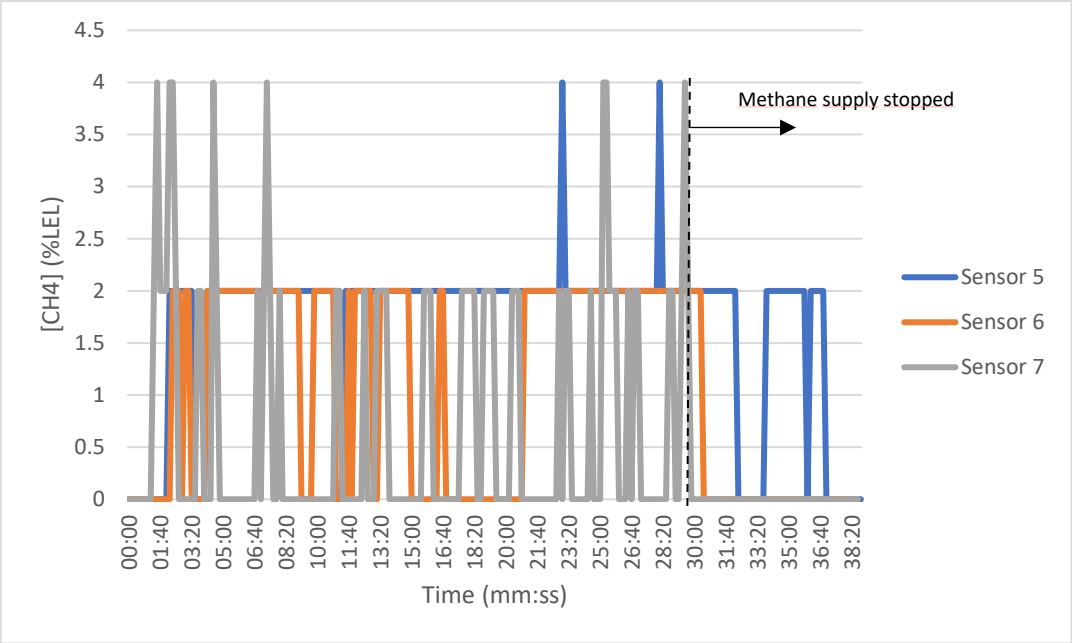

Figure 5-37: Sensors at the side measuring %LEL methane concentration levels. With flow in upward direction and open ventilation.

Table 5-12: Detection time and maximum concentration per sensor of Case 7-b: CH4 leakage with open ventilation.

Case	sensor	Detection time 4 %LEL (mm:ss)	Detection time 10 %LEL (mm:ss)	Max. concentration (%LEL)
7 - b	1	12:08	not reached	4
	2	23:18	not reached	4
	3	not reached	not reached	2
	4	not reached	not reached	2
	5	22:58	not reached	4
	6	not reached	not reached	2
	7	01:28	not reached	4

A comparison of the results of the hydrogen and the natural gas (methane) leakage in the open ventilation situation is shown in Figure 5-38. The methane in air was detected faster than the hydrogen at lower concentration level. This is explained by the concentration value at which methane gets detected (2 %LEL) and hydrogen gets detected from a concentration of 3 %LEL.

When comparing the results of the hydrogen and methane sensors only sensor no. 1 showed the same concentration levels for both gases. For the sensors close to the leakage (sensor no. 5), it is clearly seen (in Figure 5-39) for both cases, the sensors detect the gas at around the same leakage period.

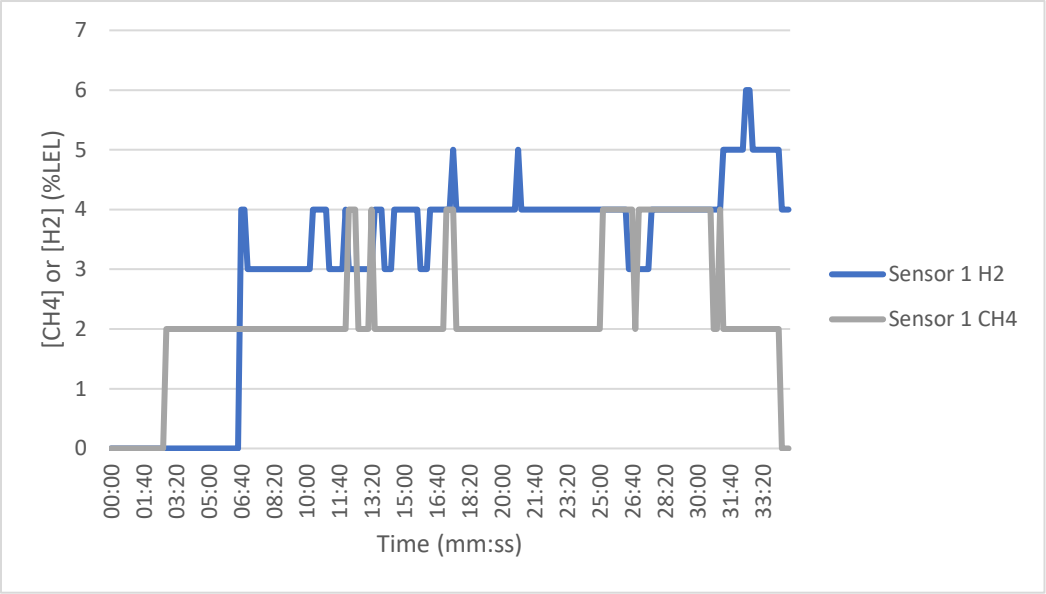

Figure 5-38: Comparison between the sensors no. 1 on the ceiling (One hydrogen sensor and one methane sensor). In both cases the ventilation was open.

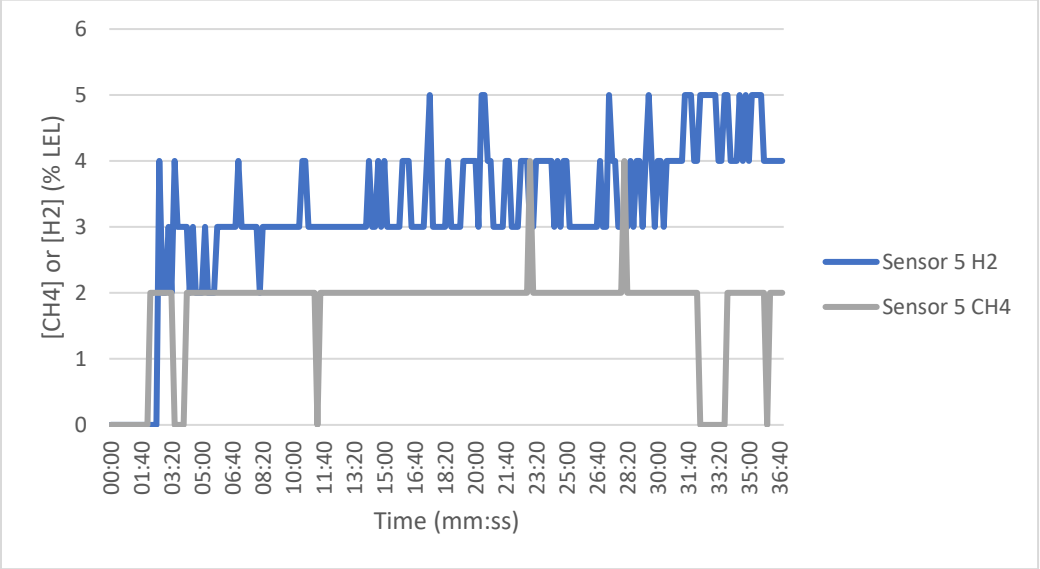

Figure 5-39: Comparison between the sensors no. 5 on the side (One hydrogen sensor and one methane sensor). In both cases the ventilation was open.

Overall, these results show that the hydrogen concentration was higher than the methane concentration in the closed and open ventilation conditions at the same leakage period. Even though, the volumetric leakage flow rate of hydrogen is higher than for natural gas through the same leak size, the concentration levels of hydrogen are not as high as might be expected. Apart from the better mixing of hydrogen in air that exists due to its tendency to easily diffuse [71], an explanation for this is found in the study of **Lowesmith (2009)** [53]. It is stated that a gas with higher hydrogen content leads to a more buoyant gas mixture which leads to an increase in the ventilation air flow.

Figures of the results of this study from **DNV (2020)** [70], shown in Appendix F (Figure F1 and Figure F2), describe the hydrogen and methane concentrations both for the same conditions. In case of worst-case leakage rates (10, 15, 20 and 25 L/h), the highest leakage rates (25 L/h) lead to a lower maximum concentration than 20 L/h. At these high leakage rates, since hydrogen is much lighter than natural gas, hydrogen would rise faster and exits faster through the upper ventilation grill.

5.4 Best sensor location

Table 5-13 in this section gives an overview of a ranking on the sensors with the fastest detection time and the ones that showed the maximum concentration. For each experiment case the top 3 of the sensors are ranked on detection time of detecting 4 %LEL hydrogen or methane concentration. This is the first significant concentration measured by the catalytic LEL-sensors. Moreover, the top 2 of the sensors that showed the maximum concentration are ranked at the right side of Table 5-13. Sensor no. 1 and sensor no. 7 showed the fastest response in most cases. Generally, the sensor no. 7 (closest to the leakage) showed the fastest detection period in the most of cases.

When focusing the attention on highest concentrations, sensor no. 1 was the sensor that in almost all cases reached the maximum concentration during the experiment period. Sensor no. 7 did not show the maximum concentrations in these cases. It showed the highest concentrations only in closed ventilation conditions when the leakage nozzle was directly pointed at the closest sensor inlet.

Except from sensor no. 7 and 6 that are at a lower height in the metering cabinet, due to the rising hydrogen a higher placed sensor would give the fastest response to concentrations above 10 %LEL. Sensor no. 1 is in the top 3 of sensors based on the fastest detection time. Considering when the leakage is on the left side of the metering cabinet sensor no. 1 at the top-center is an effective location as well. Moreover, it had a reading of the maximum concentration in almost all of the test cases or was the second highest concentration in two of the cases (3-a and 6).

Table 5-13: Catalytic LEL-sensors ranked on detection time of a 4 %LEL reading and ranked on maximum concentration.

Case		**Gas**	**Ventilation**	**Sensor (S no.) ranked based on the fastest detection time**			**Sensor (S no.) ranked based on max. concentration**	
				1	**2**	**3**	**1**	**2**
1		H_2	Closed	S6	S5, S7	S1	S1	S6
2		H_2	Open	S7	S5	S5, S4, S6	S1	S4, S6, S7
3	**a**	H_2	Closed	S7	S6	S1	S7	S1
	b	H_2	Closed	S6	S7	S4, S1	S1	*
4		H_2	Closed	S1	S4	S8	S1	*
5		H_2	Closed	S7	S6, S1	S5	S1	S2, S5, S6
6		H_2	Closed	S7	S1	S2	S7	S1
7	**a**	CH_4	Closed	S6	S5	S1	S1, S2	S5
	b	CH_4	Open	S7	S1	S5	S1	S2, S5, S7

* The rest of the sensors have shown the same results.

To have more insight in the fastest response and to have accurate responses of the sensors, the results of the detection time of the electrochemical sensors were also ranked in Table 5-14. Here, the 4 sensors at the ceiling (and in one case the sensor at the left S8) are ranked on the detection time of reaching a concentration of 200 ppm. Sensors no. 1 and 4 got the same ranks in most of the cases. This means the sensors in the top middle of the metering cabinet measured hydrogen the fastest. Because the %LEL sensor type sensor no. 1 had better results for the longer detection periods. These findings therefore suggest that sensor no. 1 has the best location according to the results.

Table 5-14: Electrochemical ppm-sensors ranked on detection time of a 200 ppm reading.

Case		Gas	Ventilation	Sensor (S no.) ranked on detection time			
				1	**2**	**3**	**4**
1		H_2	Closed	S1, S4	-	S2	S3
2		H_2	Open	S1, S4	-	S3	S2
3	**a**	H_2	Closed	S4	S1	S3	S2
	b	H_2	Closed	S1	S4	S2	S3
4		H_2	Closed	S8	S1	S4	S2
5		H_2	Closed	S1, S4	-	S2	S3
6		H_2	Closed	S4	S3	S1	S2

5.5 Discussion of the risk of hydrogen leakage

This part further discusses the risk caused during the seven different conditions of the studied experiment cases. In cases with closed ventilation, it was expected that the hydrogen builds up to high gas concentrations at the top section of the metering cabinet. The door was not completely air tight. Gas does escape from the cabinet trough small air leakages around the door. Nevertheless, closed ventilation leads to a constant increase of the hydrogen concentrations with the highest concentrations (19 %LEL) found in top of the metering cabinet. The readings of the sensors were all well below the lower explosion limit of 4 vol% (100 %LEL).

The ventilation was expected to be an important factor that should have a major effect on the response in this experiment. The ventilation causes lower concentrations of gas in the top part of the metering cabinet. The importance of ventilation is clear from the outcomes. Ventilation caused changes in the distribution mechanism, resulting in a better mixing and reduced concentration of the hydrogen. The maximum hydrogen concentration reached to 6 %LEL.

The concentrations of hydrogen observed at the ceiling were highest. Hydrogen tends to rise and stay at the top of the metering cabinet. This happens in phases as the hydrogen rises it will bounce off from the ceiling and go down. The upper ventilation grille needs to be positioned as high in the metering cabinet as possible to ensure the hydrogen exists on the top.

The lowest concentration at the ceiling was in almost all of the cases on the location that sensor no. 3 was placed (At the right side on the ceiling). This sensor measured a lower concentration level compared to the other sensors. Thus, it is not recommended to put a sensor on this position with the risk of a longer detection time.

Other directions of the leakage caused a build-up of gas concentration in the lower part of the metering cabinet. Changes in response time of the sensors on the various height levels were expected. A direction of the leakage towards the back wall of the cabinet caused an additional risk. A high concentration peak of 20 %LEL was caused due to blockage by the back wall. Hydrogen could accumulate in the lower section of the metering cabinet as more gas was continuously added. With a direction of the leakage towards the bottom, less risk is involved. A better mixture of hydrogen in air resulted in a homogeneously spread of hydrogen in the compartment.

The extra sensor on the left side would not necessarily be a better position to measure the hydrogen concentration in the case of a leakage on the left side of the gas meter. The other sensors placed on the right side of the cabinet can still detect the leakage in the left side of the cabinet due to the high

hydrogen diffusion rate. The highest hydrogen concentrations were detected in the top-center of the metering cabinet. So, the risk of having the leakage on the left side was therefore similar.

The expected response with extra obstacles present in the gas metering cabinet, was that these objects alter the hydrogen distribution inside the cabinet. The most interesting part of the response was the gas concentration on the different height levels. In this case, the blockage by the obstacles trapped hydrogen gas at the bottom of the cabinet. No dangerous concentrations (above 20 %LEL) were reached.

The expected response with a smaller leakage rate, was a lower hydrogen concentration caused by the leakage. But in some parts of the metering cabinet there might be build-up of hydrogen gas. It is observed that the period of reaching risky concentrations (above 4 %LEL) was longer for the low leakage rate compared to the 5 L/h leakage rate.

In the case of hydrogen to natural gas comparison, the size of the opening (nozzle) was kept constant. But, due to a bigger CH_4 molecule, it is assumed that the leakage rate of methane is less (2.5 L/h). The leakage rate depended on the difference in the gas properties (hydrogen and natural gas). As previously discussed, higher concentrations of hydrogen were expected at the top of the metering cabinet than in the methane case.

During closed ventilation tests, the hydrogen concentrations were higher in %LEL than the methane in the same leakage period. The hydrogen gas rises quicker to the ceiling and builds up (and stays) in the upper part. The time required for the methane gas to reach the top sensors at the ceiling was three times longer than the hydrogen leakage. This happens because of the velocity of the hydrogen gas in air is roughly 3 times higher than methane [72].

The buoyant hydrogen-air mixture rises to the top which might lead to increased ventilation. **DNV (2020)** [70] found that this was true especially for higher (worst-case) leakage rates. This was contrary to the behaviour found for methane.

6

Conclusions

6 Conclusions

In the near future, hydrogen sensors will become readily available for a wide range of hydrogen detection systems in different applications. Therefore, it is essential to understand for each application which sensor technology is the most effective and where it should be located for optimal performance. The conclusion to each sub-research question is presented in this section.

This thesis aims to contribute to our knowledge of these hydrogen sensor technologies by addressing the research objective:

> Evaluation of hydrogen sensor technologies for residential safety and determination of the sensor location with the fastest response to high hydrogen concentrations inside a metering cabinet.

6.1 What type of hydrogen sensor technology is most suitable based on the relevant criteria for residential use?

The second chapter outlined the major different sensor technologies and discussed the advantages and disadvantages for the targeted application. A multi-criteria analysis was conducted to find out the highest scoring commercially available sensor technology for residential application. The most notable criteria against which these sensors were tested are accuracy, detection limit, measuring range, lifetime, response time, and stability.

Thermal conductivity sensors showed the highest performance overall as seen from the final scores in Table 6-1. The type out-performed the rest on stability, response time and selectivity. However, it is costly and with future improvements on the detection limit, it could be considered suitable for residential applications. **Catalytic** sensors had a great performance during the evaluation of the sensors. They are accurate in measuring hydrogen and methane concentrations. However, their response is influenced by operating conditions, such as the gas leakage rate. **Metal oxide** sensors had an acceptable performance, they are unexpensive and the power consumption is reasonably low. However, the detection accuracy needs to be improved. **Electrochemical** sensors showed a variation in performance. They are highly accurate (in ppm range) but showed uncertainty of detection. The impact of environmental conditions, such as temperature and gas leakage rate, on the hydrogen detection are considerable.

Table 6-1: Final scores and ranks of the sensor technologies from the WSM multi-criteria decision-making analysis.

WSM	Cat1	Cat2	Cat3	TC	EC	MOX
Final score	0.749	0.724	0.667	0.871	0.586	0.742
Rank	2	4	5	1	6	3

6.2 What location of the hydrogen sensor shows the fastest response to high hydrogen concentrations inside the metering cabinet?

The aim of the present research was to examine a hydrogen sensors application with the focus on experiments inside a Dutch metering cabinet. This study has shown some insights through experimentation separated into 7 different case studies.

In each case, some adjustments to the testing conditions in the metering cabinet were applied to investigate the response of the sensors. The leakage flow rate of 5 liters per hour was chosen for the experiments. It is the highest rate of a gas leakage currently allowed in the existing buildings (including the old ones). The measurements setup mainly consisted of 7 or 8 sensors that were positioned at the described locations inside the metering cabinet.

The use of two different types of sensors, catalytic and electrochemical sensors, were needed to measure the entire concentration range. This helps to understand the behaviour of hydrogen in the metering cabinet. In the beginning of each experiment the attention goes to four electrochemical sensors placed at the ceiling of the cabinet. While the hydrogen concentration is above 1000 ppm, the catalytic sensors (%LEL) should be used to measure the hydrogen concentrations. These sensors only showed the hydrogen concentrations when it is above 3 %LEL.

The results showed that the sensors at the ceiling are not always giving the highest readings at the beginning, but in most of the cases, they consistently showed the highest concentrations and the fastest response during the tests. This was illustrated in the analysed results while the ventilation was closed.

The results of this study further indicate that in the cases with closed ventilation, the large concentrations could be found in the center of the ceiling. It is recommended that sensor no. 1 (at the top-center backside) has the best location to mount the hydrogen sensor according to the results (Table 5-13 and Table 5-14). Mounting the sensor on this location was also proven to be effective when assuming a gas leakage at the left side of the metering cabinet. Thus, the sensor with the position in the top-center backside of the metering cabinet is ranked with the highest concentrations in all situations.

6.3 Which conditions lead to the highest risk of hydrogen leakage inside the metering cabinet?

The experiments confirmed that the condition of closed ventilation leads to a constant increase of hydrogen concentration in the metering cabinet. The final concentration depends on the time of the hydrogen leakage into the confined space. The sensors close to the leakage measured significant concentrations in the first minutes of the test. The concentration continued to increase with a constant leakage flow of hydrogen and filled the whole cabinet to with a 2 %LEL difference concentrations as high as 19 %LEL. The readings of the sensors were all well below the lower explosion limit of 4 vol% (100 %LEL).

The experiments have also clearly shown the effect of ventilation from the fluctuating and reduced concentrations. The hydrogen mixed with air escaped through the ventilation grilles. Ventilation causes changes in the distribution mechanism, resulting in better mixing of the hydrogen. This hydrogen-air mixture brings about better distribution and reduces hydrogen concentrations. The results of the experiment with open ventilation show that the concentration fluctuated with a maximum value of 6 %LEL. The level of 10 %LEL was not reached for all sensors.

The concentrations of hydrogen at the ceiling were higher in case of no ventilation. Hydrogen tends to rise and stay at the top of the metering cabinet. Therefore, the upper ventilation grille needs to be positioned at the highest level in the metering cabinet to ensure the hydrogen exists on the top. This ventilation placed at the top area would reduce the risk of the hydrogen leakage.

The direction of the leakage of the gas towards the bottom caused a better mixture of hydrogen in the air and created a more homogeneous dispersion of the gas. This causes less risk. In the cases of

different leak direction towards the wall and extra obstacles, the sensors on the side, closer to the leakage, gave peaks in the readings during the first part of the test. The flow was impacted due to blockage and slowly moved upwards. This causes a build-up of concentration in a short period at the start of the leakage.

Compared to methane, the hydrogen gas rises quicker to the ceiling and builds up (and stays) in the upper part. The time required for the methane gas to reach the top sensors at the ceiling was three times longer than the hydrogen leakage. During closed ventilation test, the hydrogen concentrations were higher in %LEL than methane in the same leakage period.

In open ventilation conditions, the sensors located near the leakage showed a similar concentration for both hydrogen and methane. The first detection (above 2 LEL%) of hydrogen and methane happened after the same leakage period.

In comparison to methane, the hydrogen gas released leads to a more buoyant gas mixture that could have a great impact on the ventilation and better mixing of hydrogen in air due to its high diffusion factor. The buoyant hydrogen-air mixture rises to the top which might lead to increase of the ventilation, especially at higher leakage rates.

6.4 Limitations of this study

A limitation of this study which could have affected the analysis of different hydrogen sensor technologies was that the study was limited to commercially available sensors that were described in earlier research papers. Unfortunately, it is hard to find specific quantities for criteria such as the cost of the sensor types. The information about cost is often very unclear from manufacturers compared to the other criteria required for the full analysis of the hydrogen sensor technologies.

Furthermore, performances of the sensors are significantly dependent on the electronics of the sensor. This is an uncontrolled factor in this study. The electronic components of the sensor also determine the signal for a large part and therefore play an important role. They influence and correct external parameters that in other cases would negatively change the measurement signal.

Regarding the experimental research inside the metering cabinet, since the study was limited to the time that the experiment location was available, it was not possible to do measurements with much longer time spans. In spite of its limitation, the study certainly provides insight into the way hydrogen is distributed within the cabinet.

7

Recommendations

7 Recommendations

In this section, recommendations for further research are outlined. Additionally, several safety measures are proposed to assure the safety apart from applying hydrogen sensors.

7.1 Recommendations for further studies

Other research that implements a multi-criteria analysis to determine the best performing sensor should appreciate that the weights attached to criteria are essential towards the final result. It is hard to decide which of the criteria will have more influence. It is recommended that there is a discussion on the various choices, grading, and weighting. An expert's opinion is highly valued. This is done in order to get the best sensor outcome from the analysis. The outcome is highly dependent on the weights attributed to the criteria that is used in the analysis.

The risk with the multi-criteria analysis remains that some criteria show overlap. The effect of a decision towards one of the sensors gets double-counted. Furthermore, it is possible that some criteria are not taken into account as much as others in the case they will be of negative influence on the application of the sensor. Much effort has been made to minimize these risks in finding the best performing sensor.

A recommendation when doing experiments with hydrogen sensors is to find a solution to correct for the suction flow of the sensors. While the sensors pump out a small portion of the air and gas, the body of the sensors are placed outside the metering cabinet. The gas and air mixture is pumped out of the closed volume and would not flow back inside again.

Regarding the experiments, multiple conditions (factors) have been chosen that were varied per experiment. These were mostly determined by practical factors that were changed, one at a time in each experimental case. However, for further research the number of experiments need to be higher for statistical reasons. In this case the theory of **Montgomery (2013)** [65] 'Design and analysis of experiments' need to be addressed. This theory describes methods of experimenting where the factors could be simultaneously changed. With this approach, the procedures are more structured so that they are clear in execution and reporting.

Other worst-case scenarios should be examined. Experimental research with leakages for a longer period (e.g., 24 hours) need to be done. Since the study was limited to the time that the experiment location was available, it was not possible to do measurements with such time spans. It would be good to have an experiment that has a timespan of several hours to confirm if the LEL of hydrogen is reached. Furthermore, in case of a rupture in the pipeline, the major leakage of hydrogen might reach ignitable concentrations (4.0 vol% or 100 %LEL) of hydrogen much faster.

Another recommendation for further studies is to investigate the performance of the CO detection sensors to be used for detecting hydrogen. Metal oxide CO sensors are cross-sensitive to hydrogen and therefore able to detect a portion of the hydrogen in a concentration range of 100-5000 ppm (0.01 vol% - 0.5 vol%) [73]. However, the residential application of CO sensors is not yet out of the research phase. Approval and the relevant standards are first needed.

More research works are needed to evaluate the hydrogen behaviour inside closed compartments. A CFD (computational fluid dynamics) model is a recommended tool to study the gas flow. The data from this experimental study could be used to validate the outcomes of the future CFD model.

7.2 Safety measures

To add to the results of this research, some safety measures are important to take. This research made it clear that the location of the sensor is crucial to optimally detect hydrogen. In particular, the sensor should not be located too close to the ventilation opening in the metering cabinet in order to assure sufficient accuracy.

Sufficient ventilation within the metering cabinet is also essential. Although this research was focused on the highest level of hydrogen concentration for the sensors, the findings related to the effect of ventilation are important to back up safety precautions. It has been found in this thesis research that with more ventilation, the concentrations fluctuate more which results in a lower hydrogen concentration build-up. Thus, ventilation is important to keep the hydrogen concentration at safe levels.

Furthermore, since it is recommended to have sufficient ventilation the levels of hydrogen concentration to trigger the alarm in case of a metering cabinet with ventilation (open) should be lowered. In this research it has been found that in case of no ventilation in the metering cabinet, the alarm level at 10 %LEL hydrogen concentration is sufficient to provide early detection. However, in a situation where there is ventilation, and the sensor is put in the same position with highest concentration of hydrogen, a lower value of hydrogen concentration was observed than in the case of no ventilation. More specifically, the concentration fluctuated with a maximum value of 6 %LEL. Therefore, it is advised that the sensors give an alarm signal at 5 %LEL hydrogen concentration in the metering cabinet. In this way it prevents the leakage going unnoticed.

Additionally, a system to shut off the supply of hydrogen gas inside the house is an important safety measure. This works by blocking the service line of hydrogen that enters the building, even when there is a power shortage. Therefore, it should trigger at all times even in case it is electrically powered. To assure proper functioning of the system, the implementation of a valve that works with gravity is necessary [74]. It is important to consider such a system for hydrogen. But it is not currently applied for natural gas. The LEL level (4 vol%) for hydrogen is around the same level as for natural gas (5 vol%). It can be concluded that better safety regulation is needed.

Finally, due to the buoyant behaviour of hydrogen and gas escaping from the ventilation grilles, the addition of an odorant to the hydrogen gas is a good safety measure apart from the audible alarm provided by the sensors. Such an odorant would make it more likely that a leak is noticed and an accident prevented. However, this odorant should be suitable for all hydrogen systems and applications. More research still needs to be done to find the right substances that has no other negative effects. For example, sulphur based odorants have harmful effects on fuel cells [75].

8

References

8 References

[1] HySafe, “Chapter I : Hydrogen Fundamentals,” *Bienn. Rep. Hydrog. Saf.*, no. June, pp. 0–11, 2007.

[2] U. S. Department of Energy, “Hydrogen Production: Electrolysis,” 2021. [Online]. Available: https://www.energy.gov/eere/fuelcells/hydrogen-production-electrolysis. [Accessed: 29-Jun-2021].

[3] TNO, “From grey and blue to green hydrogen - TNO,” 2020. [Online]. Available: https://www.tno.nl/en/focus-areas/energy-transition/roadmaps/towards-co2-neutral-industry/hydrogen-for-a-sustainable-energy-supply/. [Accessed: 28-May-2021].

[4] SGN, “We’re preparing to deliver the world’s first 100% green hydrogen network,” 2020. [Online]. Available: https://sgn.co.uk/news/ready-deliver-worlds-first-100-green-hydrogen-network. [Accessed: 28-May-2021].

[5] U. S. Department of Energy, “Heat Pump Systems,” 2021. [Online]. Available: https://www.energy.gov/energysaver/heat-pump-systems. [Accessed: 29-Jun-2021].

[6] Thermodynamics Team B, “Heat Pump,” *UW-Green Bay*, 2019. [Online]. Available: https://blog.uwgb.edu/chem320b/heat-pump/. [Accessed: 29-Jun-2021].

[7] R. Energieloket, “Groen gas en waterstof,” *Regionaal Energieloket Kennisbank*, 2021. [Online]. Available: https://kennisbank.regionaalenergieloket.nl/aardgasvrij/groen-gas-en-waterstof/. [Accessed: 29-Jun-2021].

[8] T. Voermans, “Oudere woning beter te verwarmen met waterstofketel dan met warmtepomp,” *AD.nl*, 2021. [Online]. Available: https://www.ad.nl/wonen/oudere-woning-beter-te-verwarmen-met-waterstofketel-dan-met-warmtepomp~a0239beb/. [Accessed: 13-Jan-2022].

[9] GasTerra, “Aardgas in Nederland,” 2019.

[10] J. Gigler, J; Weeda, M.; Hoogma, R.; de Boer, “Waterstof voor de energietransitie - Topsectorenergie,” *TKI Urban Energy*, p. 145, 2020.

[11] M. Afman and F. Rooijers, “Net voor de Toekomst - Achtergrondrapport,” *Netbeheer Ned.*, p. 44, 2017.

[12] Kiwa Technology B.V., “Toekomstbestendige gasdistributienetten,” p. 95, 2018.

[13] Planbureau voor de Leefomgeving, “Waterstof voor de gebouwde omgeving; operationalisering in de Startanalyse 2020,” *Pbl*, vol. 4250, no. september, 2020.

[14] M. van de Voorde, *Hydrogen Production and Energy Transition*. De Gruyter, 2021.

[15] T. Correljé, A.; van der Linde, C.; Westerwoudt, *Natural gas in the Netherlands*, vol. 200, no. 4902. 2003.

[16] J. Caanen, “Eerste inventarisatie naar waterstofuitstromen bij kleine toelaatbare aardgas lekken,” *Kiwa*, no. april, 2019.

[17] ISO, “NPR-ISO/TR 15916 Basismetingen voor de veiligheid van waterstofsystemen,” no. december 2015, 2015.

[18] Y. Brazier, “Carbon monoxide (CO) poisoning: Symptoms, causes, and prevention,” *Medical News Today*, 2022. [Online]. Available: https://www.medicalnewstoday.com/articles/171876#tests. [Accessed: 04-Feb-2022].

[19] K. Chowdhury, “Decarbonising the Residential Space Heating Sector of the Netherlands in 2050 through Three Decarbonisation Pathways-Hydrogen Boilers, Hybrid Heat Pumps and Electric Heat Pumps,” 2020.

[20] W. Buttner, R. Burgess, M. Post, and C. Rivkin, “Summary and Findings from the NREL/DOE Hydrogen Sensor Workshop (June 8, 2011),” no. July 2012, 2011.

[21] Y. S. Najjar, “Hydrogen Leakage Sensing and Control: (Review),” *Biomed. J. Sci. Tech. Res.*, vol. 21, no. 5, pp. 16228–16240, 2019.

[22] P. S. Chauhan and S. Bhattacharya, “Hydrogen gas sensing methods, materials, and approach to achieve parts per billion level detection: A review,” *Int. J. Hydrogen Energy*, vol. 44, no. 47, pp. 26076–26099, 2019.

[23] T. Hübert, L. Boon-Brett, G. Black, and U. Banach, “Hydrogen sensors - A review,” *Sensors Actuators, B Chem.*, vol. 157, no. 2, pp. 329–352, 2011.

[24] W. J. Buttner, M. B. Post, R. Burgess, and C. Rivkin, “An overview of hydrogen safety sensors and requirements,” *Int. J. Hydrogen Energy*, vol. 36, no. 3, pp. 2462–2470, 2011.

[25] G. Manjavacas and B. Nieto, “Hydrogen sensors and detectors,” *Compend. Hydrog. Energy*, pp. 215–234, 2016.

[26] R. B. Gupta, *Hydrogen fuel: production, transport and storage*. CRC Press, 2009.

[27] R. Lockhat, “Physics: Wheatstone bridge,” *South. African J. Anaesth. Analg.*, vol. 26, no. 6, pp. 100–101, 2020.

[28] L. Boon-Brett, J. Bousek, and P. Moretto, “Reliability of commercially available hydrogen sensors for detection of hydrogen at critical concentrations: Part II - selected sensor test results,” *Int. J. Hydrogen Energy*, vol. 34, no. 1, pp. 562–571, 2009.

[29] S. Masuzawa, S. Okazaki, Y. Maru, and T. Mizutani, “Catalyst-type-an optical fiber sensor for hydrogen leakage based on fiber Bragg gratings,” *Sensors Actuators, B Chem.*, vol. 217, pp. 151–157, 2015.

[30] D. R. Lide, *Handbook of Chemistry and Physics*. 2003.

[31] HySafe, “Hydrogen safety barriers and safety measures,” *Bienn. Rep. Hydrog. Saf.*, no. May, pp. 1–78, 2006.

[32] N. L. Torad, S. Zhang, W. A. Amer, and E. Al., “Advanced Nanoporous Material–Based QCM Devices: A New Horizon of Interfacial Mass Sensing Technology,” *Adv. Mater. Interfaces*, vol. 6, no. 20, 2019.

[33] I. Simon and M. Arndt, “Thermal and gas-sensing properties of a micromachined thermal conductivity sensor for the detection of hydrogen in automotive applications,” in *Sensors and Actuators, A: Physical*, 2002, vol. 97–98, pp. 104–108.

[34] S. Chen, D. Supervisor, H. W. Supervisor, and R. Wolffenbuttel, “Surface-Micromachined Thermal Conductivity Gas Sensors For Hydrogen Detection,” no. October, 2010.

[35] T. Hübert, L. Boon-Brett, V. Palmisano, and M. A. Bader, “Developments in gas sensor technology for hydrogen safety,” *Int. J. Hydrogen Energy*, vol. 39, no. 35, pp. 20474–20483, 2014.

[36] K. Chen, D. Yuan, and Y. Zhao, “Review of optical hydrogen sensors based on metal hydrides: Recent developments and challenges,” *Opt. Laser Technol.*, vol. 137, no. December 2020, p. 106808, 2021.

[37] V. Palmisano *et al.*, “Selectivity and resistance to poisons of commercial hydrogen sensors,” *Int. J. Hydrogen Energy*, vol. 40, no. 35, pp. 11740–11747, 2015.

[38] S. Jallais *et al.*, “Pre-normative research on safe indoor use of fuel cells and hydrogen systems Hyindoor Final Report,” 2015.

[39] Y. A. Alamerew, M. L. Kambanou, T. Sakao, and D. Brissaud, “A multi-criteria evaluation method of product-level circularity strategies,” *Sustain.*, vol. 12, no. 12, pp. 1–19, 2020.

[40] V. Molkov, *Fundamentals of Hydrogen Safety Engineering I*, vol. 4. 2012.

[41] M. Crowther, G. Orr, J. Thomas, G. Stephens, and I. Summerfield, “Energy Storage Component Research & Feasibility Study Scheme: HyHouse Safety Issues Surrounding Hydrogen as an Energy Storage Vector,” no. June, p. 96, 2015.

[42] K. Pulles, “Ontmenging van waterstof,” *Kenniscentrum Gasnetbeheer*, 2019.

[43] M. R. Swain, P. Filoso, E. S. Grilliot, and M. N. Swain, “Hydrogen leakage into simple geometric enclosures,” *Int. J. Hydrogen Energy*, vol. 28, no. 2, pp. 229–248, 2003.

[44] R. W. Schefer, W. G. Houf, B. Bourne, and J. Colton, “Spatial and radiative properties of an open-flame hydrogen plume,” *Int. J. Hydrogen Energy*, vol. 31, no. 10, pp. 1332–1340, Aug. 2006.

[45] P. Adams, A. Bengaouer, B. Cariteau, V. Molkov, and A. G. Venetsanos, “Allowable hydrogen permeation rate from road vehicles,” *Int. J. Hydrogen Energy*, vol. 36, no. 3, pp. 2742–2749, Feb. 2011.

[46] R. J. M. Hermkens, H. Colmer, and H. A. Ophoff, “Modern Pe Pipe Enables the Transport of Hydrogen,” *Proc. 19th Plast. Pipes Conf.*, vol. 2018, pp. 1–12, 2018.

[47] F. M. White, *Fluid Mechanics*, 7th Editio. McGraw-Hill, 2011.

[48] Y. Zheng, “Schlieren imaging investigation of the hydrodynamics of atmospheric helium plasma jets,” *J. Appl. Phys.*, 2016.

[49] K. Stephan, P., Kabelac, S.,Kind, M., Holger, M. Mewes, D., Schaber, *VDI Heat Atlas*, no. Second Edition. 2010.

[50] M. De Stefano, X. Rocourt, I. Sochet, and N. Daudey, “Hydrogen dispersion in a closed environment,” *Int. J. Hydrogen Energy*, vol. 44, no. 17, pp. 9031–9040, 2019.

[51] A. Tripathy, “What is a gaseous example of a heterogeneous mixture,” *Quora*, 2018. [Online]. Available: https://www.quora.com/What-is-a-gaseous-example-of-a-heterogeneous-mixture. [Accessed: 23-Nov-2021].

[52] K. Prasad, W. Pitts, and J. Yang, “Effect of wind and buoyancy on hydrogen release and dispersion in a compartment with vents at multiple levels,” *Int. J. Hydrogen Energy*, vol. 35, no. 17, pp. 9218–9231, 2010.

[53] B. J. Lowesmith, G. Hankinson, C. Spataru, and M. Stobbart, “Gas build-up in a domestic property following releases of methane/hydrogen mixtures,” *Int. J. Hydrogen Energy*, vol. 34, no. 14, pp. 5932–5939, 2009.

[54] Miles Dai (MIT), “Schlieren Imaging,” 2018. [Online]. Available: http://www.mit.edu/~milesdai/projects/schlieren/index.html. [Accessed: 15-Nov-2021].

[55] Harvard Natural Sciences Lecture Demonstrations, “Schlieren Optics,” 2014. [Online]. Available: https://sciencedemonstrations.fas.harvard.edu/presentations/schlieren-optics. [Accessed: 15-Nov-2021].

[56] IWUN, “Richtlijn voor meterruimten met een gasaansluiting in laagbouwwoningen,” 2016.

[57] Gas Detector Shop, “MultiRAE Lite Portable Gas Detector,” 2021. [Online]. Available: https://www.gasdetectorshop.com.au/j2store/multirae. [Accessed: 15-Nov-2021].

[58] Norrscope, “MultiRAE Sensors, Accessories & Spares,” 2021. [Online]. Available: https://norrscope.com/product/multirae-sensors-accessories-spares/. [Accessed: 15-Nov-2021].

[59] H. F. Coward and G. W. Jones, “Limits of flammability of gases and vapors,” *Bull. 503, Bur. Mines*, p. 161, 1952.

[60] M. B. Spoelstra, “Veiligheidsaspecten van waterstof in een besloten ruimte,” *IFV*, pp. 1–57, 2020.

[61] Weather Atlas, “Weather forecast and Climate information for cities all over the Globe,” 2021. [Online]. Available: https://www.weather-atlas.com/. [Accessed: 24-Dec-2021].

[62] NEN, “NEN 1078 : 2018 nl Supply for gas with an operating pressure up to and including 500 mbar - Performance requirements - New estate,” 2018.

[63] NEN, “NEN 8078 : 2018 Supply for gas with an operating pressure up to and including 500 mbar - Performance requirements - Existing estate,” 2018.

[64] MKS, “Gas Correction Factors for Thermal-based Mass Flow Controllers,” 2021. [Online]. Available: https://www.mksinst.com/n/gas-correction-factors-for-thermal-based-mass-flow-controllers. [Accessed: 24-Dec-2021].

[65] D. C. (Arizona S. U. Montgomery, *Design and Analysis of Experiments*, Eighth. Wiley, 2013.

[66] B. Cariteau, J. Brinster, and I. Tkatschenko, “Experiments on the distribution of concentration due to buoyant gas low flow rate release in an enclosure,” *Int. J. Hydrogen Energy*, vol. 36, no. 3, pp. 2505–2512, 2011.

[67] P. Brown, S., Posta, G., McLaughlin, “Safety Assessment: Conclusions Report (Incorporating Quantitative Risk Assessment),” *Hy4Heat*, 2021.

[68] C. D. Barley, K. Gawlik, J. Ohi, and R. Hewett, “Analysis of Buoyancy-Driven Ventilation of Hydrogen From Buildings,” no. August, 2007.

[69] R. Taylor and H. A. Kooijman, “Mass Transfer in Distillation,” *Distill. Fundam. Princ.*, pp. 97–143, Jan. 2014.

[70] B. Bierling, “Proefopstelling verspreiding waterstof in de meterkast,” *DNV*, 2020.

[71] D. Hao, X. Wang, Y. Zhang, R. Wang, G. Chen, and J. Li, “Experimental Study on Hydrogen Leakage and Emission of Fuel Cell Vehicles in Confined Spaces,” *Automot. Innov.*, vol. 3, pp. 111–122, 2020.

[72] X. Shao, S. Yang, Y. Yuan, H. Jia, L. Zheng, and C. Liang, “Study on the difference of dispersion behavior between hydrogen and methane in utility tunnel,” *Int. J. Hydrogen Energy*, vol. 47, no. 12, pp. 8130–8144, Feb. 2022.

[73] V. Aroutiounian, “Metal oxide hydrogen, oxygen, and carbon monoxide sensors for hydrogen setups and cells,” *Int. J. Hydrogen Energy*, vol. 32, no. 9, pp. 1145–1158, Jun. 2007.

[74] A. v. Wijk, “Verbal communication, supervisor TU Delft,” 2021.

[75] A. Murugan, S. Bartlett, J. Hesketh, H. Becker, and G. Hinds, “Project closure report: Hydrogen Odorant and Leak Detection,” no. November, p. 186, 2020.

[76] W. Song, E. M. Lopato, S. Bernhard, P. A. Salvador, and G. S. Rohrer, “High-throughput measurement of the influence of pH on hydrogen production from BaTiO3/TiO2 core/shell photocatalysts,” *Appl. Catal. B Environ.*, vol. 269, p. 118750, Jul. 2020.

[77] Midsun Specialty Products, “DETECTAPE - A Localized Visual Detector for Hydrogen Leaks Webinar,” *U.S. Dep. Energy*, 2016.

Appendix

Appendix

Appendix A

A.1

From: Hyindoor Final Report: Pre-normative research on safe indoor use of fuel cells and hydrogen systems

Table A1: Tests results of the tested five commercially available sensors: Dark green - outstanding performance; light green - good performances; yellow - passing grade; red – unsatisfactory [38].

Performance parameter	CAT-1	TC-1	CAT-2	CAT-3	EC-1
Manufacturer Calibration	X	√	X	×	X
Accuracy and Precision	√	√	×	×	×
Short term stability	×	√	√	√	x
Pressure (p_0 = 100kPa)	√	√	×	×	
RH (RH_0 = 50%)	√	×	×	√	×
Temperature (T_0 = 20C)	x	√	√	×	X
Lower Detection Limit (LDL)	50 ppm	50 ppm	50 ppm	500 ppm	<<50 ppm
CH4 (1%)	X	x	X	X	No
SO2 (0.05%)	X	No	No	small	X
CO (0.005%)	No	No	No	No	lower
HMDS (0.001%)	No	No	No	small	No
Response/Recovery time	6 s	4 s	~10 s	~10 s	~50 s
Flow rate (F_0 = 200 ccm)	16%	3%	8%	13%	39%
ATEX	IEC60079-15	No	√	√	√

A.2

From: Reliability of commercially available hydrogen sensors for detection of hydrogen at critical concentrations: Part II – selected sensor test results

Table A2 : Results from detection limit and cross-sensitivity to CO tests [28].

CAT	**LDL 0 vol% H_2**	0.03	0.06	0.11
	Cross sensitivity vol% CO	0.21	1.03	2.00
MOX	**LDL 0 vol% H_2**	0.03	-	-
	Cross sensitivity vol% CO	none	-	-
EC	**LDL 0 vol% H_2**	0.03	0.03	0.03
	Cross sensitivity vol% CO	0.31	0.33	0.46
TC	**LDL 0 vol% H_2**	0.60	0.15	-
	Cross sensitivity vol% CO	-	0.36	-

A.3

Table A3: The advantages and disadvantages noted for the various hydrogen sensor types tested based on observations during tests [28].

Sensor type	Catalytic	MOx	Electrochemical	Thermal conductivity
Advantages	- Robust - Accurate - Low dependence on RH - Low dependence on temperature - Low dependence on pressure	- Low detection limit - Small size - Low cost - Stable baseline - Suitable mass production - Wide temperature range	- Low detection limit - Low dependence on RH - Low cost - Low power consumption	- Accuracy - Wide measuring range - O_2 not required for operation
Disadvantages	- High detection limit - Poisoning and cross sensitivity - High power consumption - Expensive - Large size	- Low accuracy - Dependence on temperature - Dependence on humidity - Sensitive to overexposure - Memory effects	- Poor performance at sub-zero temperature - Wide variation in results - Poisoning - Cross sensitivity - Operation at low pressures difficult	- High detection limit - Dependence on temperature - Expensive

A.4

From: Selectivity and resistance to poisons of commercial hydrogen sensors

Table A4: Overview of the tested sensors [37].

	CAT-1	CAT-2	EC	MOX
Measuring range	0 - 1.4 vol%	1 - 4 vol%	0 - 4 vol%	0 - 4.4 vol%
Cross sensitivity	H_2S, NO_2 slightly	-	H_2S, SO_2 NO_2 slightly	-

A.5

From: Hydrogen sensors – A review

Table A5: performance specifications of commercially available sensors (adjusted) [23].

Sensor type	Principle/Device	Performance*					
		Measuring range/vol%	Accuracy/% of indication	Response time (t_{90})/s	Power consumption/mW	Gas environment	Lifetime/years
Catalytic	Pellistor	Up to 4	<±5	<30	1000	−20–70 °C 5–95% RH 70–130 kPa	5
Thermal conductivity	Calorimetric	1–100	±0.2	<10	<500	0–50 °C 0–95% RH 80–120 kPa	5
Electrochemical	Amperometric	Up to 4	≤±4	<90	2–700	−20–55 °C 5–95% RH 80–110 kPa	2
Resistance based	Semiconducting metal–oxide	Up to 2	±10–30	<20	<800	−20–70 °C 10–95% RH 80–120 kPa	>2

A.6

From: An overview of hydrogen safety sensors and requirements

Table A6: Generalized ranking of various sensor platform to selected performance metrics (5 = ideal, 0 = poor) (adjusted) [24].

Metric	EC	MOX	CGS	TC	Optical	Pd
Analytical metrics						
Detection limit	4.0	4.0	4.0	4.0	4.0	4.0
Selectivity	3.5	3.0	3.5	3.5	4.5	4.9
Linear range	4.9	3.0 (4.5)	4.0 (4.5)	4.0	3.0	4.0
Response time	4.0	3.0 (4.5)	4.0	4.5	3.0	3.5
Repeatability	3.5	4.0	4.0	4.0	3.0	4.0
Environmental effect	3.5	3.5	4.0	3.0	4.0	4.0
Logistic metrics						
Level of maturity	5.0	5.0	5.0	4.5	3.5	4.5
Size	4.0	4.0	4.0	4.5	4.0	3.5
Power	4.0	3.0	3.0	4.5	4.5	4.0
Maintenance	3.5	3.5	4.0	4.0	5.0	4.0
Lifetime	3.5	4.0	3.5	4.0	4.0	3.8
Matrix	4.0	3.0	3.0	4.5	4	3.5

A.7

Table A7: An overview of the advantages and disadvantages of the technologies used for hydrogen sensing [22].

Sensing Method	Working principle	Advantage	Disadvantage	Physical change
Thermal	Calorimetric	• Fast response • Low cost • Stable • Wide measuring range • Simple construction • Robust	• Sensitive to interfering gases • Heating element reacts with gas • Lower detection limit is high	Thermal conductivity Resistance
Electrochemical	Amperometric Potentiometric	• Sensitive • Low power consumption • Working at high temperature is possible • Heating element is not required	• Costly • Low life • Cross sensitivity to other gases • Specific electrolyte requirement • Requires regular calibration	Electric current Voltage
Resistive	Resistance variation in presence of H_2 gas	• High sensitivity • Wide range of operating temperature • Low cost • Easy fabrication • Fast response • Low power consumption	• Cross sensitivity with interfering gases and humidity • Poor selectivity • High operating temperature • Requires O_2 to work • Affected by gas pressure	Resistance
Work function	Schottky diode MOSFET MIS capacitor	• Small size • Fast response • Low power requirement • High sensitivity and selectivity • Low cost • Less influence of ambient conditions	• Existence of Hysteresis losses • Possibility of drift • Saturation occurs at modest concentrations	Voltage Capacitance Current
Mechanical	Micro-cantilever bending	• Small size • Does not require oxygen • Ability to work in explosive atmosphere • Micromachining is possible	• Hard to fabricate, • Cross-sensitivity with interfering gases • Slow response • Aging effect	Bending Curvature
Optical	Optodes/ Interferometric	• Can work without explosion • Fast response	• Cross-sensitivity with interfering gases and ambient light	Reflectance Wavelength Colour SPR
Acoustic	QCM SAW Sound velocity measurement	• High sensitivity, • Low power consumption • Wide range of detection • Fast response	• Sensitive to interfering sound waves and vibrations • Unable to operate at high temperature • Interference of other gases is possible	Frequency Time Wave velocity
Catalytic	Pellistor Thermoelectric	• Wider operating temperature • Stability	• High power requirement • Interference with other gases • High response time	Resistance Voltage

Appendix B

B.1 Importance of criteria parameters for the residential application of hydrogen sensors

Table B1: Hydrogen sensor importance scores for residential applications [20].

Parameters	Importance			Specifications and Notes
	Low	Medium	High	
Analytical Parameters				
Selectivity			X	Sulfur, silicone resistance, CO, household solvents and paints
LDL		X		0.04 vol% (1% of LFL)
Analytical Resolution	X			Differentiation is not important other than alarm set points
Linear Range/Dynamic			X	To LFL (0.1–4 vol% H_2)
Accuracy		X		Within ±50% of reading for all working (T,P, RH) conditions
Response Time		X		30 s
Recovery Time		X		1 min
Repeatability		X		
Signal Drift			X	To avoid false positives and negatives at all alarm levels
Environmental Impacts				T and RH are more relevant than P
- T			X	-40° to +40°C to cover both northern and desert climates
- P		X		Must be calibrated for deployment altitude
- RH		X		5%–95% RH
Reversibility		X		Postexposure recovery should be >95%
Limits of Quantization	X			Quantization of trace hydrogen is not as critical as LDL
Saturation Stability	X			Unlikely to be exposed to 100% H_2 (or very high H_2)
Deployment Parameters				
Capital Cost			X	<$100
Installation Cost			X	Easily mounted (no special requirements or costs)
Physical Size		X		Size not a significant issue for wall/ceiling mounting

Parameters	Importance			Specifications and Notes
	Low	Medium	High	
Control Circuitry			X	Simple, must be part of integrated system for deployment
Electronic Interface		X		Output in engineering units (e.g., % H_2)
Pneumatic Connections	X			Passive (no power) sampling system
Shelf Life		X		>5 years
Commercial Maturity		X		Currently not available, but must be off-the-shelf by 2015
Alarm Thresholds			X	Must indicate adverse condition
- Trace (1,000 ppm_v)	X			Not required (trace background may be present)
- Low (low risk)	X			10% of the LFL, activate alarm (or 25%)
- High (pending risk)			X	25% of the LFL, activate alarm
Regulations and Codes			X	NFPA 2, possible performance specification
Deployment Placement			X	Guidance on placement is needed
Operational Parameters				
Lifetime		X		5 year minimum, 10 year desired
- Sensing Element		X		5 years
- Unit Replacement		X		5 years, 10 years desired
Consumables		X		None
Calibration Schedule			X	No calibration during operational lifetime
Maintenance			X	Maintenance free
Sample Size	X			No critical restriction
Matrix Requirements	X			Normal air environment
Signal Management		X		
- Alarm (audible, lights)			X	Alarm set at 10% or 25% of LFL, depending on AHJ)
- Displays		X		Display not necessary
- Remote Monitoring	X			Not required
Device Repeatability	X			Will be replaced as unit
Warm-Up Time		X		<1 h for initial installation, 15 min for all shutdowns
Alarm Interface				To activate audible alarm, which is part of system
- Number of set points		X		One mandatory
- Audible			X	Activate at alarm set point
- Ventilation	X			Not required
- Shutdown	X			Not relevant
- Remote			X	Perhaps useful to warn against entry
Mechanical Stability	X			No special requirements for fixed deployment
Power Requirements	X			Moderate power requirements preferred (<0.5 W)

B.2 Performance criteria (15) with their score on importance

The importance of the different performance criteria determines the weights for the multi-criteria analysis. The importance is determined by using the previous table in B1 (Table B1). The weights are adjusted by a fraction to ensure that the total of all weights added up is equal to 15. The accuracy and selectivity criteria are the ones that are given more weight regarding its importance.

	Importance	Weights (added up equal to 15)
Accuracy	4	1.5
LDL	4	1.5
Response time recovery time	2.5	1
Measuring range	3	1.3
Selectivity	4.5	2
Lifetime	3	1.3
Relative humidity	2	0.5
Pressure	2	0.5
Temperature	3	1.3
Stability	2.5	1
Calibration / Maintenance	2.5	1
Flow rate	1	0.3
Robustness	1	0.3
Cost	2.5	1
Power consumption	2	0.5 +
		15

Appendix C

C.1 Multi-Criteria Analysis Matlab code

```
clear all;

close all;

clc;


W=[ 0.1 0.12 0.066667 0.086666667 0.133333 0.086666667 0.033333 0.033333 0.066667 0.066667
0.066667 0.020 0.020 0.066667 0.033333];
%Weights per criterium

X=[4 3 3 3 1 3 3 3 2 2 2 2 2 4 2; 2 3 2 2 3 3 2 2 3 3 1 3 3 2 2; 2 2 2 2 2 3 3 2 2 3 2 2 3 2 2; 3 3 4 3 2 3 2 4
4 3 3 4 2 3 3; 2 4 1 2 2 1 2 2 1 2 1 1 3 3 3; 3 3 3 2 3 2 1 2 3 2 2 2 3 3 3];
%Scores per sensor


Xval=length(X(:,1));

for i=1:Xval

for j= 1:length(W)

Y(i,j)=X(i,j)/max(X(:,j)); %Normalized scores

end

end

for i=1:Xval

PWSM(i,1)=sum(Y(i,:).*W); %Weight Sum Method

PWPM(i,1)=prod(Y(i,:).^W); %Weight Product Method

end

Weighted_Sum_Model_Score = num2str([PWSM])

Weighted_Product_Model_Score= num2str([PWPM])
```

C.2 Results from the Weighted Product Model

Table C1: Final scores when using the Weighted Product Model.

WPM	Cat1	Cat2	Cat3	TC	EC	MOX
Final score	0.706	0.688	0.641	0.858	0.532	0.725
Rank	3	4	5	1	6	2

Appendix D

Another method for hydrogen detection: Detection tape

Realization of this idea could be done in the form of tape applied on the components that are sensitive to the leaked gas. If a leak occurs, the tape close to the location changes colour to indicate the presence of a leakage. An example of this by tape, form the company Midsun Specialty Products, is the hydrogen sensitive film Detectape [76]. The tape reacts to an increase in the local hydrogen concentration. The hydrogen sensitive film changes colour from light to dark. The colour shows differences in concentration level between 0–50 vol% H2.
Silicone is the main material of the tape that lets hydrogen permeate through. The chemo-chromic pigment changes colour when it is exposed to hydrogen. It is a good technology to identify small hydrogen leaks which would otherwise go undetected. Regular observation is needed to identify the colour changes of the tape and appropriate manual actions could be taken.

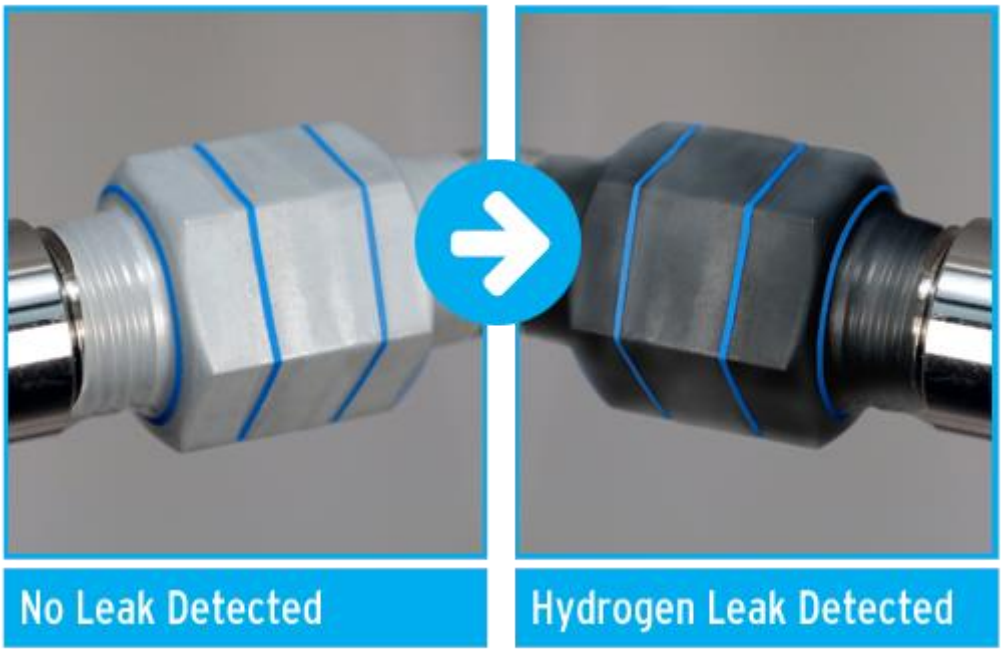

Figure D1: Detectape before and after being exposed to hydrogen [77].

Appendix E

Results of the hydrogen outflow visualised with a Schlieren technique experiment

E.1 Set up Schlieren experiment

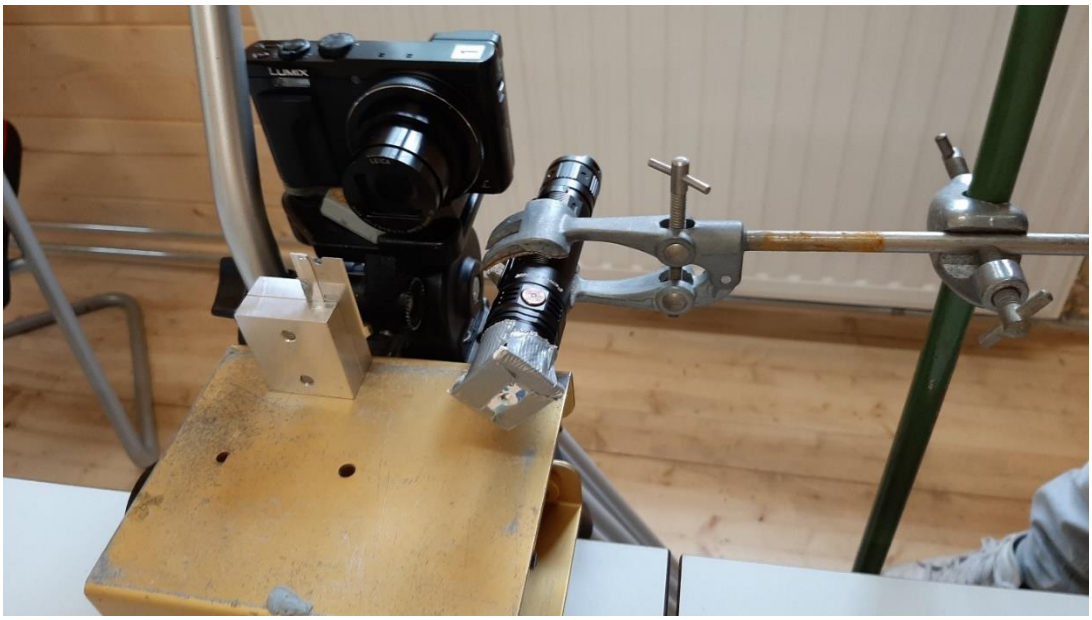

Figure E1: Schlieren technique experimental set-up at the camera end including a concentrated flash light, a razorblade and a high-res. camera.

(a)

(b)

Figure E2: (a) Schlieren technique experimental set-up seen from the camera. (b) The outflow nozzle of hydrogen gas and the mirror in position on the other end of the table.

Appendix F

From working paper of DNV: 'Proefopstelling verpreiding waterstof in de meterkast.'

F.1 Maximum concentration of hydrogen

Waterstof Lekdebiet in liters/uur	LEL 50 cm	LEL 120 cm	LEL 180 cm	LEL 220 cm
1	0.008	0.142	0.135	0.127
3 (24-uur test)	0	0.387	0.580	0.674
5	0	0.426	0.551	0.630
10 2e meting	0	0.481	0.805	0.987
15	0	1.403	1.540	1.580
20	0	1.148	1.440	1.530
25	0	0.848	1.344	1.403

(a)

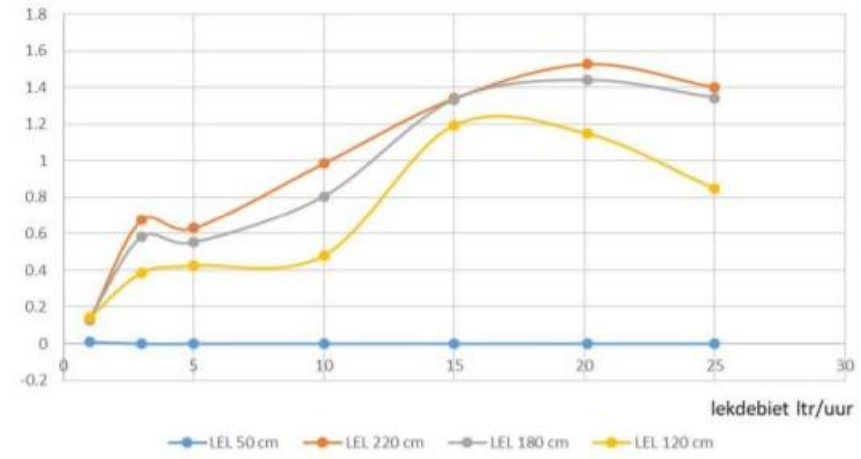

(b)

Figure F1: Maximum concentration of hydrogen gas with in (a) data of the gas concentration: horizontally the leakage rate, vertically the height. (b) Figure of the data with four lines that represent the height in the metering cabinet [70].

F.2 Maximum concentration of natural gas

	Maximaal bereikte concentraties in vol % CH4			
Aardgas **Lekdebiet in liters/uur**	**LEL 50 cm**	**LEL 120 cm**	**LEL 180 cm**	**LEL 220 cm**
1	0	0.172	0.159	0.196
3 (24-uur test)	0	0.185	0.204	0.184
5	0	0.405	0.652	0.665
10.1	0	0.823	0.961	0.947
15	0	0.734	0.782	0.774
20.1 3e meting	0	0.727	0.961	0.945
25	0	0.821	0.987	0.969

(a)

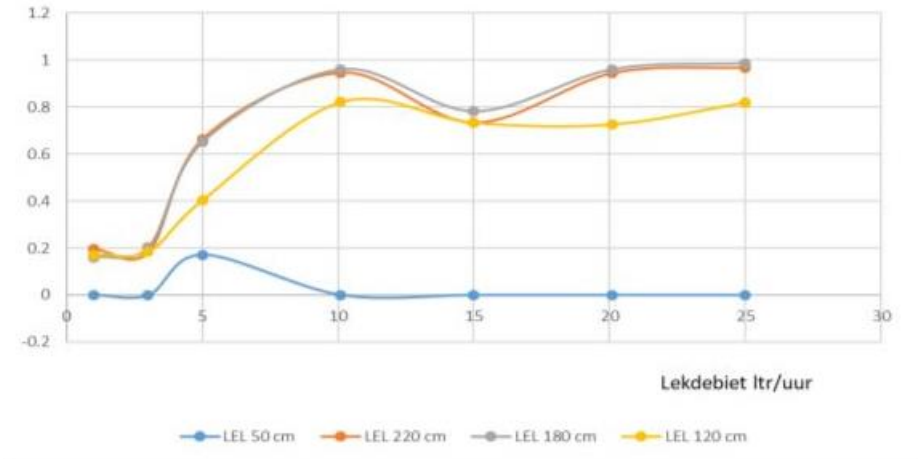

(b)

Figure F2: Maximum concentration of natural gas with in (a) data of the gas concentration: horizontally the leakage rate, vertically the height. (b) Figure of the data with four lines that represent the height in the metering cabinet [70].